The Vanadium Project Final Report

JT Steenkamp & Paul Corbett, for Shell Canada
Andy Knight & Mohammad Rashid, for the University of Calgary
Garima Chauhan & Arno de Klerk, for the University of Alberta

Disclaimer

Executive Summary

The Vanadium Project was a split-effort by Shell Canada, the Athabasca Oil Sands Project (AOSP) owners, the University of Calgary (U of C) and the University of Alberta (U of A) to explore the performance of vanadium redox flow batteries in the Alberta climate for grid applications (Shell, U of C), and the viability of extracting nuisance vanadium from oil sands processes (Shell, AOSP owners, U of A).

Vanadium is found in one of the most abundant metal complexes in Alberta oil sands. It also causes significant catalyst fouling in refinery processes. At the same time, vanadium is the key constituent in vanadium redox flow batteries (VRB) which have an important application in renewable energy integration with the grid.

The research objectives of the project were two-fold: (1) learn the performance specifications of VRB technology and benchmark against lithium-ion (Li-ion) in Alberta conditions in the context of renewable energy applications and (2) test metal removal techniques on oil sands bitumen for the efficient removal of vanadium and potentially other nuisance metals such as nickel.

For objective 1, Shell installed a li-ion battery (by Tesla), Alberta's first VRB (by WattJoule), battery testing equipment and a complimentary solar array at what was then Shell Technology Centre Calgary (STCC) in 2017. The U of C was recruited to execute the test program for the batteries over two winter seasons. Unfortunately, the U of C was unable to perform testing on the li-ion battery due to controllability issues and delayed availability of an application programming interface. For the VRB, key findings included:

1. Ability of VRB to operate in temperature conditions below rated, albeit at lower efficiency of 0.12%-0.16% per degree Celsius.
2. Impressive current densities of 300 mA / cm2 at rated power and 437 mA / cm2 at peak power in conditions below nominal temperatures.
3. VRB power stacks can be damaged by electrolyte impurities. It was the first time a particular undisclosed impurity had been encountered by the vendor in their vanadium supply chain and lead to the development of additional quality control procedures for the detection of this irregular impurity in vanadium sources going forward[1].
4. A maximum DC round trip efficiency of 78.5% was observed at rated power close to nominal temperature but can fall to low-mid 60% range at a peak power twice nominal rated power. The observed value occurred during an electrolyte contamination issue which may be the cause of the difference.
5. Mechanical reliability issues were encountered that were likely caused by operating well below rated ambient conditions

VRB chemistry shows potential resiliency for Alberta climatic conditions, and the current density of the test unit impresses. Efficiency sensitivities to temperature will matter more to some battery applications (arbitrage) than others (ancillary services).

For objective 2 (testing metal removal techniques on oil sands bitumen) U of A identified and explored three techniques. The first was ionic liquids assisted extraction. Ionic liquids have applicability in a solvent based liquid-liquid extraction method and are known for their potential to be efficient and highly selective. A range of ionic liquids were tested but yielded mixed results at U of A and in Shell's own laboratory work. Major findings of the ionic liquid assisted extraction process are listed below:

i. None of the ionic liquid demonstrated a significant V/Ni extraction in a single stage extraction. Though, out of the all investigated ionic liquids, Dimethlyammonium dimethyl-carbamate (DIMCARB) showed highest extraction of metals from dilbit samples.
ii. Along with the extraction of metals, selectivity of ionic liquids for oil extraction was also considered as a deciding factor. Selectivity of various ionic liquid was investigated by performing Simulated Distillation analysis of organic and ionic liquid phases. Dimethlyammonium dimethyl-carbamate, in spite of showing the considerable metal extraction, was observed to be a non-selective ionic liquid. Significant amount of organic content was detected in ionic liquid phase.

[1] A comment from the vendor: "As experience teaches with all new battery systems that are introduced for testing in the field, some problems present themselves that have not been discovered in laboratory testing. The solution to such problems is an essential part of continuous battery product development, and it offers the opportunity to improve the product performance, cost and lifetime. As expected, such challenges and opportunities were noted in Shell's testing of the WattJoule Electristor™ ES10. WattJoule has now incorporated these new improvements and learnings into the ElectriStor™ platform going forward. Anyone requiring more information about the ElectriStor™ platform and licensing, should reach out to WattJoule at info@wattjoule.com".

iii. On the contrary, 1-ethyl-3-methyl imidazolium thiocyanate (EMIM-SCN) and 1-methyl imidazolium chloride ([HC1im]Cl+10% H2O) were observed to be selective. No evidence was found that oil was observed in the extracted ionic liquid phase. However, the extraction efficiency for single equilibrium stage extraction was less than 10% for these ionic liquids.

iv. Efforts were also made to optimize the process parameters. Reaction parameters were optimized by varying the reaction temperature, ratio of dilbit to ionic liquid, reaction time, settling time, stirring speed. Variation of stirring speed could not show any noticeable increase in metal extraction with the increase in stirring speed. This observation indicated that the ionic liquid assisted extraction was not a mass transfer limited process over the extraction periods investigated.

v. Possibility of multi-stage extraction process was investigated. 1-ethyl-3-methyl imidazolium thiocyanate (EMIM-SCN) was chosen to study the multistage extraction, considering its high selectivity (i.e. little or no oil co-extraction with the metals). Three cycles of experiments were performed using the Athabasca bitumen/Albian dilbit sample during all cycles, while fresh ionic liquid was used in each cycle. Results indicated the possibility of multi-stage extraction process. By employing three equilibrium stages, the overall vanadium extraction was increased from around 4 to 12 % (Table 9) in case of Athabasca bitumen whereas in Albian dilbit sample, vanadium extraction was increased from 15-38%.

In conclusion, it was found that some of the ionic liquids were selective for the extraction of the metals in the presence of little or no oil. It was further found that for the selective ionic liquid that was further evaluated (EMIM-SCN), the extraction was an equilibrium limited extraction. It was therefore possible to increase extraction by employing more than one equilibrium stage. At the end of the ionic liquid work several questions remain. The irreproducibility of previous results (Appendix D) is not yet understood and Mechanisms limiting extraction efficiency require further discovery.

The second technique explored was photochemical separation, where a combination of photochemical reaction and liquid-liquid extraction is employed to recover vanadium and nickel from bitumen. In this process, the bound-type metalloporphyrins are postulated to photodissociate in presence of a hydrogen donor solvent to convert ‘bound’ into ‘free’ type metalloporphyrins. The resulting solution is photodecomposition by UV irradiation to release the metal ions into solution, which can be selectively removed by solvent extraction. This technique results in low yield extraction on dark samples, since most of the light is absorbed by the bulk medium. However, the work showed that it may have some value in removing metals from less-opaque products.

A promising technique was found to be electrochemical separation which is based on the similar hypothesis as photochemical assisted extraction process. The bitumen is subjected to electrochemical treatment to displace the metal ions in the metalloporphyrins. The released

metal ions can then be extracted by employing a liquid-liquid extraction process. In the experiment yielded up to 69% vanadium extraction from a model component and 35% vanadium removal from actual Albian dilbit. Similar to the ionic liquids work, this technique also generated new questions. Factors affecting removal efficiency from actual samples are not fully understood and the selection of electrochemical system materials not yet economically optimized.

Acknowledgements

The authors would like to thank Alberta Innovates, Alberta Economic Development and Trade and the AOSP Owners, in addition to Shell Canada, Canadian Natural Upgrading Limited, and Chevron Canada Limited for making this work possible.

Contents

Introduction

The research objectives of the project were two-fold: (1) learn the performance specifications of vanadium redox flow battery (VRB) technology and benchmark against lithium-ion (Li-ion) in Alberta conditions in the context of renewable energy applications and (2) test metal removal techniques on oil sands bitumen for the efficient removal of vanadium and potentially other nuisance metals such as nickel.

The first component of the project proposal was to consist of the deployment, integration and testing of two leading electrochemical energy storage technologies: (a) lithium-ion (Li-ion) and (b) the latest-generation VRB battery at the Shell Technology Center in Calgary. The battery performance benchmarking was to be conducted using the grid as load and source. When benchmarking tests were not being conducted, the system would default to a standard maximized-solar-self-consumption mode with a grid connected 10kW solar array.

The installation would advance the understanding of how VRB technology benchmarks with Li-ion batteries to enable renewable energy integration applications in the Alberta electricity system.

The second component of the project was to test and develop metal removal techniques for metals removal from Alberta oil sands bitumen. This element consisted of establishing a method for determining the metal content and testing three different extraction techniques; ionic liquid assisted extraction, photo-irradiation assisted extraction and electrochemical metal removal. Its focus would be on the vanadium extraction, which could become a major, exportable oil sands by-product, for use in vanadium-redox-flow batteries (VRB).

The results could enable:

- Additional and better integration of renewable energy in Alberta;
- Improved commerciality and environmental performance of the Oil Sands resource;
- Innovation capacity building in Alberta institutions and companies in a new area and nucleating a global center of excellence;
- Clean energy technology development and export opportunities for Alberta.

Battery Deployment, Integration and Testing

Objectives

The technical objectives of the battery component of the project were as follows:

- Develop and run an accelerated benchmarking program cycle that tests performance specifications of the two battery technologies before the end of 2018:
    - Power capacity
    - Energy storage capacity (MWH)
    - AC round trip efficiency
    - Ramp rates
    - Limitations of frequency, timing of switching between states, and required changes in state
    - Self-discharge rate
- Determine and report on the battery performance specifications due to:
    - Alberta ambient conditions: temperature, humidity, pressure
    - Cycle count, cycle depth, cycle frequency
- Repeat the program and reporting cycle if by September 2018 a locally sourced vanadium electrolyte is substituted into the vanadium redox flow battery through the metal extraction component;
- Allow the system to go into a maximize-solar-self-consumption mode when test programs are not being run.

Methodology

The WattJoule ES-10 VRB was delivered and installed in December 2017 at Shell Technology Centre Calgary (STCC). The arrival, installation and handling of the electrolyte is shown in Figure 1, and Figure 2 **Error! Reference source not found.**.

Figure 1 - VRB arrival in December 2017 at Shell Technology Centre Calgary

Figure 2 - The battery installation location behind STCC

Two Tesla Li-ion Powerwall 2 were delivered and installed on the outer wall of the STCC. The installation is shown inFigure 3.

Figure 3 - Tesla Powerwall 2 installation located next to the VRB shed

Figure 4 - 10kW Solar installation located on the 3rd floor

10 kW of PV solar was installed on the roof of the STCC with the grid-tied inverter installed within the mechanical room on the third floor. The installation is shown in Figure 4. The original intent of the solar PV was to allow integration with the batteries to maximize solar self-consumption when experiments were not being run, however this mode was not specifically tested due to controlled battery cycling routines taking up all project time.

Shell Canada (Shell) recruited Dr. Andy Knight and Mr. Mohammed Rashid from the U of C to execute the test program for the VRB and Li-ion batteries over two winter seasons. To enable the execution of the test program, a Battery Charge/Discharge Testing system (Chroma 69225) was programmed to execute charge/discharge routines naturally varying climatic conditions on a vanadium redox flow battery. Performance data was monitored and collected remotely from the U of C for analysis. For Lithium Ion battery testing, the original plan was to use the built-in inverter of the Tesla Powerwall 2 and an application programming interface (API) to control charge and discharge signals. Due to a delay in the availability of the API the native backup power functionality was used instead by automating power source and load relays.

Results & Discussion

The battery testing commenced in January 2018 and concluded in February 2019 with two winter seasons of testing. Dr. Knight and Mr. Rashid compiled a detailed test report for Shell and it is reproduced below.

All battery testing was done on a DC basis as core performance characteristics of batteries are DC in nature. The battery performance testing was divided into three sections:

1. Winter 2017/2018 testing of the WattJoule ES10-2DC Battery
2. Spring 2018 testing of the WattJoule ES10-2DC Battery
3. Winter 2018/2019 testing of the WattJoule ES10-0.5DC Battery

In early spring 2018, battery testing halted due to a pump coupling fault. After repair, the battery continued until late spring 2018, when an undisclosed impurity in the electrolyte was detected by the vendor, causing damage to the cell stack. In late 2018, the battery returned to service as an ES10-0.5DC model, with the cell stack reduced to 5 cells rather than the original 20. Testing of the modified battery continued until later February 2019, when operation was once again halted by a pump fault. WattJoule's specifications of the batteries and the technical stack differences are given in Appendices A and B.

Extended testing of the Tesla Powerwall 2 batteries was not possible. The functionality of the Powerwall 2 is limited by the proprietary firmware and user interface. When the Powerwall 2 system is continuously cycled by connection / disconnection of the building supply, operation is halted after 3-4 cycles.

During cold weather operation, the flow battery operated far outside the nominal temperature range. The battery is installed in a partially-insulated shed without environmental controls to allow stress-testing under Alberta climatic conditions. In winter 2019, the battery operated while

the mean daily temperature in Calgary was below -20C, with an average enclosure temperature below -10C and electrolyte temperatures dropping below -6C.

Winter 2017/18 Testing with ES10-2DC

The ES10-2DC is a 2kW/10kWh vanadium redox flow battery and has an expected life of 20 years and/or 10,000 cycles. In the period from December 21, 2017 to April 4, 2018, the ES10-2DC VRB was cycled 184 times. Of these, 164 cycles were continuous cycling at the nominal charge/discharge rate, 19 were under accelerated discharge/charge testing, and 1 was after a cold resting period.

Nominal Charge Rate, Continuous Cycles

Under continuous cycling at nominal charge and discharge rates of 75A, the energy input is close to the nominal value of 10kWh when charging, with lower energy capacity when the ambient enclosure temperature is below 15°C, shown in Figure 5. The ambient enclosure temperature is calculated as the mean of the enclosure temperature at the start and end of charge and discharge in one cycle. Under continuous operation, the internal heat produced by the battery is sufficient to keep the enclosure temperature in the acceptable ambient operating range of +10 to +35°C. In discussions with WattJoule, the electrolyte temperature during their performance benchmarking was +45°C.

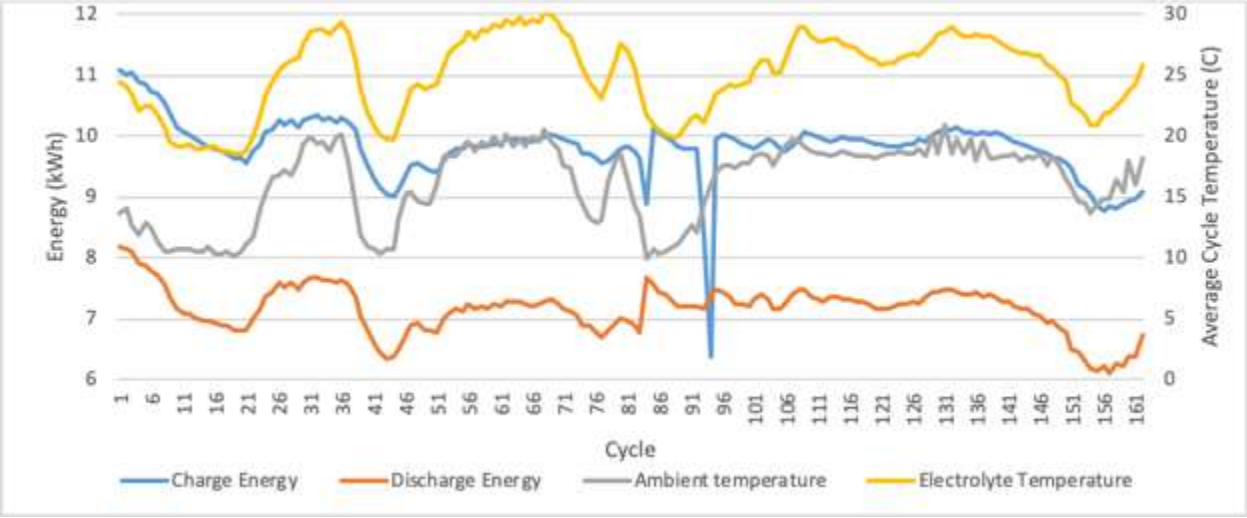

Figure 5 Charge and Discharge Energy at Nominal Rate

The round-trip energy efficiency, calculated as discharge energy/charge energy for each cycle, is plotted in Figure 6. Both the energy flow to/from the battery and round-trip efficiency appear visually correlated to the temperature of the enclosure.

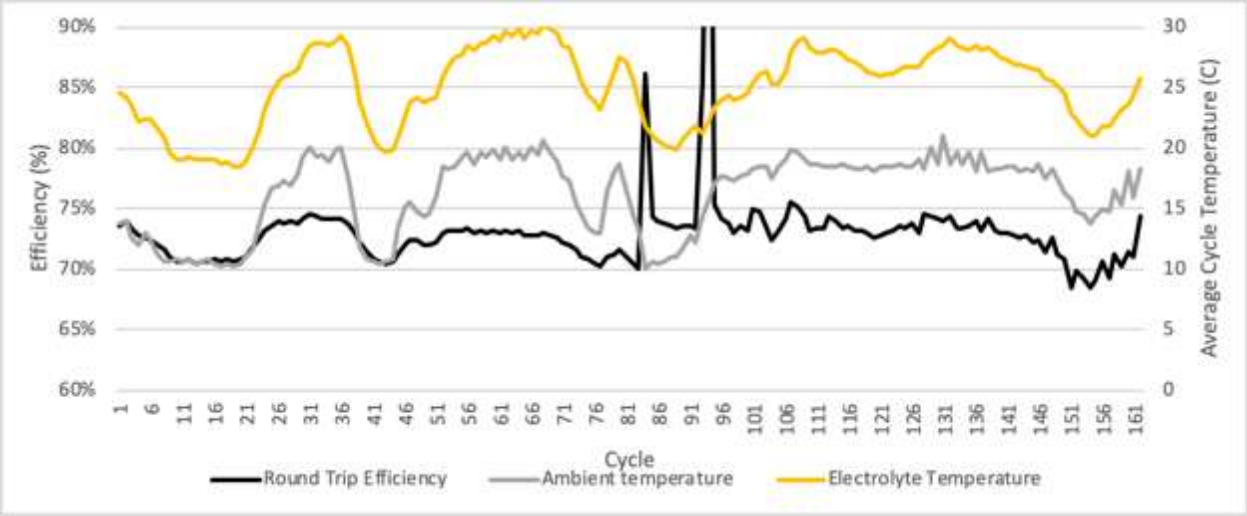

Figure 6 Round Trip Efficiency at Nominal Rate

Figure 7 shows a scatter plot of efficiency as a function of both enclosure temperature and electrolyte temperature, together with linear best fit trendlines. It can be seen that the efficiency does increase with increasing temperature, at a rate of 0.12%-0.16% per degree Celsius.

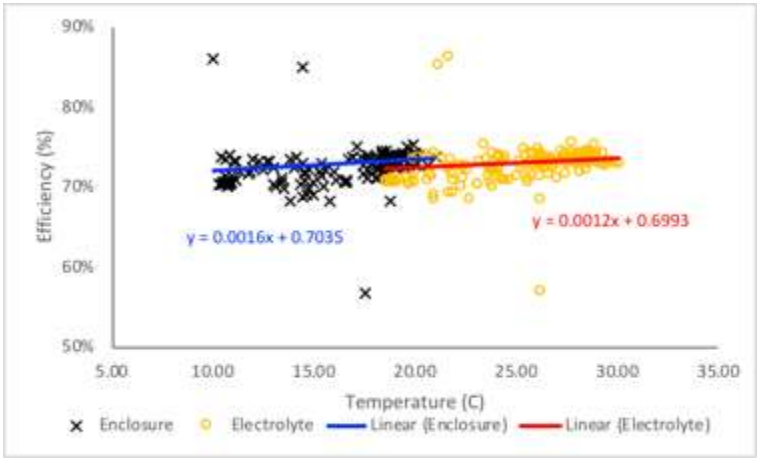

Figure 7 Correlation of Efficiency with Temperature

Under nominal charging conditions, the charge and discharge currents from the Chroma controller were set to a target value of 75A, at the voltage limits of the system. The actual voltage, current and power profiles for a typical day in the continuous cycling period are shown in Figure 8. In this plot, negative current and power indicate discharge operation. The average power in the discharge cycle beginning at 2:41am is 1514W. The average power for the charge cycle from 7:38am is 1495W. This would indicate that while the VRB does, at peak, meet the nominal 2kW discharge and 2.3kW charge power ratings in the WattJoule's specification sheet, the actual continuous power rating of the device is closer to 1.5kW at the lower temperatures encountered during the testing. It should be noted, that the supplier has data indicating that the continuous

power of 2kW is achieved at nominal electrolyte temperature of 45°C irrespective of the ambient temperature. Throughout the testing period, the battery was operated with controlled maximum current and maximum voltage constraints; the resulting variation in power during cycling is a typical characteristic of any battery.

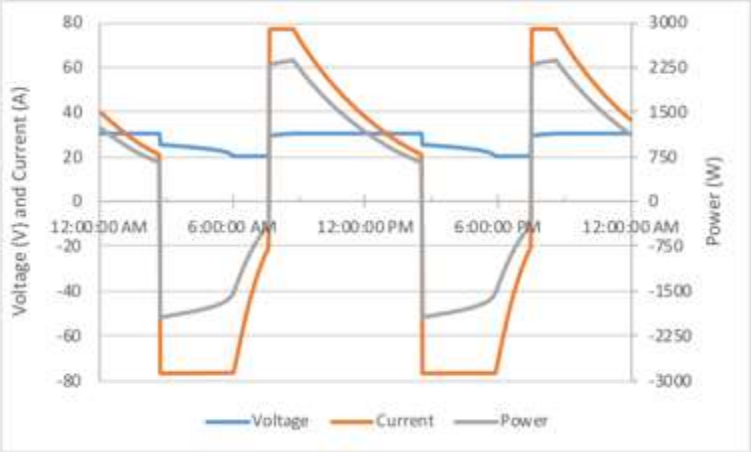

Figure 8 Voltage, Current and Power Profiles, Feb 19, 2018 (Cycle 120 begins at 7.38 am)

The data plotted in Figure 8 demonstrates the ability of the VRB to switch from charge to discharge in consecutive minutes of sampled data. This supports the "instantaneous" response time claim in the WattJoule battery specification sheet.

Analysis of this nominal operation, with a peak charge power of 2.3kW and discharge power of 2.0kW, corresponds to a nominal active cell power density of 460mW/cm^2 and 400mW/cm^2 respectively. At a current of 75A, the active cell current density is 0.3A/cm^2. From experience, such numbers are about a factor of three higher than those of a typical commercial VRB.

Beyond-Nominal Testing

In an effort to understand how performance characteristics are impacted beyond nominal conditions, the battery was operated at above nominal currents for a limited number of cycles with a mean electrolyte temperature of 26.1°C. When operating with designated charge and discharge currents of 100A and 150A respectively, the round-trip efficiency fell to 64.7%. The corresponding peak power levels were 2964W while charging and 3320W while discharging, giving peak active cell power densities of 593mW/cm^2 and 664mW/cm^2, respectively. The observed currents reached a peak charge current of 95A and discharge current of 157A, giving active cell current densities of 0.38A/cm^2 and 0.63A/cm^2, respectively.

Cold Soak Testing

In an attempt to investigate the battery performance after a period of resting, the battery was left charged on the weekend of March 17-19, 2018, as the outside temperature cooled, and the interior of the battery shed was left open to the air. The system temperatures for this period are shown in Figure 9, with the corresponding currents in Figure 10.

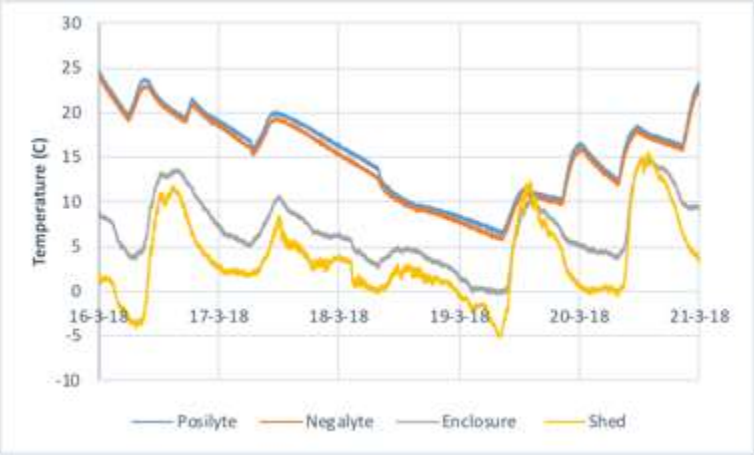

Figure 9 System Temperature for Cold Test (Battery enclosure (ambient) vs. shed temperature)

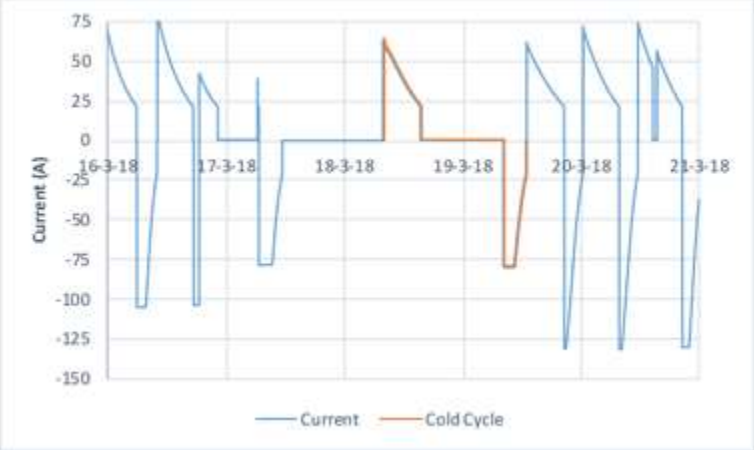

Figure 10 Currents Before, During and After Cold Test

During the cold testing, the VRB is charged from the fully discharged state when the air temperature in the shed reaches 0°C on March 18. The charge current fails to reach 75A, but the total energy into the battery is 9.4kWh during the charge. WattJoule have indicated that for future systems that are engineered for operation in cold climates, a thermal management system will not permit excursions of temperature of the electrolyte into this range.

In the morning of March 19, the ambient enclosure temperature falls to 0°C as the shed falls to -5°C so the VRB is discharged. The discharge is able to reach the designated current of 75A, and the VRB discharges 6.0kWh, a round trip efficiency of 63.9%.

It should be noted that there are occasional anomalies in the data, usually due to partial cycle operation as can be seen in Figure 10 in the afternoon of March 16 and March 20.

In April 2018, another cold cycle was scheduled. However, one of the pumps failed, and at that time a leak in one of the piping connections was discovered. At this point, cold weather testing of the ES10-2DC was halted.

Spring 2018 Testing with ES10-2DC

Investigation of the pump failure indicated an issue with third party magnetic couplings between the electrolyte pump motor and impeller. After replacement, testing of the ES10-2DC was restarted in June 2018. Unfortunately, only a limited number of cycles could be completed before gas bubbles were observed in the electrolyte. Operation of the battery was again halted while an investigation was carried out. This investigation identified a previously unencountered sub-micro-meter impurity in the electrolyte vanadium supply. The impurity was responsible for the gas production, but also caused damage to the cell stack.

The data that is available for this period is plotted in Figure 11 and Figure 12. Figure 11 shows that as the electrolyte temperature is above 20°C, the charge and discharge energies are more stable. After the first two initialization cycles, the average charging energy is 11.0kWh and the discharge energy is 8.54 kWh.

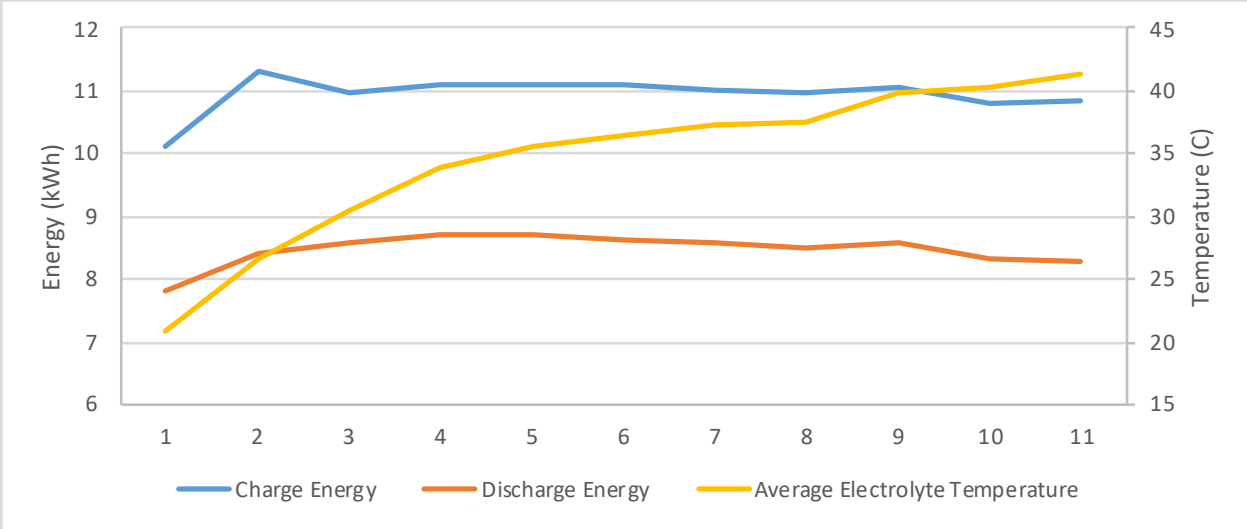

Figure 11 Charge and Discharge Energy, with Electrolyte Temperature, During Spring 2018

The round-trip efficiency by cycle is plotted in Figure 11, with an average of 77.7%, slightly below the 80% value given in the specification in Appendix A. This slight reduction in performance may be due to the impurity deposits damaging the cell stack during this phase of operation. As energy efficiency is expected to increase with temperature, which is not the case here, this is further indication of an electrolyte contamination problem. All operation during this phase was conducted at rated power and current conditions.

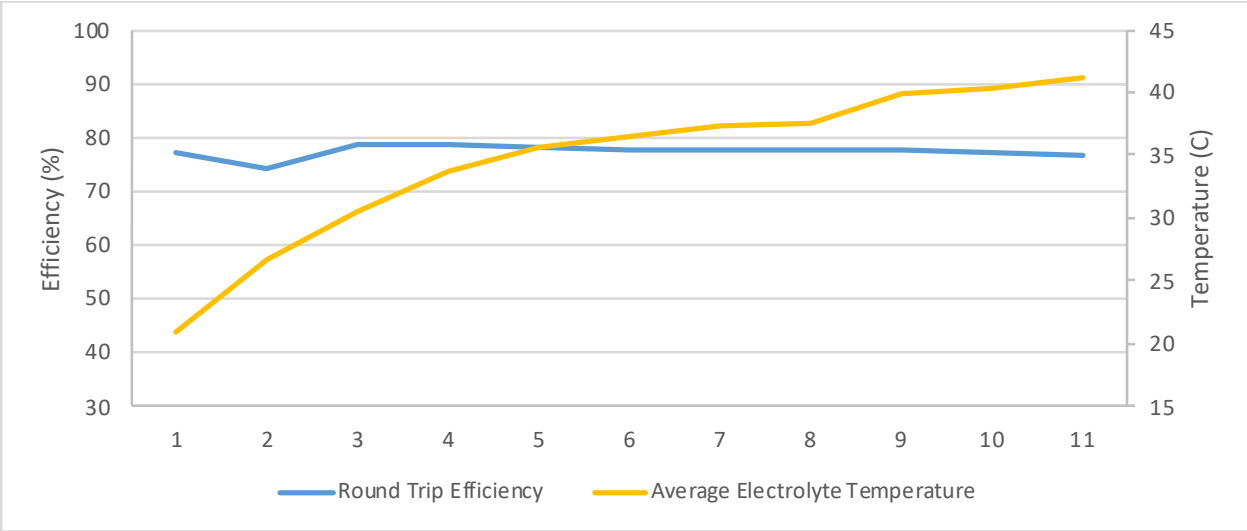

Figure 12 Round Trip Efficiency, with Electrolyte Temperature, During Spring 2018

Winter 2018/19 Testing with ES10-0.5DC

The damaged stack was replaced with a smaller stack that was readily available. The ES10-0.5DC battery is a smaller scale version of the ES10-2DC battery, where the stack is made up from only 5 cells, rather than the 20 cells in the ES10-2DC battery. The electrolyte tanks are the same, with the same volume of electrolyte. As a result, the operating current of the ES10-0.5DC is identical to the ES10-2DC, but the voltage and power are reduced by a factor of 4, while the charge and discharge time increase by a factor of 4. The time for a full charge/discharge cycle at rated current is approximately 56 hours. The power to energy capacity ratio of the ES10-0.5DC battery is 0.5 kW/10 kWh.

The extended cycle time limits the ability to test a significant number of cycles during the winter period from November 2018 to February 2019. Figure 13 plots the voltage and current as functions of time for the entire testing period for the ES10-0.5DC. One advantage of operating with a storage capacity that is now 4 times longer relative to the power rating is that it is clear that the flow battery is capable of fully discharging at rated current, if the storage capacity is large.

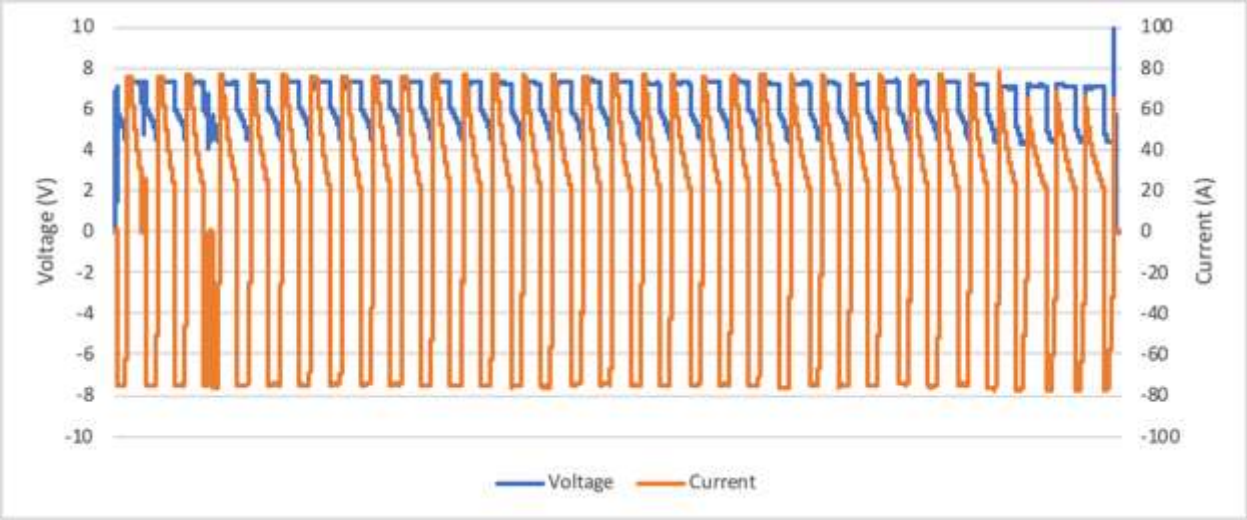

Figure 13 Voltage and Current for ES10-0.5DC Nov 30, 2018 to Feb 12, 2019.

Figure 14 plots the voltage and current for a period that approximately covers the first week of January 2019. Comparing this plot to Figure 8 the reduction in current towards the end of the discharge cycle is proportionally smaller in Figure 14

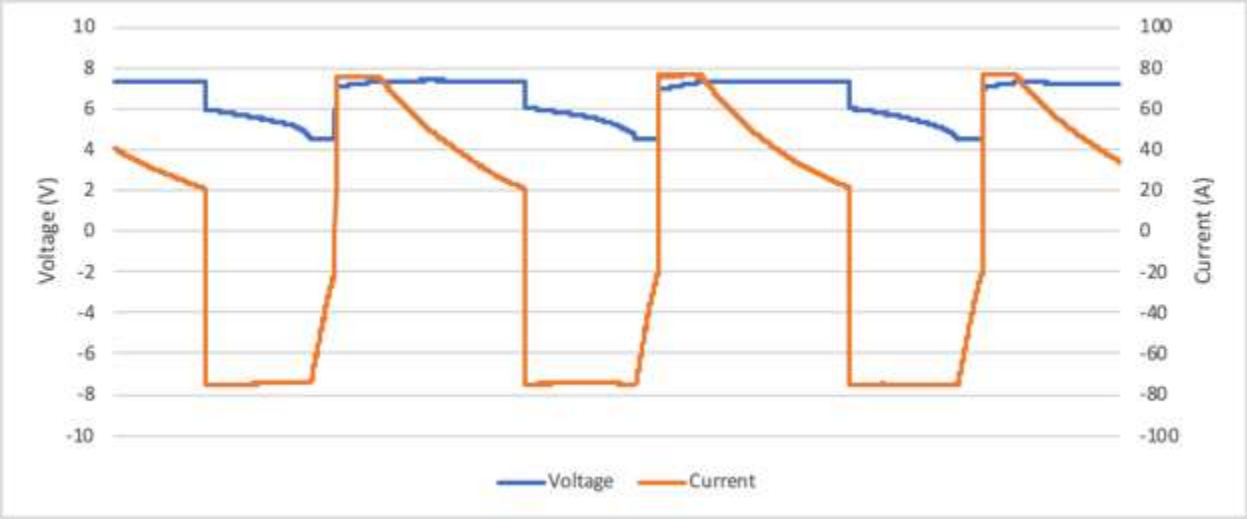

Figure 14 Voltage and Current for ES10-0.5DC Jan 1, 2018 to Jan 8, 2019.

Figure 15 plots the power flow and electrolyte temperatures for the same period as Figure 14. During the cold weather testing period at the beginning of January 2019, the weather was unseasonably warm, as can be seen from the relatively high electrolyte temperatures.

Considering the current and power densities, the peak current of 75A again corresponds to a cell current density of 0.3A/cm^2. The peak charge power of 553W corresponds to 442mW/cm^2 and the peak discharge power of 454W corresponds to 363 mW/cm^2. These numbers are consistent with previous results.

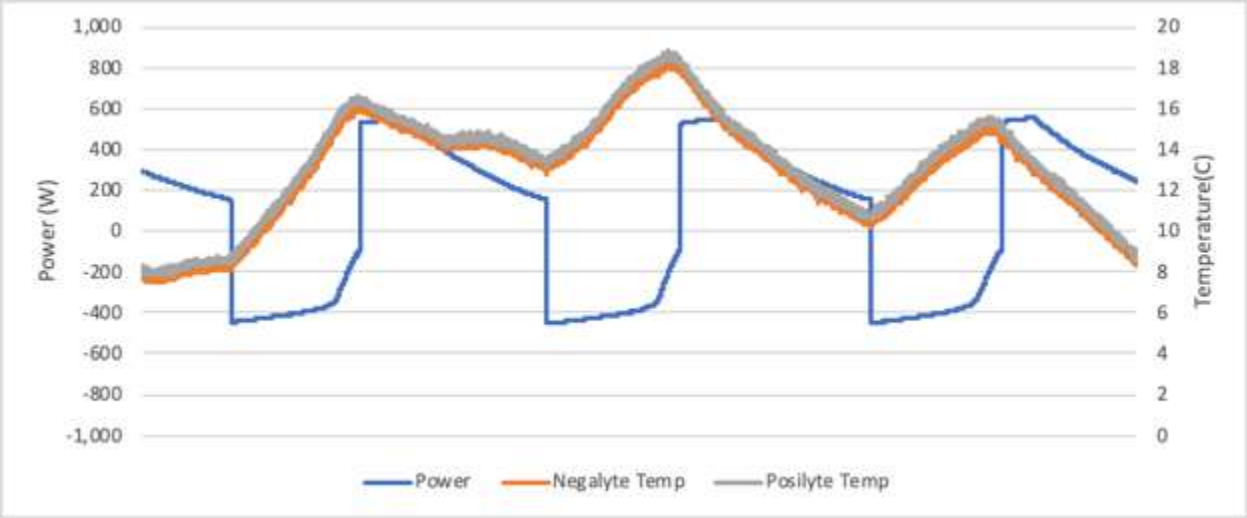

Figure 15 Power and Electrolyte Temperatures, ES10-0.5DC, Jan 1, 2018 to Jan 8, 2019.

Figure 16 and Figure 17 plot similar data for a period around Feb 4-11, 2019. During this time, the outside temperature was as much as 30°C colder than in early January, with the electrolyte temperatures dropping to as low as -6°C. By contrasting these figures with the previous two, it is clear that the peak charge current capability of the battery is substantially reduced, operating at some 50°C below the benchmark electrolyte temperature of 45°C. Interestingly, discharge current capability appears relatively unaffected in the colder period indicating the sensitivity of kinetics to temperature are different for reduction and oxidation reactions in a VRB. It is worth noting that lithium ion chemistries also exhibit a greater sensitivity to lower temperature for the charge mode.

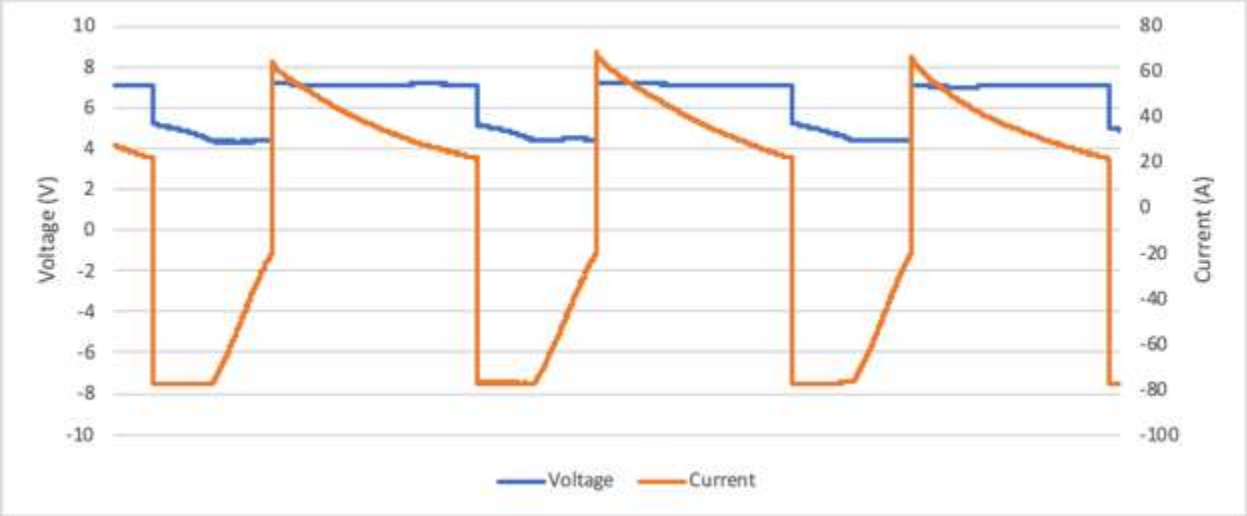

Figure 16 Voltage and Current, ES10-0.5DC, Feb 4, 2019 to Feb 11, 2019.

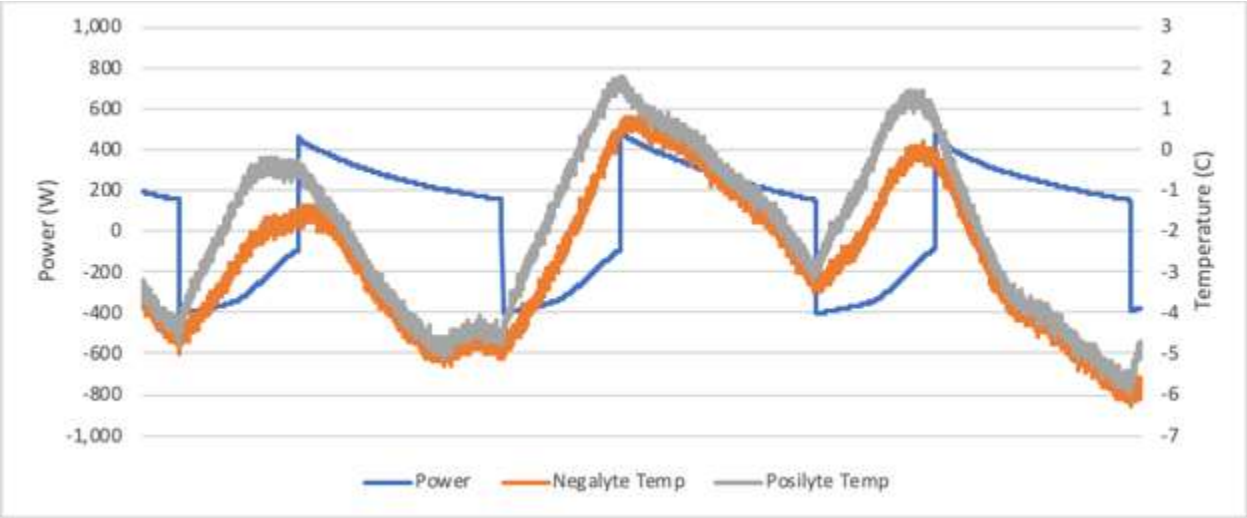

Figure 17 DC Power and Electrolyte Temperatures, ES10-0.5DC, Feb 4, 2019 to Feb 11, 2019.

Figure 18 and Figure 19 plot the Charge and Discharge Energy, Average Electrolyte Temperature over a cycle and the Round-Trip Efficiency for the ES10-0.5DC over the winter 2018/19 testing period. As with the ES10-2DC, efficiency is lower than in spring testing, and the energy capacity is substantially reduced once the electrolyte temperature falls below 10°C. Again, the manufacturer, WattJoule, has indicated that they would not normally allow operation in this temperature range.

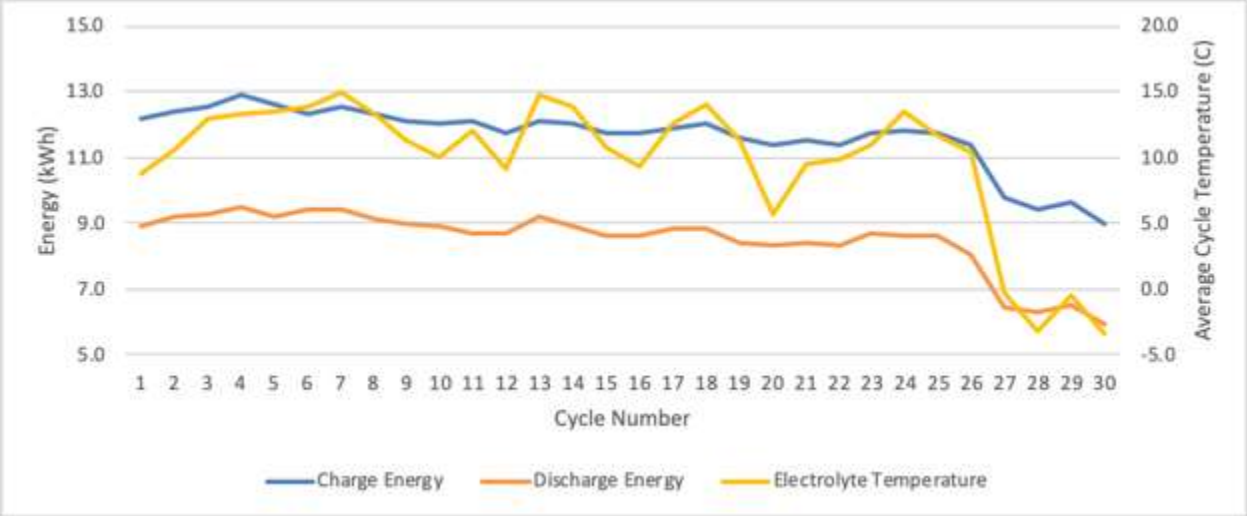

Figure 18 Charge and Discharge Energy, with Average Electrolyte Temperature, ES10-0.5DC

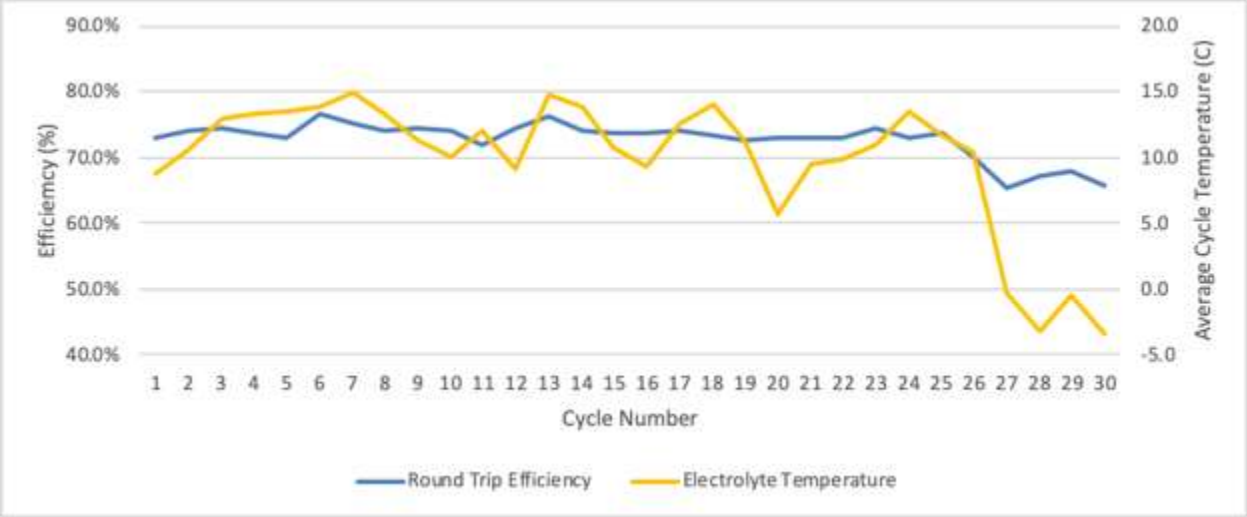

Figure 19 Round Trip Efficiency, with Average Electrolyte Temperature, ES10-0.5DC

Key Findings from Battery Testing

The objectives of the battery testing were:

1. Develop and run an accelerated benchmarking program cycle that tests performance specifications of the two battery technologies (WattJoule VRB and Tesla Powerwall 2):
    - Power capacity
    - Energy storage capacity (MWH)
    - AC round trip efficiency
    - Ramp rates
    - Limitations of frequency, timing of switching between states, and required changes in state
    - Self-discharge rate
2. Determine and report on the battery performance specifications due to:
    - Alberta ambient conditions: temperature, humidity, pressure
    - Cycle count, cycle depth, cycle frequency

Due to limitations with the installed equipment, it has not been possible to carry out any meaningful testing with the Li-Ion Tesla Powerwall 2 batteries. It has also not been possible to conduct 'accelerated' testing of the WattJoule VRB due to the large energy capacity of the cell resulting in multiple-hours cycling time.

Considering the VRB, charge and discharge power capacity is clearly scalable with the number of cells. Under normal operating conditions, the VRB is capable of operating at the nominal power rating, although we were unable to test the WattJoule specification for maximum power of 4.5kW due to capacity limitations of the testing equipment. The system was observed consistently operating at power densities over 400mW/cm^2 under non-ideal operating conditions, with sustained current density of 300mA cm^2. Peak power density obtained during testing was 664mW/cm^2 during discharge. Based on experience these values appear to be better than a typical commercial VRB by a factor of about three.

Energy storage capacity was observed to be reduced when operating significantly below the normal operating range, but otherwise, not significantly impacted during the program. The data acquisition system sampled the performance every minute, and the battery was capable of switching from charge to discharge in consecutive samples. Within the usual limitations on available energy supply, no limitations on cycle frequency or switching time were observed, however the system was not tested as a fast-acting resource (such as resources used in grid frequency regulation).

The installed system is a DC system, with round trip DC efficiency reaching a maximum observed value of 78.4% during operation at rated power at close to nominal temperature. In colder conditions the observed round-trip efficiency is closer to 74% for both the ES10-2DC and ES10-0.5DC. The efficiency falls to the low-mid 60% range when the battery was operated at either

twice the rated discharge current or with electrolyte temperature below 0°C. However, it should be stressed that the battery can still operate with electrolyte temperatures in this range.

Table 1 below provides a summary of the objectives and the results achieved.

Table 1 - VRB Summary of Results

Objective	**Result**
Power Capacity	Independently scalable from energy capacity. Depends on number of cells in power stack configuration and active area of power stack cells/number of power stacks in parallel. A peak active cell discharge current density of up to 437mA/cm^2 was observed in cold soak conditions. According to the WattJoule datasheet peak power, known cell voltage 1.52V, cell count and active electrode surface area, the peak value could be as high as 579mA/cm^2.
Energy Storage Capacity	Independently scalable from power capacity. Depends on tank size and electrolyte volume. 400 liters of electrolyte provided 10kWh of energy storage or 25Wh/l.
AC round trip efficiency	DC round trip efficiencies up to 78.4% was observed close to nominal conditions however did not cross the 80% value from the battery datasheet. The observed value occurred during an electrolyte contamination issue which may be the cause of the difference.
Ramp rates	Full power reversal is < 1min according to data collection sampling rate.
Limitations of frequency, timing of switching between states, and required changes in state	None found
Self-discharge rate	Not measured. Auxiliary systems such as pumps can power down to avoid self-discharge.
Effects of Alberta climate conditions	Charge mode power capacity and round-trip efficiency reduces for colder electrolyte temperatures which can be mitigated with basic climate controls.
Degradation effects	No degradation effects were observed from cycling

Metal Removal Technique Testing Objective

The metal content of oil affects the processing options available to refiners and low metal content is always preferred in a refining context. The presence of metals is undesirable, mainly because they cause poisoning and deactivation of the catalysts used in the refining processes. The non-volatile metal contaminants tend to accumulate during cracking and eventually get deposited on the catalyst. This causes decrease in catalyst surface area by plugging their pores, thereby rendering them inactive. A baseline approach to dealing with this problem is a costly recycle of spent catalysts Metals also promote dehydrogenation reactions during the cracking sequence, which results in an increase in the production of coke and decrease in gasoline production. Additionally, high amount of metals in crude oil makes production costly by increasing the amount of hydrogen needed for the process and by increasing yield loss due to carbon rejection.

The most abundant and troublesome metal complexes in oil are vanadium and nickel, which are known to occur naturally as vanadyl (IV)- and nickel (II)- porphyrins. Metalloporphyrins are believed to associate strongly with molecules in the asphaltene solubility fraction to form "bound"-type metalloporphyrins. Several heavy oils (including Canadian oilsands derived bitumen) have a combined Ni and V content of the order 200–300 µg/g raw bitumen. Over many decades, the removal of Ni and V from oil attracted attention. Selective metals removal is not only beneficial to refining, but also a potential source of Ni and V for removal as metal products.

The technical objectives of the metal removal component of the project were:

- Determine the feasibility of ionic liquids technique for nuisance metals removal, such as V, Ni, Ca, Fe, Zr, Ti from Alberta Oil Sands product streams. The objective is to improve the Scotford Upgrader process economics by preventing fouling in catalysts.
- The following performance data will be developed for the above feasibility analysis:
    - The ratio of ionic liquid to product feedstock
    - Cost of ionic liquid regeneration
    - Concentration of oil in ionic liquid or ionic liquid in oil after one separation
    - Percentage of metal removal from oil
    - Reaction conditions
    - Estimated cost of ionic liquid production on a per unit basis
    - Normalized capital cost estimate of an industrial scale metals extraction system
    - Capital cost estimate of a pilot system
- If the ionic liquids technique is feasible, determine the feasibility of converting vanadium removed from the Alberta Oil Sands into a locally sourced electrolyte for vanadium redox flow batteries. The objective is a step toward:
    - Creating a "made-in-Alberta" solution that has the potential to be an international export opportunity in the clean technology sector;
    - Potentially creating incentives for other oil sands companies to remove a high priority (Environment Canada) toxic metal compound from the environment (vanadium pentoxide from fly ash).

Methodology

Building off work completed by Shell and Imperial College London, the U of A was tasked with completing the objectives of the metals removal component of the project. The U of A completed the following key tasks:

- A literature review to establish a method for determining the metal content in the bitumen samples and assessing the removal options for vanadium (V) and nickel (Ni);
- Establishing a method for the analysis of V and Ni;
- Characterizing the raw material, and
- recovering metal from bitumen and dilbit samples.

In the end, U of A expanded the original metals removal technique from just ionic liquids extraction to also include photochemical separation and electrochemical separation. The U of A final report is attached in Appendix C with an overview of each investigated method and major findings given in following sections.

Ionic Liquid (IL) Assisted Extraction of Metals

A range of ILs were selected to determine which cationic and anionic components of ILs are effective in the extraction of V and Ni from dilbit samples. Specific to the structures, the imidazolium-based cations contain a delocalized charged ring whereas the ammonium-based cations provide a charged atom. The anion will play the key part in chelation to the metal center, therefore the effect of anions was monitored while imidazolium-based cation was the same for most of the employed ionic liquids. The anions in this study were employed for several reasons in addition to being thought of as suitable candidates to coordinate the metals.

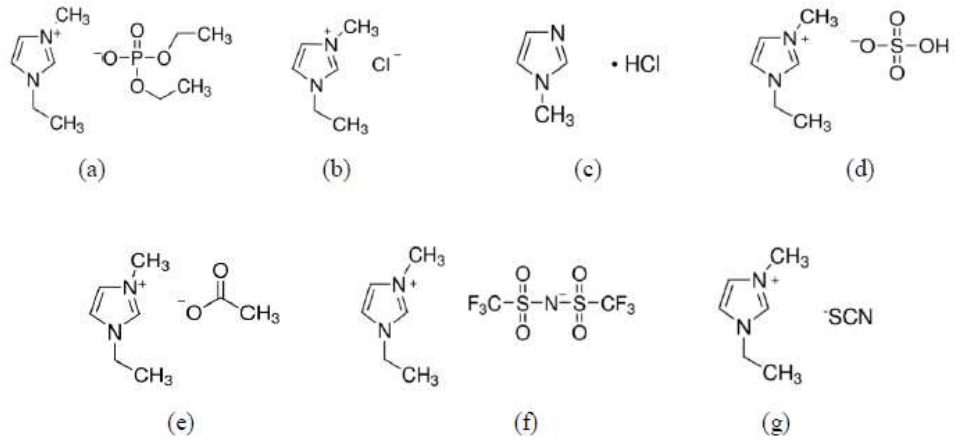

Figure 20 - Chemical Structure of various ionic liquids of interest (a) 1-Ethyl-3-methyl-imidazolium diethyl phosphate (EMIM-DEP) (b) 1-Ethyl-3-methylimidazolium chloride (c) 1-Methylimidazolium chloride (d) 1-Ethyl-3-methylimidazolium hydrogen sulfate (e) 1-Ethyl-3-methylimidazolium acetate (f) 1-Ethyl-3-methylimidazolium bis(trifluoromethylsulfonyl) imide (g) 1-Ethyl-3-methylimidazolium thiocyanate

Photo-irradiation Assisted Extraction for Demetallization of Dilbit Samples

In photochemical separation, a combination of photochemical reaction and liquid-liquid extraction is employed to recover vanadium and nickel from bitumen. In this process, the bound-type metalloporphyrins are postulated to photodissociate in presence of a hydrogen donor solvent to convert 'bound' into 'free' type metalloporphyrins. The resulting solution is photodecomposition by UV irradiation to release the metal ions into solution, which can be selectively removed by solvent extraction. To examine the photoreactivity of vanadyl(IV)tetraphenyllporphyrin (VOTPP), a model compound, the tetralin solution containing VOTPP was photoirradiated under air bubbling in the absence of an aqueous phase.

Electrochemical Demetallization of Dilbit samples

Electrochemical separation is based on the similar hypothesis as photochemical assisted extraction process. An electrochemical treatment is followed by liquid-liquid extraction. The bitumen is subjected to electrochemical treatment to displace the metal ions in the metalloporphyrins. The released metal ions can then be extracted by employing a liquid-liquid extraction process.

Experiments were carried out in the presence of inert atmosphere. A three-electrode electrochemical cell was used, and electrolysis was carried out at room temperature for 24 hours, under magnetic stirring. Solid residue was obtained in the bottom of the flask as well as on anode at the end of the reaction. Toluene was added to wash the solid residue and then, the residue was separated by filtration. The remaining solvent was removed in rotary evaporator under vacuum and the resultant product were analyzed for nickel and vanadium content using ICP-OES.

Results & Discussion

Ionic Liquid Assisted Extraction of Metals

Table 2 lists the noted major observation during/after the experiments using different ionic liquids. Specific details of selecting ionic liquids are below:

Table 2 - Observation for various Ionic Liquid of interest (Initial meta concentration in Suncor dilbit samples V:166.06 µg/g, Ni: 65.006 µg/g; Reaction Temp: 50°C, Reaction time: 1h, Settling time: 4h, Ratio of ILs to dilbit ratio =1:1, stirring speed: 550rpm)

S. No.	Ionic Liquids	% Recovery	Selectivity	Remarks	ICL Results
1	Dimethlyammonium dimethyl-carbamate (DIMCARB)	13.8 ± 0.5%V, 9.4 ± 1.0 % Ni	Non-Selective	Clear biphasic layer separation	13.3% V, 4.3% Ni
2	1-Ethyl-3-methyl-imidazolium bis-(trifluoromethylsulfonyl) imide (EMIMim)	0.3 ± 0.04%V, 2.3 ± 0.16%Ni	Non-Selective	Longer settling time and higher temperature (100C) is required to attain V/Ni extraction. Clear biphasic separation was not visible.	40% V, 36% Ni
3	1-methyl imidazolium chloride [HC1im]Cl + 10% H_2O	1.6 ± 0.7 %V, 6.1± 0.1 %Ni	Selective	ILs froze as soon as the vial was taken out from the oil bath at 80C reaction temp. Therefore, further experiments were conducted with 10% H2O.	45.8% V, 43.8%Ni
4	1-Ethyl-3-methyl-imidazolium chloride (EMIC) +10% H_2O	2.8 ± 0.9 %V, 5.2 ± 0.1 %Ni			-
5	1-Ethyl-3-methyl-imidazolium diethyl phosphate (EMIM-DEP)	7.0 ± 1.4 %V, 6.0 ± 0.8 %Ni	Non-Selective	Clear biphasic separation at higher temperature (80C).	-
6	1-Ethyl-3-methyl-imidazolium hydrogen sulfate	0.02 ± 0.01 %V, 0.1 ± 0.01 %Ni	-	Not suitable for metal extraction. <1% V and Ni were extracted.	-
7	1-Ethyl-3-methyl-imidazolium acetate (EMIM Ac)	-	-	No biphasic layer separation.	-
8	1-ethyl-3-methyl imidazolium thiocyanate (EMIM-SCN)	4.1 ± 0.1 % V, 1.5 ± 0.1 % Ni	Selective	Clear biphasic layer separation.	-

Multistage Extraction

Only some of the ILs were selective for metal extraction without co-extracting oil. In those instances where the extraction was not selective, the metals were co-extracted with oil.

It was observed that variation of stirring speed could not show any noticeable increase in metal extraction. This observation indicated that the ionic liquid assisted extraction was not a mass transfer limited process over the extraction periods investigated. Therefore the possibility of multistage extraction process was investigated using Athabasca dilbit samples. The table below illustrates the data for vanadium and nickel extraction from Athabasca/Cold Lake dilbit samples using DIMCARB and EMIM-SCN ionic liquid.

Results illustrated in Table 3 below indicate the possibility of multi-stage extraction process. By employing three equilibrium stages, the overall vanadium extraction was increased from around 4% to 12% and 10% to 19% using EMIM-SCN and DIMCARB respectively.

Table 3 - Multi-stage extraction of metal (Reaction conditions: Initial metal concentration in Suncor dilbit samples V:166.06 µg/g, Ni: 65.006 µg/g; Reaction Temp: 50°C, Reaction time: 1 h, Settling time: 4 h, Ratio of ILs to dilbit ratio =1:1, stirring speed: 550rpm

Sample	Ionic Liquid	Stage	Initial Metal Content (ppm)		Metal recovery (ppm)		% Metal recovery	
			V	Ni	V	Ni	V	Ni
Suncor Dilbit	EMIM-thiocyanate	I	166.1	65.0	6.1 ± 0.1	1.0 ± 0.1	4.1 ± 0.1	1.5 ± 0.1
Dilbit recovered from Stage I		II	160.0	64.0	7.7 ± 0.5	2.2 ± 0.4	4.8 ± 0.2	3.4 ± 0.1
Dilbit recovered from Stage II		III	152.3	61.8	5.5 ± 0.3	1.1 ± 0.3	4.7 ± 0.2	3.3 ± 0.7
Overall Recovery							11.6 ± 0.3	6.6 ± 0.2
Suncor Dilbit	DIMCARB	I	166.1	65.0	16.7 ± 0.3	4.3 ± 0.09	10.1 ± 0.2	6.6 ± 0.1
Dilbit recovered from Stage I		II	149.3	60.7	12.4 ± 0.2	3.6 ± 0.1	8.3 ± 0.3	5.9 ± 0.2
Dilbit recovered from Stage II		III	138.9	57.1	3.0 ± 0.8	1.8 ± 0.6	2.2 ± 0.5	3.1 ± 0.8
Overall Recovery							19.4 ± 0.6	14.9 ± 0.4

Effect of diluent (Naphthenic vs paraffinic) on V/Ni extraction

None of the selected ionic liquids showed a satisfactory extraction efficiency. It was suspected that naphthenic diluent may pose a negative effect on the chemistry of Vanadium metals with ionic liquids. To replicate the results reported in Imperial College London Benchtest report (

Appendix D –Benchtest Report) and to investigate the effect of diluent, experiments were designed based on commercial parameters. Experiments were performed in the similar manner as mentioned before. Four different ionic liquids were employed in this study and results are reported in Table 4 below.

Table 4 - Effect of diluent on metal reduction from diblit samples (Initial metal concentration in samples prepared using paraffinic diluent - V: 168.73 µg/g, Ni: 64.87 µg/g; samples prepared using napthenic diluent - V:166.06 µg/g, Ni: 65.006 µg/g)

Sample	Ionic Liquid	V (%)			Ni (%)		
		C5/C6 diluent	Napthenic diluent[2]	ICL results (Albian dilbit)[3]	C5/C6 diluent	Napthenic diluent	ICL results (Albian dilbit)
Athabasca	DIMCARB	7.9 ± 0.9	13.8 ± 0.5	13.33	6.1 ± 0.4	9.3 ± 1.0	4.35
	EMIM-Phos	2.3 ± 0.3	19.5 ± 0.3	-	1.4 ± 0.4	11.2 ± 0.5	-
	EMIM-NTf_2	2.9 ±0.6	2.7 ± 0.9	40	0.6 ± 0.1	0.9 ± 0.0	36
	[HC1m-Cl]	0.07 ± 0.02	6.4 ± 0.4	45.83	0.9 ± 0.1	7.1 ± 0.01	43.89
Cold Lake	DIMCARB	1.02 ± 0.05	15.3 ± 0.8		1.6 ± 0.4	13.3 ± 0.1	
	EMIM-Phos	2.5 ± 0.5	20.5 ± 1.0		5.9 ± 0.3	16.3 ± 0.8	
	EMIM-NTf_2	2.7 ± 0.3	8.1 ± 0.2		1.4 ± 0.06	4.9 ± 0.04	
	[HC1m-Cl]	0.01 ± 0.003	5.9 ± 0.2		1.3 ± 0.08	7.9 ± 0.1	

[2] Reaction conditions: diluent addition: 30%; ionic liquid to dilbit ratio: 1:1; reaction temp: 50°C; reaction time: 1 h; settling time: overnight (approx. 14 h); stirring speed: 550 rpm; centrifugation time: 10 min; centrifugation speed: 5000rpm

[3] All the ICL results have been reported at reaction temp: 50°C, ratio of IL to dilbit: 1:1, reaction time : 1 h, settling time: overnight).

Contrary to the expected results, extraction efficiency was even lesser in case of paraffinic diluent than that of naphthenic diluent. The reason behind this observation was not determined.

Metal extraction using ionic liquids from partially deasphalted oil (DAO) samples

To obtain a sample which should match the properties of Albian dilbit samples, it was suggested to work on the partially DAO samples. Rigorous stirring was provided for one hour and then the solution was kept in the dark for 24 hours. After 24 hours, the solution was filtered with the aid of a vacuum filter and the filtrate was collected. This filtrate was stored in an airtight container for further use in extraction experiments. Experiments were performed in triplicates in the similar manner as described in Appendix B, Section 5.1.1.

Table 5 = (%) metal reduction from Deasphalted oil (DAO) samples using Ionic liquids (a) 1-methyl immidazolium chloride ([HC1im]Cl+10% H2O) and (b) 1-ethyl 3-methyl immidazolium diethyl phosphate (EMIM-DEP) - Reaction conditions: ionic liquid to DAO ratio: 1:1*

Ionic Liquid	Initial Metal Content (µg/g)		Metal recovery in ILs Phase (µg/g)		(%) Metal Recovery	
	V	Ni	V	Ni	V	Ni
EMIM-DEP	112.2	63.1	9.7 ± 0.8	4.5 ± 0.04	8.7 ± 0.15	7.2 ± 0.6
[HC1im]Cl + 10%H_2O			1.4 ± 0.1	24.3 ± 2.3	1.24 ± 0.02	38.5 ± 2.1

Performance investigation of Acid saturated ILs

Although vanadium removal is still an unresolved issue in the process of ionic liquid assisted metal extraction, the ionic liquid 1-methyl immidazolium chloride ([HC1im]Cl+10% H2O) showed nearly 40% extraction of Ni from partially DAO samples. Based on the hypothesis that porphyrins are prone to successive hydrogenation of the porphyrin leading to a chlorin metal structure and, finally, the demetallization is accomplished via the ring fragmentation, further investigation were carried out in excess of H+ ion to accelerate the reactions at the olefin groups on the outer ring of the porphyrin. Figure 21 demonstrates the metal extraction at different molar HCL concentrations.

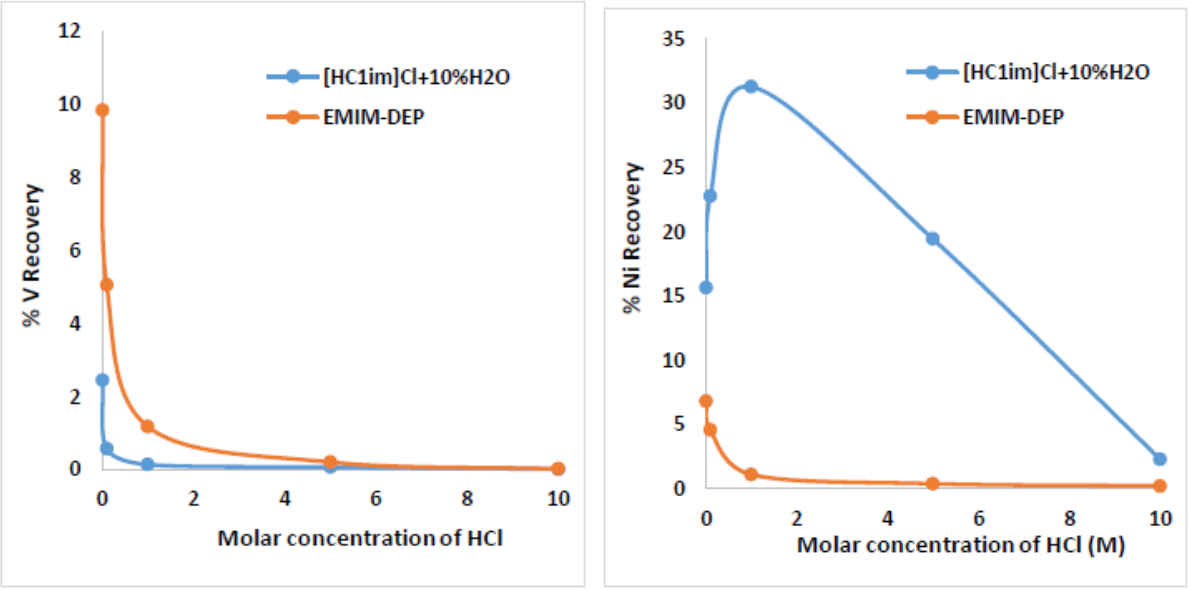

Figure 21 - (%) V and (%) Ni Reduction from Bitumen using HCl Saturated Ionic lIquids 1-methyl immidazolium chloride ([HC1im]Cl+10% H2O) and 1-ethyl 3-methyl immidazolium diethyl phosphate (EMIM-DEP)

It was observed that the presence of acidic sites substantially affects the reduction of nickel, however, no improvement was observed in the reduction of Vanadium. It may be related with

charge density. Volume of Vanadyl ion is much higher than its charge and therefore due to less concentrated charge density, less extraction may be achieved.

Ionic Liquid Assisted Extraction Using Albian Dilbit Samples

Ionic Liquid assisted metal extraction experiments were performed using Albian Dilbit samples. Four ionic liquids namely DIMCARB, EMIM-NTF2, HC1imCl+10%H2O and EMIM-SCN were chosen based on their performance with Athabasca dilbit samples.

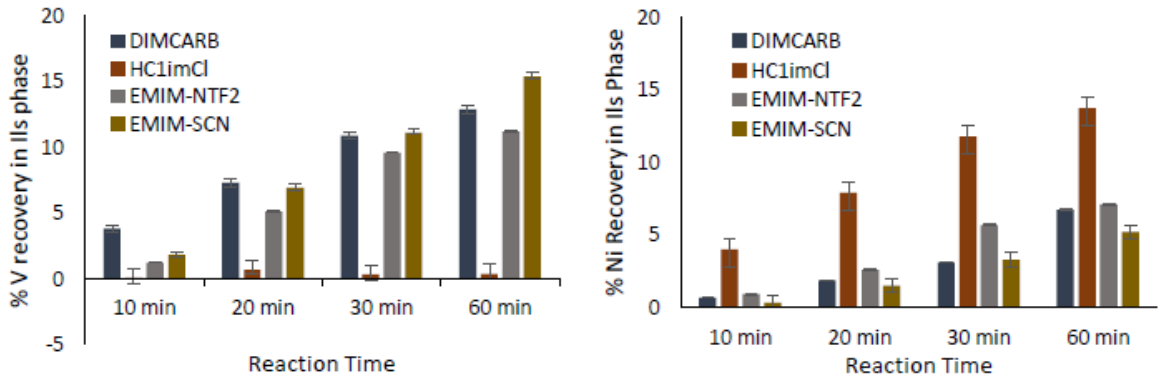

Figure 22 - Effect of reaction time on metal extraction from Albial dilbit sample (Metal content in dilbit sample V = 143 ± 5.8 µg/g; Ni = 59.7± 2.3 µg/g; Reaction conditions: ionic liquid to dilbit ratio: 1:1 (w/w); reaction temp: 50°C; settling time: 4 h; stirring speed: 550 rpm; centrifugation time: 10 min; centrifugation speed: 5000rpm)

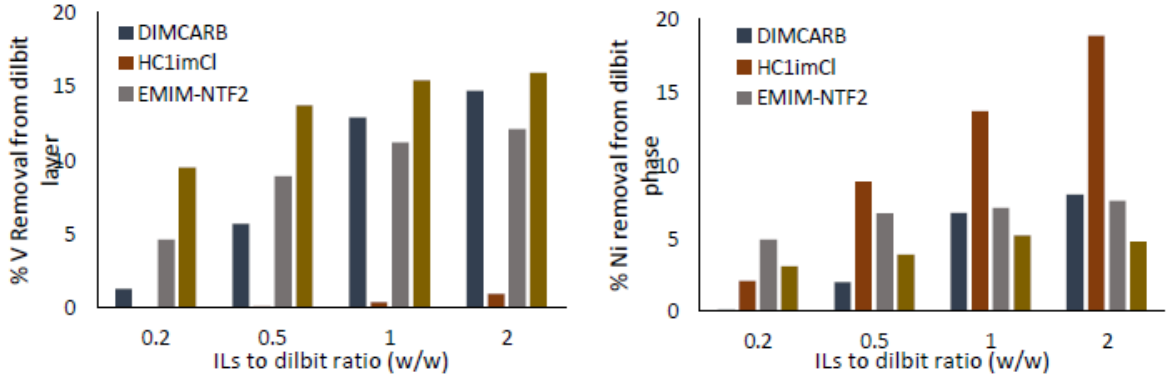

Figure 23 - Effect of reaction time on metal extraction from Albial dilbit sample (Metal content in dilbit sample V = 143 ± 5.8 µg/g; Ni = 59.7± 2.3 µg/g; Reaction conditions: reaction temp: 50°C; reaction time : 1 h; settling time: 4 h; stirring speed: 550 rpm; centrifugation time: 10 min; centrifugation speed: 5000rpm)

Further experiments were conducted to ensure the possibility of multi-stage extraction process using Albian dilbit samples. Three cycles of experiments were performed using the same dilbit sample during all cycles, while fresh ionic liquid was used in each cycle. Results indicated the possibility of multistage extraction process. Figure 24 illustrates the data for vanadium and nickel extraction from Albian dilbit samples using DIMCARB and EMIM-SCN ionic liquid.

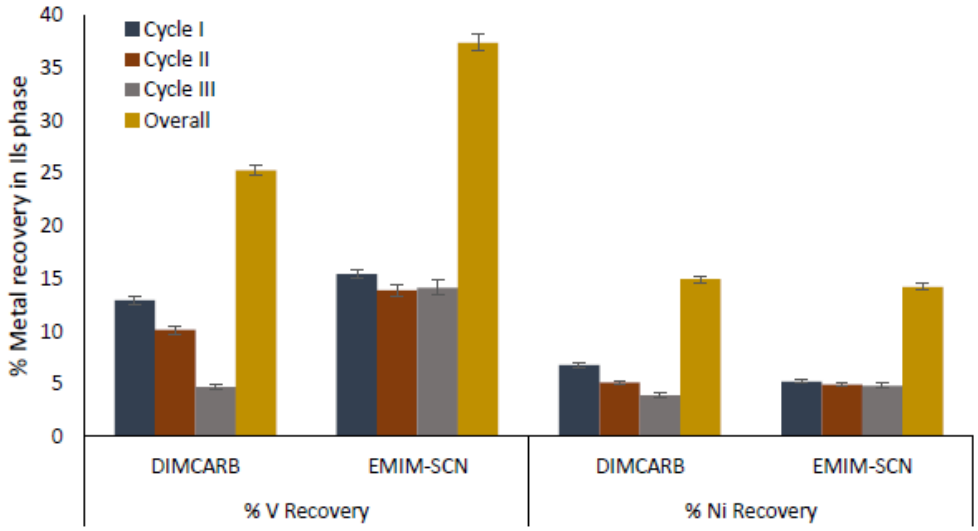

Figure 24 - Multi-stage extraction of metal (Reaction conditions: Initial metal concentration in Albian dilbit samples 143 ± 5.8 µg/g; Ni = 59.7± 2.3 µg/g; Reaction Temp: 50°C, Reaction time: 1h, Settling time: 4h, Ratio of ILs to dilbit ratio =1:1, stirring speed: 550rpm)

Key findings for Ionic Liquid Assisted Extraction

Major findings of the illustrated ionic liquid assisted extraction process are listed below:

i. None of the ionic liquid demonstrated a significant V/Ni extraction in a single stage extraction. Though, out of the all investigated ionic liquids, Dimethlyammonium dimethyl-carbamate (DIMCARB) showed highest extraction of metals from dilbit samples.

ii. Along with the extraction of metals, selectivity of ionic liquids for oil extraction was also considered as a deciding factor. Selectivity of various ionic liquid was investigated by performing Simulated Distillation analysis of organic and ionic liquid phases. Dimethlyammonium dimethyl-carbamate, inspite of showing the considerable metal extraction, was observed to be a non-selective ionic liquid. Significant amount of organic content was detected in ionic liquid phase.

iii. On the contrary, 1-ethyl-3-methyl imidazolium thiocyanate (EMIM-SCN) and 1-methyl imidazolium chloride ([HC1im]Cl+10% H2O) were observed to be selective. No evidence was found that oil was observed in the extracted ionic liquid phase. However, the extraction efficiency for single equilibrium stage extraction was less than 10% for these ionic liquids.

iv. Efforts were also made to optimize the process parameters. Reaction parameters were optimized by varying the reaction temperature, ratio of dilbit to ionic liquid, reaction time, settling time, stirring speed. Variation of stirring speed could not show any noticeable increase in metal extraction with the increase in stirring speed. This observation indicated that the ionic liquid assisted extraction was not a mass transfer limited process over the extraction periods investigated.

v. Possibility of multi-stage extraction process was investigated. 1-ethyl-3-methyl imidazolium thiocyanate (EMIM-SCN) was chosen to study the multistage extraction, considering its high selectivity (i.e. little or no oil co-extraction with the metals). Three cycles of experiments were performed using the Athabasca bitumen/Albian dilbit sample during all cycles, while fresh ionic liquid was used in each cycle. Results indicate the possibility of a multi-stage extraction process. By employing three equilibrium stages, the overall vanadium extraction was increased from around 4% to 12% (Table 9) in case of Athabasca bitumen whereas in Albian dilbit sample, vanadium extraction was increased from 15% to 38%.

In conclusion, it was found that some of the ionic liquids were selective for the extraction of the metals in the presence of little or no oil. It was further found that for the selective ionic liquid that was further evaluated (EMIM-SCN), the extraction was an equilibrium limited extraction. It was therefore possible to increase extraction by employing more than one equilibrium stage.

Photo-irradiation Assisted Extraction for Demetallization of Dilbit Samples

The overview of results for this phase of the project are summarized in Table 6.

Table 6 - Demetallization of dilbit samples using photo irradiation assisted extraction process

Sample	Initial V conc. [mg/kg]	Initial Ni conc. [mg/kg]	Final V conc. in aqueous phase [mg/kg]	V removal [wt%]*	Final Ni conc. [mg/kg]	% Ni removal
1 hour irradiation - Model compound (VOTPP)	15	NA	0.74	9.9	NA	NA
4 hours irradiation - Model compound (VOTPP)	15	NA	4.3	57.3	NA	NA
6 hours irradiation - Bitumen/HCl extraction	228	93	0.02	0.1	0.13	1.4
6 hours irradiation - Bitumen/HCl extraction	228	93	0.01	0.0	0	0

* Removal based on the determined concentration in the IL.
NA = Not applicable because the model compound tested contained only V.

In conclusion, photo-irradiation assisted extraction cannot be used on dark samples, since most of the light is absorbed by the bulk medium. However, the work showed that this technique may have some value in removing metals from less-opaque products. Therefore, it was decided to assess a different methodology of assisted extraction via electrochemistry.

Electrochemical Demetallization of Dilbit samples

For this technique a 69.4% vanadium removal rate was inferred from emission signals in ICP-OES for a model compound. An actual dilbit sample from Albian yielded 35.4% removal. Results are summarized in Table 7.

Table 7 - Demetallization of dilbit samples using Electrochemical assisted extraction process

Sample	Initial V conc. [µg/g]	Initial Ni conc. [µg/g]	Final V conc. in dilbit sample [µg/g]	V removal [wt%][a]	Final Ni conc. [µg/g]	% Ni removal	Residue collected (g)
6 hour electrolysis - Model compound (VOTPP)	25	NA	12.2	51.1	NA[b]	NA	nd[c]
24 hours electrolysis - Model compound (VOTPP)	25	NA	7.6	69.4	NA	NA	0.74 ± 0.1
24 hours electrolysis – Athabasca Dilbit + 10% Methanol-THF solution	166	65	136.9±3.8	17.5± 1.2	61.9 ± 1.1	4.7 ± 0.41	0.31± 0.04
24 hours electrolysis- Athabasca Dilbit + 20% Methanol-THF solution	166	65	126.5 ± 5.1	23.8 ± 3.5	61.7 ± 2.3	5.1±0.87	0.49 ± 0.13
24 hours electrolysis – Albian Dilbit + 10% Methanol-THF solution	143	59.7	103.5	27.6	54.9	8.0	nd
24 hours electrolysis- Albian Dilbit + 20% Methanol-THF solution	143	59.7	92.3 ± 6.9	35.4 ± 4.1	54.7 ± 4.8	8.3 ± 0.6	0.08 ± 0.0

[a]Removal based on the determined concentration in the dilbit layer.

[b]NA = Not applicable because the model compound tested contained only V.

[c]nd = not determined.

In conclusion, it was possible to remove the metals from dilbit by electrochemical metal removal. This phase is the least developed of the techniques investigated but proves promising; work on this method commenced only during late stages of the project.

Conclusions

The research objectives of the project were two-fold: (1) Learn the performance specifications of Vanadium Redox Battery (VRB) technology and benchmark against lithium-ion (Li-ion) in Alberta conditions in the context of renewable energy applications and (2) Test metal removal techniques on oil sands bitumen for the efficient removal of vanadium and potentially other nuisance metals such as nickel. For objective 1, VRB technology is found to be a feasible option for Alberta conditions but basic care must be taken upfront to ensure chemical and mechanical reliability in the design of a commercial plant. For objective 2, it is possible to reduce vanadium and nickel from Alberta Bitumen but no clear preferred technique for doing so has emerged at this point.

For objective 1, the battery electrolyte tested is chemically robust in low temperatures with no sign of crystallization or irreversible performance degradation issues over the period tested. In a stress-test, the battery was able to be charged at negative electrolyte temperatures with limited power derating and reduced efficiency. In this area the VRB appears to signal a possible advantage over commercial lithium ion chemistries which are known to risk permanent damage if charged below freezing. Further work would be needed to validate VRB resiliency in these conditions over longer periods of time. In other areas, the power density of the WattJoule VRB stack impressed. Power density is an area where VRBs are currently economically outclassed by lithium ion batteries. The power stacks of VRBs require large quantities of material and hydraulic integration to achieve active electrode surface areas that rival power output of inherently integrated cells of lithium ion batteries. Elsewhere, energy density is an area where VRB remains unimpressive compared to lithium ion. The issue here is that the cell potential of vanadium is much lower than lithium and that vanadium solubility in the current generation of electrolytes is limited. For the foreseeable future VRBs are expected to remain relegated exclusively to stationary applications such as renewable energy integration into the grid.

For objective 2, the U of A work raises new questions and recommendations for next steps which involve further exploration of ionic liquids and electrochemical extraction. The report screens out photo irradiation as a technique on the basis of bitumen being dark preventing significant penetration of light energy. However, although dark samples indicate an opaqueness to the visible range of the electromagnetic radiation spectrum, it does not offer conclusions about wavelengths for which bitumen may be transparent nor variation in radiation intensity.

Appendix A – WattJoule Flow Battery Specifications

		ES10 Product Datasheet		
1	**Document Control**			
	Product Model Number	**ES10-3.5DC (48V version)**	**ES10-2DC (24V version)**	**ES10--0.5DC (6V version)**
	Document Version Number	V1.4		
	Last Revision Date	2018-11-06		
2	**Electrical Performance (at 45C electrolyte temperature)**			
	Energy Storage Capacity at full discharge with full tank capacity	10 kWh	10 kWh	10 kWh
	Nominal DC Voltage	48VDC	24VDC	6VDC
	DC Voltage Range, Discharge	37 - 56.2 V	20 - 30.4 V	5 - 7.6 V
	DC Power Output, Nominal	3.5 kW, at 75 A	1.9 kW, at 75 A	0.5 kW, at 75 A
	DC Power Output, Max	8.5kW at 190A	4.5kW at 190A	1.1kW at 190A
	DC Voltage Range, Charge	44.2 - 57.4 V	23.9 - 31 V	6.0 - 7.8 V
	DC Power Input, Max (with recommended profile)	4.3 kW, at 75 A	2.3 kW, at 75 A	0.6 kW, at 75 A
	DC Round-Trip Efficiency @ 3 kW discharge, constant power and recommended profile	>80%		
	Response Time, Charge to Discharge and vice versa	Instantaneous		
3	**Physical & Environmental**			
	Ambient Operating Temperature for Beta 1 Unit	+10 to +35˚C		
	Ambient Operating Temperature with Environmental Control	-20 to +50˚C		
	Footprint	1.44 (W) x 0.72 (D) m		
	Height	1.35 m		
	Weight without Electrolyte	160 kg	150 kg	140 kg
	Weight with 400 Liters of Electrolyte	760 kg	750 kg	740 kg
	Maximum Allowable Site Pad Level Tilt	<10 mm over footprint		
4	**System Lifetime & Service**			
	Calendar Life	20 Years		
	Cycle Life	10,000 Cycles		
	Preventive Maintenance Interval (replace air filters & system check)	1 Year		
	Pump & Stack Service Interval	5 Years		
5	**Safety Compliance & Ratings**			
	Energy Storage System Safety: UL 9540	Designed to be compliant		
	Telecom DC Power & Safety: ETS300 132-2 & NEBS-GR78	Designed to be compliant		
	Fire Safety: IEC 60950, NFPA 70	Designed to be compliant		
	Environmental Ingress Protection: IP 14, NEMA 3R (not supported for Beta 1 unit)	Designed to be compliant		
	Electrolyte Spillage Containment: ISO 14001 & IEC 60950	Designed to be compliant		
	Chemical & Electrical Safety: IEC 60950 & IEC 60529 (MSDS, Labels, Nameplate)	Designed to be compliant		
6	**System Software, Remote and Local Monitoring**			
	WattJoule PLC based local DC battery software with local control panel and remote data monitoring, acquisition and control			
	Emergency stop button for full shutdown and DC disconnect, automatic shutdown and DC disconnect when required by error and fault conditions			

Appendix B – Additional WattJoule Flow Battery Data

Stack Dimensions	24.13 cm x 31.75 cm
Cell Area (cm^2)	766.13
Cell Active Area (cm^2)	250
ES10-2DC (Original Battery)	
Number of Cells	20
Total Active Stack Area (cm^2)	5000
ES10-0.5DC (Modified Battery)	
Number of Cells	5
Total Active Stack Area (cm^2)	1250

Appendix C – U of A Metal Removal Final Report

Final_Report_Vanadium_Opportunity.pdf

UNIVERSITY OF ALBERTA

Department of Chemical and Materials Engineering
9211 – 116th Street
Edmonton, AB, T6G 1H9- CANADA

The Vanadium Opportunity

The report is re-issued with potentially sensitive information removed.

Prepared by
Garima Chauhan & Arno de Klerk

March 2020

Table of Contents

List of Tables

List of Figures

1. Introduction

The metal content of oil affects the processing options available to refiners and low metal content is always preferred in a refining context. The presence of metals is undesirable, mainly because they cause poisoning and deactivation of the catalysts used in the refining processes. The non-volatile metal contaminants tend to accumulate during cracking and eventually get deposited on the catalyst. This causes decrease in catalyst surface area by plugging their pores, thereby rendering them inactive. Metals also promote dehydrogenation reactions during the cracking sequence, which results in an increase in the production of coke and decrease in gasoline production[1]. Additionally, high amount of metals in crude oil makes production costly by increasing the amount of hydrogen needed for the process and by increasing yield loss due to carbon rejection[2].

The most abundant and troublesome metal complexes in oil are vanadium and nickel, which are known to occur naturally as vanadyl(IV)- and nickel(II)- porphyrins. Metalloporphyrins are believed to associate strongly with molecules in the asphaltene solubility fraction to form "bound"-type metalloporphyrins. Several heavy oils (including Canadian oilsands derived bitumen) have a combined Ni and V content of the order 200–300 μg/g raw bitumen. Over many decades, the removal and recovery of Ni and V from oil attracted attention. Selective metals removal is not only beneficial to refining, but also a potential source of Ni and V for recovery as metal products.

The primary objective of this work was to develop an efficient demetalation process to recover vanadium and nickel, which can be further used in potential applications such as vanadium as an electrolyte in vanadium redox flow batteries (VRFB). The project was subcategorized into two sections:

a) Determination of V and Ni content in dilbit samples

b) Recovery of V and Ni from dilbit samples

2. Review of Literature

This section provides a brief review of literature on determination of metal content and recovery of V and Ni from dilbit samples.

2.1. Establishing a method for determination of metal content

Development of analytical methods for metals determination is essentially required for the quality control of petroleum samples. Such methods must present suitable sensitivity and must be as simple as possible to allow their use in routine analysis laboratories.

Electroanalytical[3], laser-induced breakdown spectroscopy[4] and X-Ray Fluorescence spectroscopy[5] methods have been reported for the determination of metals, though majority of analytical methods mentioned in the literature are based on atomic spectrometric techniques such as flame atomic absorption spectroscopy (F-AAS)[6,7,] electrothermal (ET-AAS)[8,9,10,] inductively coupled plasma mass spectrometry[11,12] and inductively coupled plasma optical emission spectrometry (ICP-OES)[13,14,15]. It is argued that ET-AAS does not allow the simultaneous determination of multielements present in solution[16]. Also, it may cause loss of volatile analytes during processing. F-AAS gives a high limit of detection due to the low sensitivity for some elements[17,18]. Considering the limitations associated with F-AAS and ET-AAS techniques, inductively coupled plasma (ICP) based technique are found to be more attractive for the metal content determination in petroleum based products. Both ICP-OES and ICP-MS provide a wider dynamic range than atomic absorption and allow simultaneous multi-elemental analyses. Nevertheless, the use of plasma-based techniques for the direct analysis of samples still remains as a challenge due to high carbon content, intrinsic heterogeneity and unfavorable physical characteristics such as high viscosity and turbidity of the crude oil. Therefore, designing optimal pre-treatment of crude oil is critical for reliable metal determination in such a complex matrix.

Several sample preparation strategies have been proposed to circumvent the aforementioned limitations. Figure 1 illustrates various sample preparation methods and the associated limitations with each of the methods.

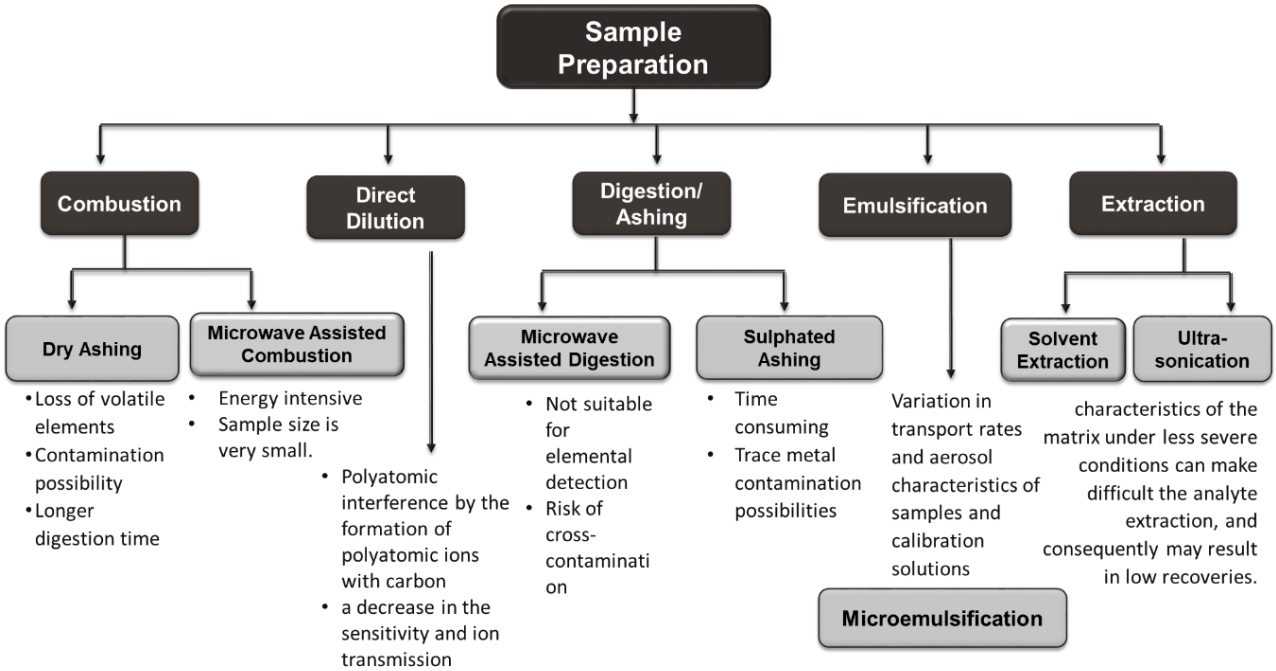

Figure 1: Overview of sample preparation methods

The samples can be mineralized before injection into the instrument[19,20] or injected using special approaches to minimize the amount of carbon that reaches the plasma source[21,22]. Dry ashing is conventionally used for the pre-treatment due to its ease of operation, however loss of volatile elements at high operating temperature and contamination possibility were the major limitations which restrict the applicability of dry ashing. Another traditional way to introduce oil samples into ICP is directly diluting with an appropriate organic solvent which may overcome the limitation of volatile losses. Nonetheless, this procedure does not minimize the problems associated with the high organic load, and necessarily requires the use of expensive and unstable organometallic standards for calibration. Polyatomic interference by the formation of polyatomic ions with carbon, carbon fouling of the spectrometer interface, a decrease in the sensitivity and ion transmission, matrix effects due to the introduction of organic solvents perturbation or extinction of the plasma are the associated concerns with the organic dilution methods. Recently, other sample preparation techniques including microwave digestion, oil-in-water emulsification, microemulsion, ultrasound assisted extraction and wet-ashing have also been proposed with significant efficiency, though each technique has its certain advantages and limitations as mentioned in Figure 1. In this project, some effort was expended to evaluate and confirm the validity of the analytic protocol for diluted bitumen.

2.2. Technology Option Review for Recovery of V and Ni from bitumen sample

Since the most common metal contaminants are nickel and vanadium, which are generally present in the form of porphyrins and are concentrated in residues, much work has been devoted to the treatment of crude oil residues for their removal. Several different reactive demetalation schemes including oxidative demetalation, electrolytic demetalation, ultrasonic irradiation, adsorption, photochemical reaction, liquid-liquid extraction have been reported in literature, nevertheless, the success of any demetalation scheme will depend on how accessible these metals are in the sample. This section presents a literature review on various demetallization approaches.

2.2.1. Conventional Methods

Most demetallization studies focus on the conventional process of hydrodemetallization (HDM). In HDM, nearly 90% metals can be reportedly removed by hydrogenation[23-25], however metals have a tendency to accumulate in the pores of the HDM catalysts. To offset this disadvantage, hydroprocessing units are generally installed before HDM units. Various reactor configurations for HDM are available, which include trickle bed reactors, fixed bed reactors, ebullated bed reactors, and

slurry bed reactors. Most of the studies are conducted on HDM improvised parameters such as operating temperature, catalyst pore size, catalyst surface area, doping of catalysts, feedstock, and residence time[26-28]. This approach can be used for low Ni+V, typically 25 μg/g or less. At higher metal concentration the cycle time for catalyst replacement becomes impractically short[29].

Another conventional method distillation, of atmospheric residues from California crude oil at 358 °C removed 98% of metallopetroporphyrins. The vapor phase contained metal complexes 92% of which were metallopetroporphyrins. The hydrotreatment of this distillate diluted with gas oil in a fixed bed of a low-activity catalyst removed all the metallopetroporphyrins. The spectroscopic analysis of metallopetroporphyrins remaining in the distillate-gas oil after very mild treatment suggested that they were degraded to chlorines, which were intermediates in either thermal or catalytic residuum demetallization[30]. Though, recovery of metal complexes is high in the distillation process, the process was found to be nonselective in nature and therefore cannot be considered a feasible option.

Acid leaching has been one of the most widely commercially employed method for treatment of petroleum fraction. A number of patents for the use of sulfuric acid were issued at the very beginning of the petroleum industry[31-32]. In the process of treating crude oil using sulphuric acid, some of the acid is reduced to sulfur dioxide. This sulfur dioxide may also react with some of the unsaturated hydrocarbons, forming various addition products and thus complicating still further the nature of the basic reactions. The fact that sulfuric acid reacts with and promotes reactions of hydrocarbons is a drawback to its use as an agent for removing metals, sulfur and nitrogen from oil. The hydrocarbon reactions increase the quantity of acid required and decrease the yield of fuel products. Hydrofluoric acid, Hydrochloric, sulfuric, sulfonic, polyphosphoric, hydrobromic, and other acids also have shown significant activity as a demetallization reagent. Metals can be removed (90%) with a high yield of the liquid fraction (85–90 wt.%) particularly in the presence of hydrocarbon solvents[33]. Unfortunately, the associated disadvantages including extensive side reactions and product contamination limits the applicability of acid leaching for metal removal from crude oil. None of these methods appeared promising for treating a diluted bitumen, especially if one considers the capacity needed and cost of the large volume of acid required.

2.2.2. Unconventional Methods

a) Physical Methods

Processes based on membrane technology have been described for demetallization in recent studies. Most of these methods use membranes for the recovery of solvent from an initial extraction, phase

separation, or dilution step. Only a few reports are available on the direct use of membranes for the removal of asphaltene, sulfur, and metals from heavy oil. Arod et al.[34] of Energie Atomique, France, described the ultrafiltration of a vacuum residue at high temperature (330°C) using a ceramic membrane with an average pore diameter of 10 nm. The membrane was operated at a cross-flow velocity of 5.6 m/s and a trans-membrane pressure of 500 kPa. The asphaltene content of the heavy oil was reduced from 6.3 to 4.1 wt.%. The vanadium content was also reduced (from 195 to 90 ppm) and the permeate flux was reportedly at 667 L/m^2 per day i.e. about 4 barrels/m^2 per day. However the effect of time on-stream and membrane fouling was not examined, and it is not clear if the permeate flux was stable during the operation. Duong et al.[35] described an ultra-filtration study on Cold Lake heavy oil using ceramic membranes with average pore diameter of less than 0.1 μm. The ultra-filtration experiments were carried out under relatively mild conditions (600 kPa and 110°C). The results showed a significant reduction in density, viscosity, and Ni and V contents. However, the permeate flux data showed a strong effect of fouling that significantly reduced the permeate flux but increased asphaltene retention.

A recent demetallization study targeted the application of Molecularly Imprinted Polymers (MIPs) to adsorb metalloporphyrins from crude oil[36]. MIPs were synthesized by a reversible interaction of a template molecule with suitable monomers having a high degree of cross-linking. By dissolving using a suitable solvent, a complementary cavity was formed. The synthesized MIPs were combined with electrospun fibers, termed as molecularly imprinted nanofibers (MINs) and were used as sorbents. Their performance was compared to that of nonimprinted nanofibers (NINs). Results indicated that MINs were much more selective than NINs in regard to the adsorption of NiTPP from organic media. While MIN showed a maximum recovery of 99.9%, NINs could only recover 18% of NiTPP, without overloading active sites. Challenges associated with this method are due to the memory sites (selectively recognize the template molecule) being embedded in the inner helices of the particles. Also, the highly cross-linked rigid structure of the monomer restricts the movement of the template molecule.

Liquid–liquid extraction is the most widely applied technology for metal ion separations due to its advantages including operation in a continuous mode, employment of simple equipment, achievement of high sample throughput and easy scale-up. Various solvents such as g-butyrolactone, acetonitrile, phenol, furfural, 2-pyrrolidone, dimethylformamide, pyridine–water mixtures, ethylene carbonate, propylene carbonate, ethylene trithiocarbonate, and dimethylsulfoxide have been reported in literature

for the efficient recovery of vanadium from crude oil[24,37]. However, the conventional liquid–liquid extraction process utilizes water-immiscible molecular solvents, which are flammable, volatile or toxic. To overcome these limitations, solvent extraction using Ionic liquids (ILs), have garnered interest in the demetallization of crude oil. Ionic liquids (ILs) are solvents that consist entirely of ions. Typically, they are organic salts with a melting point below 100°C. Major advantages of ionic liquids for application in solvent extraction processes are their low volatility and low flammability. Although certain IL-extractant combinations have been shown to yield metal ion extraction efficiencies far greater than those obtained with molecular organic solvents, other work suggests that the utility of ILs may be limited by solubilization losses and difficulty in recovering extracted metal ions. The mechanisms for extraction of metal ions into ionic liquids are in many cases different from what is observed for extraction into molecular solvents. Extraction of metal ions from an aqueous/organic phase into an ionic liquid phase often takes place via an ion-exchange mechanism[38,39]. This means that upon extraction ionic liquid components are solubilised in the organic phase. Ionic liquid cations are lost during extraction of a metal ion with a neutral extractant such as a crown ether, whereas ionic liquid anions can be lost during extraction of anionic metal complexes. These losses of ionic liquid by solubilisation in the organic phase are a serious problem that hampers the general application of ionic liquids for liquid–liquid extraction processes. Although these losses of ionic liquid can be reduced by structural variation of the ionic liquid, e.g., by increasing the alkyl chain length or fluorination of the alkyl chain, these modifications often have a negative effect on the distribution ratios and the extraction efficiency[40]. Based on preliminary studies on IL extraction of bitumen at Imperial College, London, much effort was devoted to the investigation of IL extraction of bitumen.

b) Chemical Methods

Various oxidizing agents have been investigated for the demetallization of crude oil in recent studies. Oxidative demetallization process using a variety of oxidizing agents was used for the treatment of Cold Lake asphaltenes, Arabian Heavy asphaltenes and Cold Lake vacuum residuum. Of these, reagents such as air at 100°C and NaOH/air were found to have no appreciable demetallization activity while oxidants such as sodium hypochlorite and peroxyacetic acid exhibited high demetallization activity coupled with the ability to remove or destroy petroporphyrins[41]. The sodium hypochlorite, however, was found to suffer from the disadvantage of causing chlorine incorporation into the feed. This oxidative demetallization appears to be rather unselective reaction with both metals and porphyrin removal being proportional to the amount of oxidant used.

Strong chlorinating compounds such as Cl_2, $SOCl_2$, or inorganic salts like $FeCl_2$, $SnCl_2$, $ZnCl_2$, $TiCl_4$, $RuCl_3$, $CrCl_3$, $COCl_2$, or their aqueous solutions have also been employed for nickel and vanadium removal from heavy oils. Up to 70% of the metals are reported to be removed at temperatures ranging from 40 to 300 °C. The metals were converted to insoluble constituents and removed by filtration. The use of these reagents, however, results in chlorine and metal incorporation into the production and, therefore, degrades rather than improves the quality of the oil.

Recently, Acevedo et al.[42] conducted research on the electrochemical-assisted conversion of model metalloporphyrins (VOTPP and Ni-TPP) as well as crude oil porphyrinic extracts in oil/water for demetallization from crude oil. The conversions were ~20% for VO-TPP and 18% for Ni-TPP. Porphyrinic extracts from Venezuelen crude oil in emulsified and nonemulsified media were less reactive than the model metalloporphyrins. Welter et al.[43] used protonating agents in their study of electrochemical demetallization to enhance the degradation of VO-MTPP and VOOEP, extracted from Ayacucho Venezuelan crude oil. The effect of different electrodes (platinum, graphite, and glassy carbon) and different protonating agents (tetrahydrofuran (THF), methanol, and perchloric acid) was observed. Quantities of 84% of VO-MTPP and 78% of VOOEP were hydrodemetallized through the electrochemical method. Ovalles et al.[44] assessed the effectiveness of the electrochemical demetallization method on the extra-heavy crude oil Orinoco Belt with high nickel and vanadium concentrations. Nearly 73% and 81% of Hamaca petroporphyrin was removed at current densities of 0.02 A cm^{-2} and 0.01 A cm^{-2}, respectively. Greany et al.[45] showed an electrochemical method of demetallization of Arabian Light atmospheric residue. After stirring for some time in a commercially available coulometry cell, 53% vanadium, 50% nickel, and 65% iron was removed.

Supercritical (SC) methods were also tested by many researchers for heavy crude. Water or carbon dioxide was usually used as solvents in these studies. Supercritical water (SCW) above a temperature of 374°C and a pressure of 22.1 MPa (critical points), behave as a solvent, a reactant in hydrolyses-based reactions, and a collision partner. Its dielectric constant ranges from 2 to 30 (nonpolar solvents to polar solvents), increasing the ion product of water. Both these changes gave SCW acidic or basic characteristics. Mandal et al.[46] conducted a laboratory-scale experiment to study the removal of Nickel etio-porphyrin using SCW in a toluene environment in the absence of catalyst and reported a promising conversion of 95.02%. While the reaction was highly sensitive to temperature, it was unaffected by variations in water partial pressure. Removal of vanadyl etio-porphyrin under supercritical conditions was also investigated using xylene and toluene as solvents and ~90.51%

conversion of porphyrin was reported at temperature of 490°C and a reaction time of 180 min[47]. The conversion increased with increasing reaction time and temperature.

Shiraishi et al.[48] studied a unique photochemical method for the extraction of vanadium and nickel porphyrins from residua. They dissolved model VOTPP or NiTPP in tetralin and treated it to photoirradiation by subjecting it to a high-pressure mercury lamp. The emulsion formed was demulsified electrically and analyzed. Removal of 98% of the nickel and 93% of the vanadium from atmospheric residue, and 85% of the nickel and 73% of the vanadium from vacuum residue were reported. With the exception of the electrochemical assisted removal, chemical and photochemical methods appear infeasible for application at large scale due to cost and potential side-reactions.

c) Other alternative methods

In the case of crude oil, another class of methods is focused on using radiation, such as ultrasonic and microwave irradiation, to enhance the demetallization potential of traditional treatment procedures. Tu and Yen[49] used ultrasonic radiation (20 kHz) on a mixture of metalloporphyrins (NiTPP and VOTPP), solvent, and hydrogen peroxide. Argon gas (5 psig) was passed over the mixture to reduce the oxidation of metal porphyrins into nonporphyrinic forms. Using chloroform as a solvent, the maximum recovery of nickel was 89.7% and that of vanadium was 86.3%. Some researchers also investigated the effect of microwave irradiation on the electric desalting process in Iranian and Shengli crudes. At a microwave intensity of 350 W, vanadium removal efficiencies were 92% for Iranian crude and 88% for Shengli crude, compared to 25.5% and 8.20% without applying radiation[50]. Other unconventional processes being investigated for heavy crude include ultrasonication. The effect of different operating conditions, such as power intensity, surfactant, oxidant, pH value, solvent, temperature, and reaction time, was studied[51]. Power of ultrasonic radiations affected chemical reactions the most by increasing its sonochemical effects. Surfactants were found to promote the ultrasonic reaction by providing a stable emulsion system. Under optimum conditions, 92.9% NiTPP and 88.8% of VOTPP were removed. Demetallization of crude oil was also attempted using micro-organisms who degrade metalloporphyrins by using them as their sole source of carbon. Salehizadeh et al.[52] studied the action of Aspergillus sp. on model vanadium compound. It was found that 55% of model compound was degraded in 7 days, by the micro-organism, into the form of free metal ions.

Table 1 lists the major advantages and disadvantages associated with unconventional methods for demetallization of crude oil.

Table 1: Major advantages and disadvantages associated with unconventional methods for demetallization of crude oil

Method	Advantages	Disadvantages	References
Membrane based methods	Significant recovery of metals	Membrane fouling, high asphaltene retention	[34], [35]
Molecular Imprinted Polymers	low cost, high durability, high selectivity, retention of selectivity for long durations, large surface area, versatility	memory sites embedded in the inner helices of the particles and the highly cross-linked rigid structure of the monomer restricts the movement of the template molecule	[36]
Ionic Liquids	Low volatility, low flammability than molecular solvents	Poor selectivity,	[38],[40]
Oxidative Demetallization	High metal recovery	loss of oxidant, non-selective operations	[41]
Chlorination	High demetallization effiiciency	chlorine and metal incorporation into the production, degrades the quality of the oil	[24]
Electrochemical Methods	Significant extraction of metals	High energy required, voltage sensitive	[43],[44]
Supercritical Methods	highly efficient, 100% removal in certain cases	temperature sensitive	[46]
Photochemical Methods	energy saving, solvent recovery, safe demetallization	difficulty in removing bound-type metalloporphyrins without solvent addition	[48]
Radiation based methods	higher efficiency of metal removal	applicable only to mild noncatalytic operations, Energy intensive	[49],[50]
Biological Methods	Environmental Friendly, minimum usage of hazardous chemicals	High contamination susceptibility, slow and time consuming process	[52]

3. Establishing a method for analysis of vanadium and nickel

***Analytical technique: Inductive coupled plasma-Optical Emission Spectroscopy**

Athabasca bitumen, Cold Lake Bitumen and Albian Dilbit samples were used as raw material in the present study. Literature review indicated that the search for novel approaches to sample preparation is still a challenge in most analytical laboratories. Considering that no official method is available for fingerprinting of petroleum samples related to their metal content, feasibility of different sample preparation methods (ultrasound assisted extraction, microemulsion, dry ashing, sulphated ashing) was investigated for the determination of metals in crude oil. Direct dilution, despite of its easy operation, was not considered for investigation in present study due to high organic vapor loading, analyte signal suppression and carbon fouling of the spectrometer interface. Comparative evaluation of the analytical methods was performed with regard to accuracy, precision, applicability for routine analysis and preparation time. All experiments were conducted in triplicates to ensure the reproducibility of each analytical technique.

3.1. Instrumentation & Apparatus

A time programmable ultrasonic cleaner bath (BRANSON 2800) operating with a frequency of 40 kHz was used for the ultrasound-assisted extraction and agitation of oil samples. Micro-emulsification and ultrasounication experiments were conducted in polyprypelene centrifuge tubes. A variable speed mini vortex mixer (FisherbrandTM BV213) with speed range 500 to 2800 rpm was employed to facilitate efficient mixing. Samples were kept in porcelain crucibles and ignited using Carbolite CWF1100 oven during dry ashing and sulphated (wet) ashing experiments. A Fisher Scientific model Isotemp hot plate was used for heating of the samples. The weighing was performed using a Mettler Toledo XP1203S balance (capacity 1210 g, readability 1 mg).

Determination of trace metal content in Athabasca bitumen samples was carried out using Agilent ICP-OES 5100 (Agilent Technologies Canada Inc.) equipped with SPS3 autosampler, an easy-fit torch, a seaspray nebulizer, a double-pass spray chamber, and ultra-high purity compressed Argon gas. The analytical emission ionic lines chosen were: V (311.8 nm), Ni (230.2 nm). The conditions for the analysis were: radial viewing mode, pump speed 10 rpm, nebulizer flow 0.7 L/min, plasma flow 12 L/min, auxiliary flow 1 L/min, delay time 26 s, stabilization time 15 s, read time 5 s, power 1.2 kW and Rf-generator of 27 MHz. The aqueous phase samples were not acidified for this analysis. Each sample was measured in triplicate.

3.2. Experimental Methodology

3.2.1. Ultrasound assisted extraction

Ultrasound assisted extraction of metals was performed in the similar manner as described in literature[13,53]. Samples, 0.2 g of Athabasca/cold lake bitumen, were directly weighted into 15 mL centrifuge tubes and diluted using 0.5 ml toluene in order to make the sample more fluid. 10 mL concentrated HNO_3 acid solution was added into the tube. Sample was agitated vigorously for 2 min in order to prepare a homogeneous solution. These samples were heated in a water bath at 85°C for 30 min and then the tube was placed in an ultrasonicator for 20 min to improve the contact between acid and bitumen. A transparent brown color solution was obtained in the bottom layer of the solution, while bitumen was present in the top layer. Phase separation was performed with the aid of separating funnel. The extracted liquid sample was diluted up to 25ml with Milli-Q water. The aqueous calibration standard solutions were prepared by adding adequate volumes of inorganic analyte standards in concentrated nitric acid in order to minimize acid non-spectral interferences when comparing analyte signals with the ones of the sample aqueous extracts.

3.2.2. Detergentless microemulsification

Detergentless microemulsions were prepared as described in literature[54] using propan-1-ol as the co-solvent and water. 0.2 g of the Athabasca/Cold Lake bitumen was mixed with 0.5 ml of xylene and 0.4 mL of concentrated HNO_3 in a centrifuge tubes and vigorously shaken in a vortex for 5 min. Then, 1.1 ml of Propan-1-ol followed by 0.25 ml of water were added in an alternate way until a final mass of 10 g was achieved. Vortex agitation was used after each alternate addition in order to make the mixture as homogeneous as possible. The final composition of the microemulsion was approximately bitumen/co-solvent/water/HNO_3 (6/70/20/4 w/w/w). The mixtures were then placed in an ultrasonic bath for 15 min. A dark transparent brown solution was obtained which was diluted up to 50 ml with Milli-Q water. The aqueous calibration standard solutions were prepared in the similar manner except the bitumen sample was replaced by adding adequate volumes of inorganic analyte standards.

3.2.3. Dry Ashing

A mass of 10.0 g of bitumen sample was accurately weighed in a porcelain crucible and heated on a hot plate until completely dried. The dried sample was then transferred to the oven and progressively heated (20°C/min) until 550°C. After achieving this temperature, sample was kept for 4 h in the oven.

The resulting ash was then acid digested in 10 mL concentrated HNO_3 until the final volume remains 5 ml and then finally diluted to 25ml with Milli-Q water.

3.2.4. Wet Ashing

10.0 g of raw material was weighed in a porcelain crucible and sulphuric acid was added in a certain oil to acid ratio (w/v). After additions of sulphuric acid, the sample was subjected to heating on hot plate until completely dried. Sample was stirred occasionally using glass rod to minimize sample splashing and foaming. The dried sample was then subjected to progressive heating (20°C/min) until 550°C in an oven and kept there for 4 h in order to get rid of all carbonaceous content. The resulting ash was digested in presence of 10 mL concentrated HNO_3 and finally diluted up to 25 ml with Milli-Q water.

3.3. Observations & Inferences

Figure 2 illustrates the metal content (µg/g) determined using different aforementioned methods. It was observed that wet digestion demonstrated highest concentration of vanadium and nickel in raw material with least standard deviation.

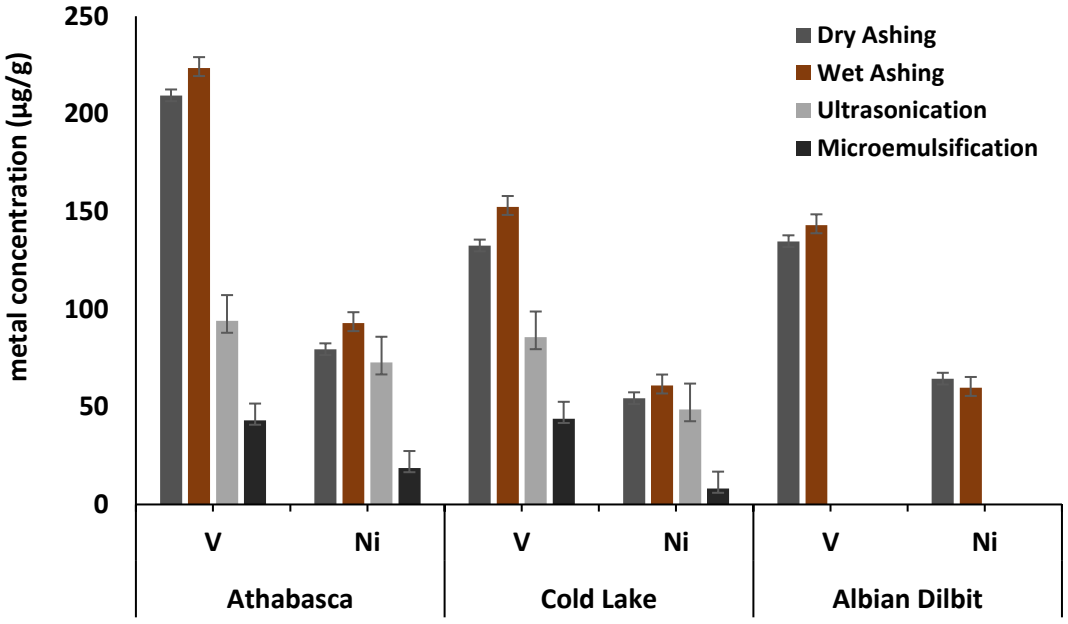

Figure 2: Comparative performance analysis of different sample preparation methods

Observations from experimental investigations indicated wet ashing as the most suitable analytical technique for quantitative analysis of nickel and vanadium. Based on the observations for different sample preparation methods, following inferences were drawn:

i) Dry ashing results into lesser metal content at the same ignition temperature and exposure time as wet ashing. It may be inferred that some of the analyte content is lost during dry ashing and therefore exact determination of metal content could not be achieved using dry ashing.

ii) Ultrasonication and microemulsification demonstrated nearly 94 ppm and 43 ppm of vanadium content in the Athabasca bitumen sample which is far less than the expected metal content. Also, excessive use of acids and organic solvent were used in experiments and therefore, these methods were not observed to be competitive.

iii) Wet ashing suggested nearly 223 μg/g, 152μg/g and 143μg/g of vanadium in the Athabasca bitumen, Cold Lake bitumen and Albian dilbit sample which meets the literature information. Effect of acid to oil ratio, ignition time and ignition temperature were investigated to optimize the metal content determination.

iv) 550°C and 4 h were found to be optimum for complete ignition of the samples. Experiments were performed at 350°C, 450°C and 700°C also, however samples could not be ignited completely at lower temperature (350°C & 450°C) and lot of coke was seen in crucible after 4 h of ignition time. When experiments were performed at 700°C, significantly less vanadium content (168 μg/g and 112μg/g) was obtained in Athabasca bitumen and Cold Lake bitumen respectively than vanadium at 550°C which indicated loss of volatile analytes at higher temperature.

v) Similarly, samples were ignited for different time duration varying from 2 h to 6 h. 4 h was observed to be optimum ignition time for wet ashing. On the other hand, 2 h was observed to be too less for complete oxidation of samples whereas 6 h did not show any considerable difference in metal content determination than 4 h.

vi) Variation in acid to oil ratio did not show any considerable difference in vanadium content. 1.5:1 was considered optimum for the present study.

vii) Validation experiments for sulphated ashing were conducted in triplicates by spiking the bitumen samples with model metalloporphyrins VO-TPP. The investigated method gave satisfactory results with less than ± 2.7% deviation in vanadium content.

4. Characterization of Raw Material

Raw materials (Athabasca bitumen, cold lake bitumen, albian dilbit) were characterized on the basis of physical properties, elemental analysis, determination of metal content, deasphalting and boiling point distribution analysis. The asphaltenes fraction was precipitated from the bitumen using *n*-pentane solvent deasphalting. In a typical solvent deasphalting experiment, 10 g of bitumen was mixed with 400 mL of n-pentane in a 500 mL flask. Then, it was placed in the fume hood at ambient conditions for 1 h while continuously stirring the mixture with a stirrer bar on a magnetic stirrer. At the end of this period the mixture was left for 24 h in the dark, before the mixture was filtered with a 0.22 μm Millipore nitrocellulose membrane filter under vacuum and rinsed with fresh n-pentane. Finally, the membrane filter was transferred to an aluminum cup and dried in the fume hood for 48 h. The membrane filter and aluminum cup were previously weighed in order to calculate the asphaltenes content in bitumen. The maltenes, or deasphalted oil (DAO), was obtained by evaporating n-pentane in a rotary evaporator at 50°C. The bitumen and its prepared fractions, asphaltenes and maltenes, were characterized and properties are listed in Table 2. Albian Dilbit sample was provided by Canadian Natural Resources Limited, Canada. Physical Properties (Density, viscosity, refractive index), elemental content (CHNS analysis), metal content, boiling point distribution analysis are reported in Table 2.

Sulphated ashing method was used for the determination of vanadium and nickel content in the raw material. Elemental analyses were performed by the Analytical Services of the Chemistry Department at University of Alberta using a Carlo Erba Elemental Analysis EA1108 Analyzer. During a typical analysis a small amount of sample is oxidatively pyrolized at 1700−1800°C in order to produce N_2, CO_2, H_2O, and SO_2. The product gases pass through a reactive column with helium as the carrier. The first section of the column contains tungsten trioxide (WO_3) on alumina (Al_2O_3), which is used to ensure that complete oxidation occurs. The second section of the column contains a layer of reduced copper where excess oxygen is removed. The products are then separated on a chromatographic column at 70°C and are detected by a thermal conductivity detector. A calibration curve based on the concentration of known standards is used to quantify the gases.

Liquid density measurement of the bitumen and the maltenes was performed using a density meter from Anton Paar, model DMA 4500M. Densities were recorded at a controlled temperature of 25°C. The refractive indexes of bitumen and maltenes were determined relative to that of air using the sodium D-line (589 nm). The measurements were performed at a controlled temperature of 25°C.

Table 2: Characterization of Raw Material (Athabasca Bitumen, Cold Lake Bitumen, Albian Dilbit)

Description	Athabasca Bitumen			Cold Lake Bitumen			Albian Dilbit
	Bitumen	Maltene	Asphaltene	Bitumen	Maltene	Asphaltene	
Fraction of bitumen (wt%)	100	82.3 ± 0.16	16.6 ± 0.12	100	80.5 ± 0.17	18.4 ± 0.09	NA
Physical Properties							
Density (kg/m^3)	1001.5 ± 0.33	943.9 ± 0.91	na	990.3 ± 0.26	803.1 ± 0.29	na	
Refractive Index (nD)	1.5683 ± 0.001	1.5423 ± 0.001	na	1.5514 ± 0.002	1.5353 ± 0.004	na	1.5317 ± 0.003
Elemental Analysis (wt%)							
Carbon	83.2 ± 0.06	83.7 ± 0.09	80.7 ± 0.059	66.8 ± 0.15*	84.0 ± 0.06	79.0 ± 0.11	82.8 ± 0.01
Hydrogen	10.4 ± 0.008	11.0 ± 0.04	8.1 ± 0.04	10.5 ± 0.08	11.3 ± 0.02	8.1 ± 0.02	10.9 ± 0.01
Nitrogen	0.5 ± 0.001	0.4 ± 0.006	1.2 ± 0.018	0.4 ± 0.003	0.3 ± 0.02	1.1 ± 0.003	0.4 ± 0.003
Sulfur	4.5 ± 0.113	3.6 ± 0.16	8.0 ± 0.104	3.3 ± 0.106	3.6 ± 0.08	7.4 ± 0.22	4.3 ± 0.01
†Oxygen (by difference)	1.3 ± 0.036	1.3 ± 0.190	1.9 ± 0.104	-	0.8 ± 0.20	4.4 ± 0.37	1.5 ± 0.01
SIMDIST Analysis (wt%)							
<200°C	0	0	0	0	0	0	6.10
200-450°C	28.65	35.12	0	26.53	40.23	2.03	29.89
451-700°C	42.36	45.55	21.19	31.64	42.23	27.55	37.54
>700°C	28.99	19.33	78.81	41.83	17.54	70.42	26.38
Metal Content (ppm) (ICP Anaysis)							
V	220 ± 7.89	nd	nd	132 ± 6.31	nd	nd	143.0 ± 5.8
Ni	83 ± 4.19	nd	nd	52 ± 1.62	nd	nd	59.7 ± 2.3

*The cold lake sample used in this study contains lot of water content (~20%), therefore the (%) carbon content was found lesser in the specific sample than Suncor Bitumen and Albian dilbit sample.

5. Demetallization of bitumen and dilbit samples

The present study investigated three unconventional methods for the demetalation of Athabasca bitumen. The investigated methods are photochemical separation, electrochemical separation and ionic liquid extraction. A detailed description of each investigated method and major findings are given in following sections:

5.1. Ionic Liquid Assisted Extraction of Metals

Ionic liquids can be used for the direct extraction of metals from the bitumen and can also be employed in combination with photochemical and electrochemical separation. The molecules in the ionic liquid is selected to compete with metal ions for coordination in the porphyrin, analogous to an ion exchange reaction.

5.1.1. Ionic Liquid DIMCARB

Preliminary experiments were performed to assess the feasibility of Dimethlyammonium dimethyl-carbamate (DIMCARB) ionic liquid (recommended by ICL, London) for the extraction of metals from dilbit samples. Athabasca and Cold Lake Dilbit samples were prepared by adding 30% of Napthenic diluent with raw bitumen. The chemical structure of DIMCARB is shown in Figure 3:

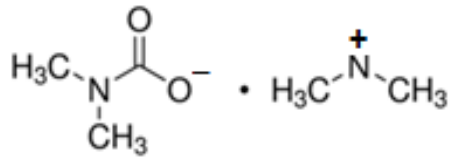

Figure 3: Chemical Structure of Dimethylammonium dimethylcarbamate (DIMCARB)

DIMCARB was used in the preliminary study for the extraction of vanadium from bitumen and extraction efficiencies of 80% at 40:1 (dilbit:IL) ratio was reported in the feasibility report carried out at Imperial College London. Therefore, DIMCARB was chosen to perform preliminary experiments.

Ionic liquid DIMCARB was added to the dilbit samples (Athabasca/Cold Lake) at different ratios of ionic liquid to dilbit samples in a glass vial along with a cross magnetic stirrer. Continuous stirring at 550rpm was provided in order to ensure sufficient interaction between ionic liquid and dilbit samples. Samples were heated to 50℃ for one hour and then the sample was left to settle for 4 h at the same reaction temperature. Under LED light, a two-phase separation (Figure 4) could be clearly observed.

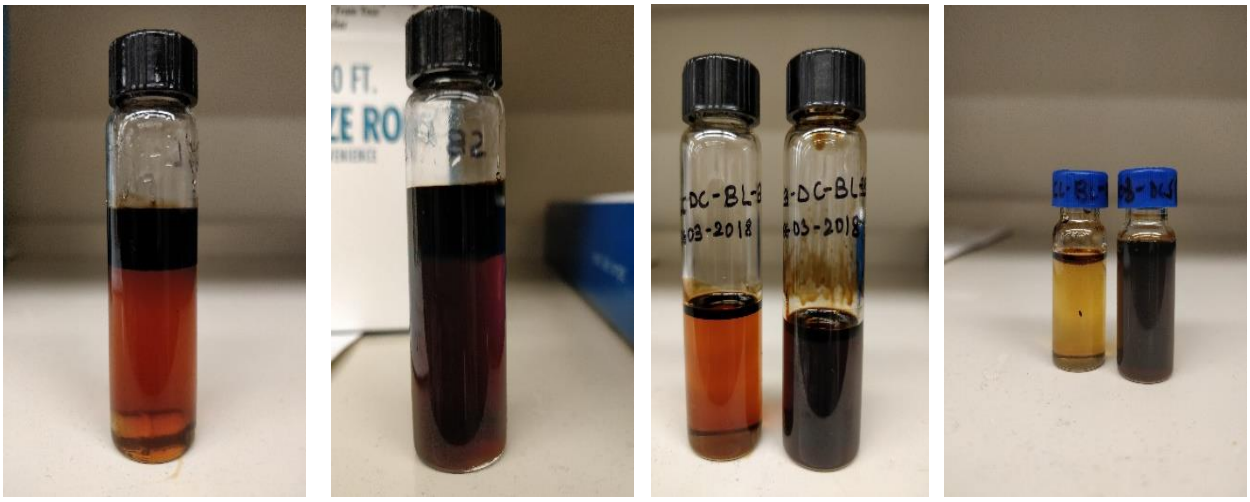

Figure 4: Biphasic Separation for (a) Cold Lake dilbit (b) Athabasca dilbit sample (c) ILs layer at ILs to Dilbit ratio 2:1 (d) ILs layer at Ils to dilbit ratio 1:1 (Cold Lake)

The samples were processed for ICP analysis via acid digestion. 300 mg of each sample was digested using 10ml of HNO_3. The digested samples were then diluted to 10 ml and analyzed via ICP-OES. Reaction parameters were optimized by varying the reaction temperature (50°C - 100°C), ratio of dilbit to ionic liquid (1:1 – 4:1), reaction time (0.5 h- 3 h), settling time (1 h, 2h, 4h, 8h, 24 h), stirring speed (0, 300rpm, 550 rpm, 800rpm). Results are shown here in Table 3 - Table 7 for the metal extraction from Athabasca/Cold Lake dilbit samples at different reaction conditions:

Table 3: Effect of ratio of ILs to dilbit ratio on the recovery of V/Ni from dilbit samples using DIMCARB ionic liquid (Initial concentration of metals in Cold Lake (V: 152.3 µg/g, Ni: 60.9 µg/g), in Suncor Bitumen (V: 223.4 µg/g, Ni: 92.8 µg/g), Reaction conditions: Temperature: 50°C, reaction time: 1 h, settling time: 4 h, stirring speed: 550 rpm)

ILs : Dilbit	Cold Lake		Athabasca		ICL Results*
	V(%)	Ni(%)	V(%)	Ni(%)	
0.5:1	3.05	2.13	2.87	2.31	13.33% V and 4.35% Ni
1:1	9.03	10.10	10.1	6.67	
2:1	11.95	13.35	14.67	11.66	
3:1	14.07	14.78	17.40	13.13	
4:1	16.82	17.36	19.1	14.93	

Table 4: Effect of reaction temperature on the recovery of V/Ni from dilbit samples using DIMCARB ionic liquid (Initial concentration of metals in Cold Lake (V: 152.3 µg/g, Ni: 60.9 µg/g), in Suncor Bitumen (V: 223.4 µg/g, Ni: 92.8 µg/g), Reaction conditions: Ils to dilbit ratio: 1:1, reaction time: 1 h, settling time: 4 h, stirring speed: 550rpm)

Reaction Temp.	Cold Lake		Athabasca	
	V(%)	Ni(%)	V(%)	Ni(%)
50°C	9.03	10.10	10.1	6.67
80°C	17.55	16.12	13.08	9.20
100°C	High Pressure inside the vessel. Sample was lost as soon as the vessel was opened.		Vessel broke due to high pressure build up.	

Table 5: Effect of reaction time on the recovery of V/Ni from dilbit samples using DIMCARB ionic liquid (Initial concentration of metals in Cold Lake (V: 152.3 µg/g, Ni: 60.9 µg/g), in Suncor Bitumen (V: 223.4 µg/g, Ni: 92.8 µg/g), Reaction conditions: Ils to dilbit ratio: 1:1, reaction temp: 50°C, settling time: 4 h, stirring speed: 550rpm)

Reaction Time	Cold Lake		Athabasca	
	V(%)	Ni(%)	V(%)	Ni(%)
0.5 h	7.61	8.01	8.98	5.24
1 h	9.03	10.10	10.10	6.67
2 h	8.21	11.35	10.53	7.03
3 h	9.17	9.78	9.40	6.13

Table 6: Effect of settling time on the recovery of V/Ni from dilbit samples using DIMCARB ionic liquid (Initial concentration of metals in Cold Lake (V: 152.3 µg/g, Ni: 60.9 µg/g), in Suncor Bitumen (V: 223.4 µg/g, Ni: 92.8 µg/g), Reaction conditions: Ils to dilbit ratio: 1:1, reaction temp: 50°C, reaction time: 1 h, stirring speed: 550rpm)

Settling Time	Cold Lake		Athabasca	
	V(%)	Ni(%)	V(%)	Ni(%)
1 h	9.03	10.10	10.10	6.67
2 h	10.37	10.12	12.41	8.08
4 h	9.41	9.12	13.94	9.01
8 h	9.17	9.01	10.38	7.93
24 h	11.68	12.91	9.79	6.86

Table 7: Effect of stirring speed on the recovery of V/Ni from dilbit samples using DIMCARB ionic liquid (Initial concentration of metals in Cold Lake (V: 152.3 µg/g, Ni: 60.9 µg/g), in Suncor Bitumen (V: 223.4 µg/g, Ni: 92.8 µg/g), Reaction conditions: Ils to dilbit ratio: 1:1, reaction temp: 50°C, reaction time: 1 h, settling time: 4 h)

Stirring Speed	Cold Lake		Athabasca	
	V(%)	Ni(%)	V(%)	Ni(%)
Without stirring	0.64	1.03	0.14	0.97
300 rpm	5.79	8.43	6.82	6.34
550 rpm	9.03	10.10	10.10	6.67
800 rpm	8.56	10.98	11.43	6.02

5.1.2. Selection of various ionic liquids and their applicability for metal extraction

DIMCARB assisted metal extraction process could not show the significant metal extraction efficiency at optimized reaction conditions. Therefore, applicability of other ionic liquids was investigated in order to improve the metal extraction efficiency. Selectivity of various ionic liquids was also investigated using Simulated Distillation Analysis.

The range of ILs were selected to determine which cationic and anionic components of ILs are effective in the extraction of V and Ni from dilbit samples. Specific to the structures, the imidazolium-based cations contain a delocalized charged ring whereas the ammonium-based cations provide a charged atom. The anion will play the key part in chelation to the metal center, therefore effect of anions was monitored while imidazolium based cation was same for most of the employed ionic liquids. The anions in this study were employed for a number of reasons in addition to being thought of as suitable candidates to coordinate to the metals.

i) The $[N(Tf)_2]^-$ anion were selected due to being widely used and thus there exists vast amounts of physical property data about them. Due to the electron withdrawing fluorine groups it would be expected that IL based in this anion will have a lower ability than the other ILs in the extraction of the target metals, however, it can be seen from a patent in this area[55], that $[C_2C_1im][N(Tf)_2]^-$ was able to remove both V and Ni in good yield from Medium Arabian Crude Oil.

ii) The $[HSO_4]^-$ anion was employed to allow the determination of whether anion-based H bond donation could have a major role in chelation. The $[HSO_4]^-$ based alkylammonium ILs are

particularly inexpensive thus if they perform well in the metal extraction they would be very appealing to a scale up application.

iii) The chloride (Cl^-) anion was selected to examine possible formation of a metal precipitate within the extraction (after strong direct metal-anion coordination), and to determine how this could affect the purification approach. Cl^- based ILs have been known to also perform well in pervious extraction of metals from hydrocarbon streams due being small and highly charged thus having a large charge density.

iv) Phosphate and thiocyanate groups were specifically selected to examine the effect of anion size and charge to volume ratio of anion vs metal on the metal extraction efficiency.

Ionic liquids (Shown in Figure 5) were purchased from Sigma Aldrich and experiments were performed in the similar manner as with DIMCARB.

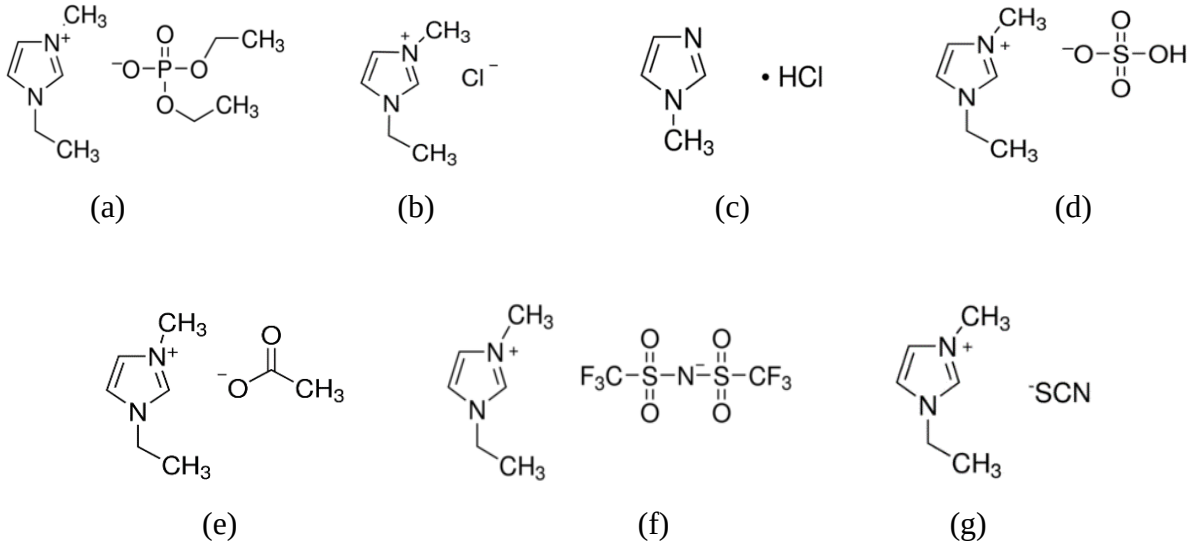

Figure 5: Chemical Structure of various ionic liquids of interest (a) 1-Ethyl-3-methyl-imidazolium diethyl phosphate (EMIM-DEP) (b) 1-Ethyl-3-methylimidazolium chloride (c) 1-Methylimidazolium chloride (d) 1-Ethyl-3-methylimidazolium hydrogen sulfate (e) 1-Ethyl-3-methylimidazolium acetate (f) 1-Ethyl-3-methylimidazolium bis(trifluoromethylsulfonyl) imide (g) 1-Ethyl-3-methylimidazolium thiocyanate

Table 8 lists the noted major observation during/after the experiments using different ionic liquids. Specific details of selecting ionic liquids are below:

Table 8: Observation for various Ionic Liquid of interest (Initial meta concentration in Suncor dilbit samples V:166.06 µg/g, Ni: 65.006 µg/g; Reaction Temp: 50°C, Reaction time: 1h, Settling time: 4h, Ratio of ILs to dilbit ratio =1:1, stirring speed: 550rpm)

S. No.	Ionic Liquids	% Recovery	Selectivity	Remarks	ICL Results
1	Dimethlyammonium dimethyl-carbamate (DIMCARB)	13.8 ± 0.5%V, 9.4 ± 1.0 % Ni	Non-Selective	Clear biphasic layer separation	13.3% V, 4.3% Ni
2	1-Ethyl-3-methyl-imidazolium bis-(trifluoromethylsulfonyl) imide (EMIMim)	0.3 ± 0.04%V, 2.3 ± 0.16%Ni	Non-Selective	Longer settling time and higher temperature (100C) is required to attain V/Ni extraction. Clear biphasic separation was not visible.	40% V, 36% Ni
3	1-methyl imidazolium chloride [HC1im]Cl + 10% H_2O	1.6 ± 0.7 %V, 6.1± 0.1 %Ni	Selective	ILs froze as soon as the vial was taken out from the oil bath at 80C reaction temp. Therefore, further experiments were conducted with 10% H2O.	45.8% V, 43.8%Ni
4	1-Ethyl-3-methyl-imidazolium chloride (EMIC) +10% H_2O	2.8 ± 0.9 %V, 5.2 ± 0.1 %Ni			-
5	1-Ethyl-3-methyl-imidazolium diethyl phosphate (EMIM-DEP)	7.0 ± 1.4 %V, 6.0 ± 0.8 %Ni	Non-Selective	Clear biphasic separation at higher temperature (80C).	-
6	1-Ethyl-3-methyl-imidazolium hydrogen sulfate	0.02 ± 0.01 %V, 0.1 ± 0.01 %Ni	-	Not suitable for metal extraction. <1% V and Ni were extracted.	-
7	1-Ethyl-3-methyl-imidazolium acetate (EMIM Ac)	-	-	No biphasic layer separation.	-
8	1-ethyl-3-methyl imidazolium thiocyanate (EMIM-SCN)	4.1 ± 0.1 % V, 1.5 ± 0.1 % Ni	Selective	Clear biphasic layer separation.	-

Only some of the ILs were selective for metal extraction without co-extracting oil. In those instances where the extraction was not selective, the metals were co-extracted with oil.

5.1.3. Multistage Extraction

It was observed in section 5.1.1 that variation of stirring speed could not show any noticeable increase in metal extraction with the increase in stirring speed. This observation indicated that the ionic liquid assisted extraction was not a mass transfer limited process over the extraction periods investigated. Therefore, possibility of equilibrium assisted extraction process was investigated using Athabasca dilbit samples. Three cycles of experiments were performed using the same dilbit sample during all cycles, while fresh ionic liquid was used in each cycle. Results indicated the possibility of multistage extraction process. Table 9 illustrates the data for vanadium and nickel extraction from Athabasca/ cold lake dilbit samples using DIMCARB and EMIM-SCN ionic liquid.

Results illustrated in Table 9 indicated the possibility of equilibrium assisted extraction process. By employing three equilibrium stages, the overall vanadium extraction was increased from around 4 to 12 % and 10% to 19% using EMIM-SCN and DIMCARB respectively.

Table 9: Equilibrium assisted extraction of metal (Reaction conditions: Initial metal concentration in Suncor dilbit samples V:166.06 µg/g, Ni: 65.006 µg/g; Reaction Temp: 50°C, Reaction time: 1 h, Settling time: 4 h, Ratio of ILs to dilbit ratio =1:1, stirring speed: 550rpm)

Sample	Ionic Liquid	Stage	Initial Metal Content (ppm)		Metal recovery (ppm)		% Metal recovery	
			V	Ni	V	Ni	V	Ni
Suncor Dilbit	EMIM-thiocyanate	I	166.1	65.0	6.1 ± 0.1	1.0 ± 0.1	4.1 ± 0.1	1.5 ± 0.1
Dilbit recovered from Stage I		II	160.0	64.0	7.7 ± 0.5	2.2 ± 0.4	4.8 ± 0.2	3.4 ± 0.1
Dilbit recovered from Stage II		III	152.3	61.8	5.5 ± 0.3	1.1 ± 0.3	4.7 ± 0.2	3.3 ± 0.7
Overall Recovery							11.6 ± 0.3	6.6 ± 0.2
Suncor Dilbit	DIMCARB	I	166.1	65.0	16.7 ± 0.3	4.3 ± 0.09	10.1 ± 0.2	6.6 ± 0.1
Dilbit recovered from Stage I		II	149.3	60.7	12.4 ± 0.2	3.6 ± 0.1	8.3 ± 0.3	5.9 ± 0.2
Dilbit recovered from Stage II		III	138.9	57.1	3.0 ± 0.8	1.8 ± 0.6	2.2 ± 0.5	3.1 ± 0.8
Overall Recovery							19.4 ± 0.6	14.9 ± 0.4

5.1.4. Effect of diluent (Naphthenic vs paraffinic) on V/Ni extraction

As illustrated in the section 5.1.2., performance of different ionic liquids have been tested for extraction of metals from dilbit samples, however none of the investigated ionic liquids showed a satisfactory extraction efficiency. It was suspected that naphthenic diluent may pose a negative effect on the chemistry of Vanadium metals with ionic liquids. In order to replicate the results reported in ICL bench test report and to investigate the effect of diluent, fresh dilbit samples were prepared using a paraffinic mixture to simulate dilbit.

Experiments were performed in the similar manner as mentioned before in section 5.1.1. Four different ionic liquids were employed in this study and results are reported in Table 10.

Table 10: Effect of diluent on metal recovery from diblit samples

Sample	Ionic Liquid	V (%)			Ni (%)		
		Paraffinic diluent[1]	**Napthenic diluent[2]**	**ICL results (Albian dilbit)[3]**	**Paraffinic diluent**	**Napthenic diluent**	**ICL results (Albian dilbit)**
Athabasca	DIMCARB	7.9 ± 0.9	13.8 ± 0.5	13.3	6.1 ± 0.4	9.3 ± 1.0	4.4
	EMIM-Phos	2.3 ± 0.3	19.5 ± 0.3	-	1.4 ± 0.4	11.2 ± 0.5	-
	EMIM-NTf_2	2.9 ±0.6	2.7 ± 0.9	40	0.6 ± 0.1	0.9 ± 0.0	36
	[HC1m-Cl]	0.07 ± 0.02	6.4 ± 0.4	45.8	0.9 ± 0.1	7.1 ± 0.01	43.9
Cold Lake	DIMCARB	1.02 ± 0.05	15.3 ± 0.8		1.6 ± 0.4	13.3 ± 0.1	
	EMIM-Phos	2.5 ± 0.5	20.5 ± 1.0		5.9 ± 0.3	16.3 ± 0.8	
	EMIM-NTf_2	2.7 ± 0.3	8.1 ± 0.2		1.4 ± 0.06	4.9 ± 0.04	
	[HC1m-Cl]	0.01 ± 0.003	5.9 ± 0.2		1.3 ± 0.08	7.9 ± 0.1	

[1] Reaction conditions: diluent to bitumen ratio: [redacted]; ionic liquid to dilbit ratio: 1:1 ; reaction temp: 50°C; reaction time: 1 h; settling time: overnight (approx. 14 h); stirring speed: 550 rpm; centrifugation time: 10 min; centrifugation speed: 5000rpm

[2] Reaction conditions: diluent addition: 30%; ionic liquid to dilbit ratio: 1:1; reaction temp: 50°C; reaction time: 1 h; settling time: overnight (approx. 14 h); stirring speed: 550 rpm; centrifugation time: 10 min; centrifugation speed: 5000rpm

[3] All the ICL results have been reported at reaction temp: 50°C, ratio of IL to dilbit: 1:1, reaction time : 1 h, settling time: overnight).

Contrary to the expected results, extraction efficiency was even less in the case of paraffinic diluent than that of naphthenic diluent. The reason behind this observation was not determined.

5.1.5. Metal extraction using ionic liquids from partially DAO samples

Partial deasphalting was performed in an attempt to make the material more representative of industrial practice. Solvent was added and rigorous stirring was provided for one hour and then the solution was kept in dark for 24 hour[56]. After 24 hour, solution was filtered with the aid of vacuumSer filter and the filtrate was collected. This filtrate was stored in an airtight container for further use in extraction experiments. Experiments were performed in triplicates in the similar manner as described previously in section 5.1.1. Results are shown here in Table 11.

Table 11: (%) metal recovery from Deasphalted oil (DAO)* samples using Ionic lIquids (a) 1-methyl immidazolium chloride ([HC1im]Cl+10% H_2O) and (b) 1-ethyl 3-methyl immidazolium diethyl phosphate (EMIM-DEP) - Reaction conditions: ionic liquid to DAO ratio: 1:1; reaction temp: 50°C; reaction time: 1 h; settling time: 4 h; stirring speed: 550 rpm; centrifugation time: 10 min; centrifugation speed: 5000 rpm.

Ionic Liquid	Initial Metal Content (µg/g)		Metal recovery in ILs Phase (µg/g)		(%) Metal Recovery	
	V	Ni	V	Ni	V	Ni
EMIM-DEP	112.2	63.1	9.7 ± 0.8	4.5 ± 0.04	8.7 ± 0.15	7.2 ± 0.6
[HC1im]Cl + 10%H_2O			1.4 ± 0.1	24.3 ± 2.3	1.24 ± 0.02	38.5 ± 2.1

5.1.6. Performance investigation of Acid saturated ILs

Although, vanadium recovery is still an unresolved issue in case of ionic liquid assisted metal extraction process, the ionic liquid 1-methyl immidazolium chloride ([HC1im]Cl+10% H_2O) showed nearly 40% extraction of Ni from partially DAO samples. Based on the hypothesis that porphyrins are prone to successive hydrogenation of the porphyrin leading to a chlorin metal structure and, finally, the demetallization is accomplished via the ring fragmentation, further investigation were carried out in excess of H^+ ion to accelerate the reactions at the olefin groups on the outer ring of the porphyrin.

Acid saturated [HC1im]Cl+10% H_2O ILs was prepared by varying the molar concentration of solution from 0.01M to 10M HCl concentration. Figure 6 demonstrates the metal extraction at different molar HCl concentration. It was observed that presence of acidic sites substantially affect the recovery of

nickel, however, no improvement was observed in the recovery of Vanadium. It may be related with charge density. Volume of Vanadyl ion is much higher than its charge and therefore due to less concentrated charge density, less extraction may be achieved. In case of EMIM-DEP, size of the phosphate ion is relatively larger (bulky) than the chloride ions and consequently charge density difference cause the difference in their extraction behaviour. In order to investigate the effect of cation, experiments were performed using EMIM-Cl +10% H_2O ILs at various molar concentration of HCl acid. Similar extraction behaviour was obtained which infers the dominant role of anion in metal extraction process. Also, experiments were performed using NaCl salt rather than HCl acid to investigate the effect of H^+ ion. It was observed that extraction efficiency of Nickel was increased upto 1M concentration and then it becomes constant. This observation infers the effect of H^+ ion which results into emulsion formation at higher H^+ concentration.

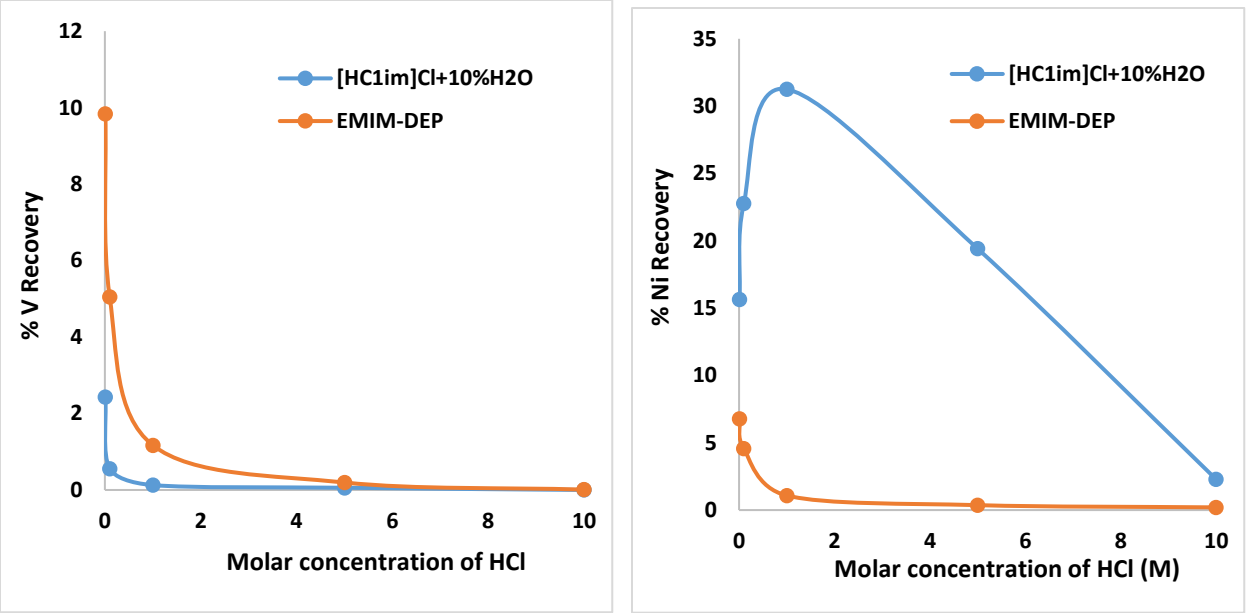

Figure 6: (%) V and (%) Ni Recovery from Bitumen using HCl Saturated Ionic lIquids 1-methyl immidazolium chloride ([HC1im]Cl+10% H_2O) and 1-ethyl 3-methyl immidazolium diethyl phosphate (EMIM-DEP)

5.1.7. Extraction experiments at High pressure

Extraction experiments at high pressure were planned in order to replicate the exact 'quick & dirty' experiments which were reported in the ICL feasibility report. These experiments were performed at 300°C and dilbit to IL ratio 40:1 using heat gun and nearly 80% V extraction was reported (ICL, London). Therefore, large scale experiments were performed using Athabasca dilbit samples in

autoclave (150 psi) at the same reaction conditions as reported. Also, experiments were performed in microreactor using 8g of partially deasphalted oil (PDAO) samples and max pressure 225 psi was attained during the reaction. However, these experiments also could not replicate the (%) extraction of vanadium. Another batch of experiments were conducted in microreactor at ratio of PDAO to DIMCARB 1:1 and 200°C reaction temperature. Max. pressure 700 psi was attained during the reaction. Reaction at such high temperature and pressure may decompose the organic component of the raw material and thus not recommended for demetallization.

Table 12: % V and % Ni recovery at high temperature and high pressure reaction conditions and ratio of sample to Ils 40:1

Sample	Sample Size	Ionic Liquid (DIMCARB)	System	Reaction condition	Max Pressure Attained	% V	% Ni
Dilbit (Suncor Bitumen + Naptha)	150g	3.5g	Autoclave	Temp. 300°C, Reaction Time : 1 h, Stirring: 300rpm, Dilbit to ILs ratio: 40:1	150 psi	1.753	1.764
DAO (using C5/C6 mixture)	8g	~0.2g	Micro-reactor in sandbath	Temp. 300°C, Reaction Time : 1 h, Stirring: Not provided, DAO to Ils ratio: 40:1	225 psi	0.4 ± 0.07	3.5 ± 0.1
DAO (using C5/C6 mixture)	8g	~0.2g	Micro-reactor+ hot- plate	Temp. 200°C, Reaction Time: 1 h, Stirring: 550rpm, DAO to Ils ratio: 40:1	200 psi	0.5 ± 0.2	5.8 ± 0.7

5.1.8. Ionic Liquid Assisted Extraction Using Albian Dilbit Samples

Ionic Liquid assisted metal extraction experiments were performed using Albian Dilbit samples . Four ionic liquids namely DIMCARB, EMIM-NTF_2, HC_1imCl+10%H_2O and EMIM-SCN were chosen on the basis of their performance with Athabasca dilbit samples. Ionic liquid (20.0 g) was added to the equal amount of dilbit samples in a glass vial along with a cross magnetic stirrer. Continuous stirring at 550rpm was provided in order to ensure sufficient interaction between ionic liquid and dilbit samples. Samples were heated to 50°C for one hour and then the sample(s) were left to settle for 4

hour at the same reaction temperature. Under LED light, a two-phase separation could be clearly observed. Both phases were separated and centrifuged at 5000 rpm for 10 min. in order to remove any contaminants from the opposing phase. All the experiments were performed in triplicates. Metal content was determined in both of the recovered phases using ICP-OES analysis.

Reaction parameters (ratio of ionic liquid to dilbit and reaction time) were optimized by varying the reaction time from 10min to 60 min and ratio of ILs to dilbit from 0.2 to 2 (w/w). Results are shown in Figure 7 and Figure 8 to illustrate the effect of reaction time and ratio of Ils to dilbit respectively.

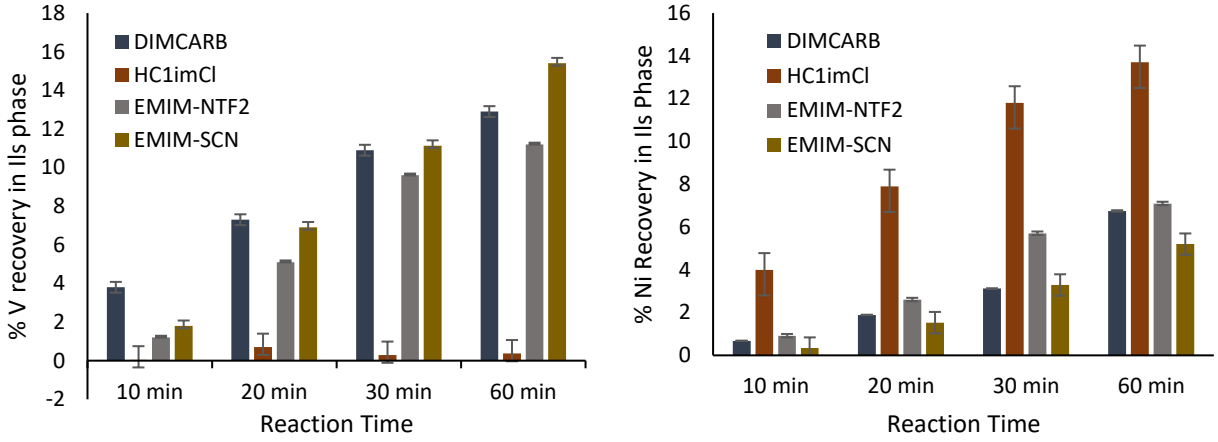

Figure 7: Effect of reaction time on metal extraction from Albial dilbit sample (Metal content in dilbit sample V = 143 ± 5.8 µg/g; Ni = 59.7± 2.3 µg/g; Reaction conditions: ionic liquid to dilbit ratio: 1:1 (w/w); reaction temp: 50°C; settling time: 4 h; stirring speed: 550 rpm; centrifugation time: 10 min; centrifugation speed: 5000rpm)

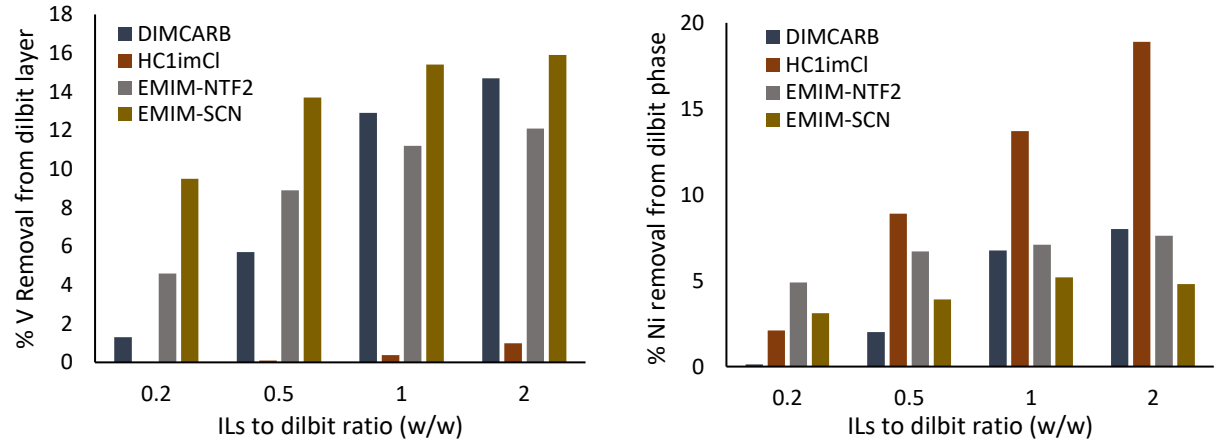

Figure 8: Effect of reaction time on metal extraction from Albial dilbit sample (Metal content in dilbit sample V = 143 ± 5.8 µg/g; Ni = 59.7± 2.3 µg/g; Reaction conditions: reaction temp:

50°C; reaction time : 1 h; settling time: 4 h; stirring speed: 550 rpm; centrifugation time: 10 min; centrifugation speed: 5000rpm)

Further experiments were conducted to ensure the possibility of equilibrium assisted extraction process using Albian dilbit samples. Three cycles of experiments were performed using the same dilbit sample during all cycles, while fresh ionic liquid was used in each cycle. Results indicated the possibility of multistage extraction process. Figure 9 illustrates the data for vanadium and nickel extraction from Albian dilbit samples using DIMCARB and EMIM-SCN ionic liquid.

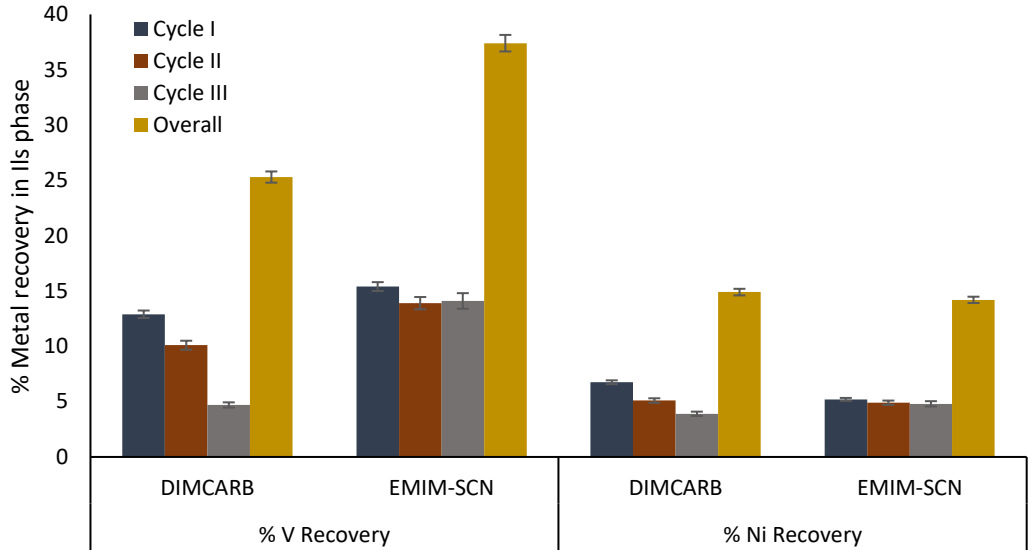

Figure 9: Equilibrium assisted extraction of metal (Reaction conditions: Initial metal concentration in Albian dilbit samples 143 ± 5.8 µg/g; Ni = 59.7± 2.3 µg/g; Reaction Temp: 50°C, Reaction time: 1h, Settling time: 4h, Ratio of ILs to dilbit ratio =1:1, stirring speed: 550rpm)

5.1.9. Inferences

Major findings of the illustrated ionic liquid assisted extraction process are listed below:

i) None of the ionic liquid demonstrated a significant V/Ni extraction in a single equilibrium stage extraction. Though, out of the all investigated ionic liquids, Dimethlyammonium dimethyl-carbamate (DIMCARB) showed highest extraction of metals from dilbit samples.

ii) Along with the extraction of metals, selectivity of ionic liquids for oil extraction was also considered as a deciding factor. Selectivity of various ionic liquid was investigated by performing Simulated Distillation analysis of organic and ionic liquid phases. Dimethlyammonium dimethyl-carbamate, inspite of showing the considerable metal extraction, was observed to be a non-selective ionic liquid. Significant amount of organic content was detected in ionic liquid phase.

iii) On the contrary, 1-ethyl-3-methyl imidazolium thiocyanate (EMIM-SCN) and 1-methyl imidazolium chloride ([HC1im]Cl+10% H_2O) were observed to be selective. No evidence was found that oil was observed in the extracted ionic liquid phase. However, the extraction efficiency for single equilibrium stage extraction was less than 10% for these ionic liquids.

iv) Efforts were also made to optimize the process parameters. Reaction parameters were optimized by varying the reaction temperature, ratio of dilbit to ionic liquid, reaction time, settling time, stirring speed. Variation of stirring speed could not show any noticeable increase in metal extraction with the increase in stirring speed. This observation indicated that the ionic liquid assisted extraction was not a mass transfer limited process over the extraction periods investigated.

v) Possibility of equilibrium assisted extraction process was investigated. 1-ethyl-3-methyl imidazolium thiocyanate (EMIM-SCN) was chosen to study the multistage extraction, considering its high selectivity (i.e. little or no oil co-extraction with the metals). Three cycles of experiments were performed using the same dilbit sample during all cycles, while fresh ionic liquid was used in each cycle. Results indicated the possibility of equilibrium assisted extraction process. By employing three equilibrium stages, the overall vanadium extraction was increased from around 4 to 12 %.

In conclusion, it was found that some of the ionic liquids were selective for the extraction of the metals in the presence of little or no oil. It was further found that for the selective ionic liquid that was further evaluated (EMIM-SCN), the extraction was an equilibrium limited extraction. It was therefore possible to increase extraction by employing more than one equilibrium stage.

5.2. Photo-irradiation Assisted Extraction for Demetallization of Dilbit Samples

In photochemical separation, a combination of photochemical reaction and liquid-liquid extraction is employed to recover vanadium and nickel from bitumen. In this process, the bound-type metalloporphyrins are postulated to photodissociate in presence of a hydrogen donor solvent to convert 'bound' into 'free' type metalloporphyrins. The resulting solution is photodecomposed by UV irradiation to release the metal ions into solution, which can be selectively removed by solvent extraction. To examine the photoreactivity of vanadyl(IV)tetraphenyllporphyrin (VOTPP), the tetralin solution containing VOTPP was photoirradiated under air bubbling in the absence of an aqueous phase. Practically no decrease in the VOTPP concentration was observed using a LED light source.

Further, photochemical reaction was performed in a photoreactor. A medium pressure mercury lamp was employed to provide UV wavelength range for the photodecomposition of porphyrin compounds

in dilbit samples. Preliminary experiments were performed using model compound 5,10,15,20-Tetraphenyl-21H,23H-porphine vanadium(IV) oxide. 15 ppm vanadium concentration solution was prepared in tetralin solvent and deionized water was added into equal proportion. The organic-aqueous solution was photo-irradated for 1hour and 4 hour. After the reaction, the aqueous layer was analyzed in ICP. Nearly 10% and 50% Vanadium was obtained in aqueous solution after 1h and 4h photo-irradiation respectively.

Another experiment was carried out using dilbit sample. 100g tetralin-decalin solution was prepared with 10% dilbit sample. 50g 2-propanol was added to the solution as a hydrogen donating solvent and photo-irradiated for 6h. After the reaction, the propanol was evaporated using rotary evaporator and then liquid liquid extraction was performed using 1N HCl solution. Centrifugation was performed at 7000 rpm for 30 minutes and the bottom layer was analyzed. Only 0.13% V was extracted in the bottom layer. Table 13 lists the major observations based on photo irradiation assisted demetallization process.

Table 13: Demetallization of dilbit samples using photo irradiation assisted extraction process

Sample	Initial V conc. [mg/kg]	Initial Ni conc. [mg/kg]	Final V conc. in aqueous phase [mg/kg]	V removal [wt%]*	Final Ni conc. [mg/kg]	% Ni removal
1 hour irradiation - Model compound (VOTPP)	15	NA	0.74	9.9	NA	NA
4 hours irradiation - Model compound (VOTPP)	15	NA	4.3	57.3	NA	NA
6 hours irradiation - Bitumen/HCl extraction	228	93	0.02	0.1	0.13	1.4
6 hours irradiation - Bitumen/HCl extraction	228	93	0.01	0.0	0	0

* Removal based on the determined concentration in the IL.
NA = Not applicable because the model compound tested contained only V.

In conclusion, photo-irradiation assisted extraction cannot be used on dark samples, since most of the light is absorbed by the bulk medium. However, the work showed that this technique may have some value in removing metals from white products.

5.3. Electrochemical Demetallization of Dilbit samples

Electrochemical separation is based on the similar hypothesis as photochemical assisted extraction process. An electrochemical treatment is followed by liquid-liquid extraction. The bitumen is subjected to electrochemical treatment in order to displace the metal ions in the metalloporphyrins. The released metal ions can then be extracted by employing a liquid-liquid extraction process.

Experiments were conducted using model compound 5,10,15,20-Tetraphenyl-21H,23H-porphine vanadium(IV) oxide (VOTPP) to ensure the applicability of electrochemical process for demetallization of dilbit samples. 25-ppm vanadium concentration solution was prepared by dissolving certain amount of VOTPP in the solvent mixture of 80 ml tetrahydrofuran and 20 ml methanol. Lithium perchlorate ($LiClO_4$) was used as an electrolyte during the experiments. A three-electrode electrochemical cell was used and electrolysis was carried out at - 2.5V vs. Ag/Ag+ constant potential using a lead working electrode of 3 cm^2 and a glassy carbon electrode as counter electrode at room temperature for 24h, under magnetic stirring. Solid residue was obtained in the bottom of the flask as well as on anode at the end of the reaction. 100ml of toluene was added in order to wash the solid residue and then, the residue was separated by filtration. The remaining solvent was removed in rotary evaporator under vacuum and the resultant product were analyzed for nickel and vanadium content using ICP-OES. Nearly 69.4% vanadium was recovered in the residue.

Similar experiments were conducted using Athabasca and Albian dilbit sample. Control experiments were conducted with raw dilbit sample without adding any electrolyte or protonating agent. To decrease the viscosity of the sample, 50% toluene was added to the raw Albian dilbit sample. Eletrolysis was performed for 24 hours however, no reaction was observed. Further experiments were conducted with the addition of electrolyte and protonating agent. 100g THF-Methanol solution was prepared with 5 wt% of dilbit sample and varying concentration of protonating agent methanol. Electrolysis was carried out in the similar manner as described for model compounds. 23.8 % Vanadium was removed from Athabasca dilbit sample whereas nearly 35.4% Vanadium was removed from Albian dilbit sample when 20% methanol was used as protonating agent during the reaction. Recovery of nickel was less than 8 % for both dilbit samples. Major findings have been listed here in Table 14.

Table 14: Demetallization of dilbit samples using Electrochemical assisted extraction process

Sample	Initial V conc. [µg/g]	Initial Ni conc. [µg/g]	Final V conc. in dilbit sample [µg/g]	V removal [wt%]*	Final Ni conc. [µg/g]	% Ni removal
6 hour electrolysis - Model compound (VOTPP)	25	NA	12.2	51.1	NA	NA
24 hours electrolysis - Model compound (VOTPP)	25	NA	7.6	69.4	NA	NA
24 hours electrolysis – Athabasca Dilbit + 10% Methanol-THF solution	166	65	136.9±3.8	17.5± 1.2	61.9 ± 1.1	4.7 ± 0.41
24 hours electrolysis- Athabasca Dilbit + 20% Methanol-THF solution	166	65	126.5 ± 5.1	23.8 ± 3.5	61.7 ± 2.3	5.1±0.87
24 hours electrolysis – Albian Dilbit + 10% Methanol-THF solution	143	59.7	103.5	27.6	54.9	8.0
24 hours electrolysis- Albian Dilbit + 20% Methanol-THF solution	143	59.7	92.3 ± 6.9	35.4 ± 4.1	54.7 ± 4.8	8.3 ± 0.6

* Removal based on the determined concentration in the dilbit layer.

NA = Not applicable because the model compound tested contained only V.

In conclusion, it was possible to remove some metals from dilbit by electrochemical demetallization. This is the least developed of the techniques investigated; work on this method commenced only during October 2018.

6. Conclusions & Recommendations

The project to investigate and evaluate vanadium removal from oilsands bitumen is approaching the end of its funding period. None of the processes investigated enabled high V and Ni removal from bitumen. Based on current best understanding the following recommendations for future work are made:

a) In case of Ionic Liquid assisted demetallization process, some of the ionic liquids were found to be selective for the extraction of the metals in the presence of little or no oil. It was further found that

for the selective ionic liquid which was further evaluated (EMIM-SCN), the extraction was an equilibrium limited extraction. It was therefore possible improve the recovery from selective extraction by adding equilibrium stages. However, following points are still need to be investigated in order to design an effective ionic liquid assisted demetallization process:

i) Nature of the separation: There are indications that extraction is limited by equilibrium, but it is not clear whether this is due to a chemical equilibrium between the VO^{2+} and porphyrin, or a partitioning of vanadyl porphyrins between phases. The nature of the equilibrium will influence potential engineering strategies to improve extraction effectiveness.

ii) Yield Loss: What is the nature of the yield loss associated with vanadium extraction? Due to the large volumes of bitumen that need to be processed, even small losses could undermine the economic viability.

iii) Equilibrium staged separation: Obtain equilibrium curves for ionic liquids with high selectivity to enable multi-stage separator design.

iv) Effect of demetallization on bitumen samples: How does demetalization affect the properties of the demetalized bitumen? It would be important to make sure that the ionic liquid demetalation process did not negatively affect bitumen for further upgrading (i.e. ionic liquids performed a physical separation only and did not lead to chemical reactions).

b) Electrochemical demetallization of model compounds and dilbit samples illustrated considerable metal recovery. Yet, this approach is still in an early stage of investigation. It is important to look for a solution to some unanswered questions:

i) Electron transfer Mechanism: Bitumen may contain variety of metalloporphyrins and the potential range may differ for different metalloporphyrins. Therefore, it is important to understand the electron transfer mechanism occurring in metalloporphyrins at different potential range in order to improve the vanadium recovery.

ii) What could be the important internal (structural) and external (operating conditions) factors which may affect the demetallization efficiency?

iii) What type of electrode material could be used to perform the electrochemical demetallization in a cost-effective manner?

References

1. Wang, S.; Yang, J.; Xu, X. Effect of the cationic starch on removal of Ni and V from crude oils under microwave irradiation. Fuel 2011, 90, 987−991.
2. Beach, L.; Shewmaker, J. The Nature of Vanadium in Petroleum. Extraction and Volatility Studies. Ind. Eng. Chem. 1957, 49, 1157−1164.
3. Munoz, R. A. A.; Oliveira, P. V.; Angnes, L. Combination of Ultrasonic Extraction and Stripping Analysis: An Effective and Reliable Way for the Determination of Cu and Pb in Lubricating Oils. Talanta 2006, 68 (3), 850–856.
4. Zheng, L.; Cao, F.; Xiu, J.; Bai, X.; Motto-Ros, V.; Gilon, N.; Zeng, H.; Yu, J. On the Performance of Laser-Induced Breakdown Spectroscopy for Direct Determination of Trace Metals in Lubricating Oils. Spectrochim. Acta - Part B At. Spectrosc. 2014, 99, 1–8.
5. Cinosi, A.; Andriollo, N.; Pepponi, G.; Monticelli, D. A Novel Total Reflection X-Ray Fluorescence Procedure for the Direct Determination of Trace Elements in Petrochemical Products. Anal. Bioanal. Chem. 2011, 399 (2), 927–933.
6. Santos, D. S. S.; Guida, M. a B.; Lemos, V. a; Teixeira, L. S. G. Determination of Copper, Iron, Lead and Zinc in Gasoline by Sequential Multi- Element Flame Atomic Absorption Spectrometry after Solid Phase Extraction. J. Brailian Chem. Soc. 2011, 22 (3), 552–557.
7. El-Gayar, M. S. Utilization of Trace Metals and Sulfur Contents in Correlating Crude Oils and Petroleum Heavy Ends. Pet. Sci. Technol. 2003, 21 (5), 719–726.
8. Resano, M.; Vanhaecke, F.; de Loos-Vollebregt, M. T. C. Electrothermal Vaporization for Sample Introduction in Atomic Absorption, Atomic Emission and Plasma Mass Spectrometry—a Critical Review with Focus on Solid Sampling and Slurry Analysis. J. Anal. At. Spectrom. 2008, 23 (11), 1450.
9. Aucélio, R. Q.; Doyle, A.; Pizzorno, B. S.; Tristão, M. L. B.; Campos, R. C. Electrothermal Atomic Absorption Spectrometric Method for the Determination of Vanadium in Diesel and Asphaltene Prepared as Detergentless Microemulsions. Microchem. J. 2004, 78 (1), 21–26.
10. Cassella, R. J.; Brum, D. M.; de Paula, C. E. R.; Lima, C. F. Extraction Induced by Emulsion Breaking: A Novel Strategy for the Trace Metals Determination in Diesel Oil Samples by Electrothermal Atomic Absorption Spectrometry. J. Anal. At. Spectrom. 2010, 25 (11), 1704.

11. He, Y.-M.; Zhao, F.-F.; Zhou, Y.; Ahmad, F.; Ling, Z.-X. Extraction Induced by Emulsion Breaking as a Tool for Simultaneous Multi-Element Determination in Used Lubricating Oils by ICP-MS. Anal. Methods 2015, 7, 4493–4501.
12. Cassella, R. J.; Brum, D. M.; Lima, C. F.; Caldas, L. F. S.; de Paula, C. E. R. Multivariate Optimization of the Determination of Zinc in Diesel Oil Employing a Novel Extraction Strategy Based on Emulsion Breaking. Anal. Chim. Acta 2011, 690 (1), 79–85.
13. de Souza, R. M.; Saraceno, A. L.; da Silveira, C. L. P.; Aucélio, R. Q. Determination of Trace Elements in Crude Oil by ICP-OES Using Ultrasound-Assisted Acid Extraction. J. Anal. At. Spectrom. 2006, 21 (11), 1345–1349.
14. Oliveira, J. S. S.; Picoloto, R. S.; Bizzi, C. A.; Mello, P. A.; Barin, J. S.; Flores, E. M. M. Microwave-Assisted Ultraviolet Digestion of Petroleum Coke for the Simultaneous Determination of Nickel, Vanadium and Sulfur by ICP-OES. Talanta 2015, 144, 1052–1058.
15. Pereira, L. S. F.; Iop, G. D.; Flores, E. M. M.; Burrow, R. A.; Mello, P. A.; Duarte, F. A. Strategies for the Determination of Trace and Toxic Elements in Pitch: Evaluation of Combustion and Wet Digestion Methods for Sample Preparation. Fuel 2016, 163, 175–179.
16. Duyck, C.; Miekeley, N.; Porto da Silveira, C. L.; Aucélio, R. Q.; Campos, R. C.; Grinberg, P.; Brandão, G. P. The Determination of Trace Elements in Crude Oil and Its Heavy Fractions by Atomic Spectrometry. Spectrochim. Acta - Part B At. Spectrosc. 2007, 62 (9), 939–951.
17. Silva, M. M.; Damin, I. C. F.; Vale, M. G. R.; Welz, B. Feasibility of Using Solid Sampling Graphite Furnace Atomic Absorption Spectrometry for Speciation Analysis of Volatile and Non-Volatile Compounds of Nickel and Vanadium in Crude Oil. Talanta 2007, 71 (5), 1877–1885.
18. Sperling, M.; Welz, B.; Hertzberg, J.; Rieck, C.; Marowsky, G. Temporal and Spatial Temperature Distributions in Transversely Heated Graphite Tube Atomizers and Their Analytical Characteristics for Atomic Absorption Spectrometry. Spectrochim. Acta - Part B At. Spectrosc. 1996, 51 (9–10), 897–930.
19. Sant'Ana, F. W.; Santelli, R. E.; Cassella, A. R.; Cassella, R. J. Optimization of an Open-Focused Microwave Oven Digestion Procedure for Determination of Metals in Diesel Oil by Inductively Coupled Plasma Optical Emission Spectrometry. J. Hazard. Mater. 2007, 149 (1), 67–74.

20. Hearn, R.; Berglund, M.; Ostermann, M.; Pusticek, N.; Taylor, P. A Comparison of High Accuracy Isotope Dilution Techniques for the Measurement of Low Level Sulfur in Gas Oils. Anal. Chim. Acta 2005, 532 (1), 55–60.

21. Caumette, G.; Lienemann, C. P.; Merdrignac, I.; Paucot, H.; Bouyssiere, B.; Lobinski, R. Sensitivity Improvement in ICP MS Analysis of Fuels and Light Petroleum Matrices Using a Microflow Nebulizer and Heated Spray Chamber Sample Introduction. Talanta 2009, 80 (2), 1039–1043.
22. Giusti, P.; Nuevo Ordóñez, Y.; Philippe Lienemann, C.; Schaumlöffel, D.; Bouyssiere, B.; Łobiński, R. μFlow-injection–ICP Collision Cell MS Determination of Molybdenum, Nickel and Vanadium in Petroleum Samples Using a Modified Total Consumption Micronebulizer. J. Anal. At. Spectrom. 2007, 22 (1), 88–92.
23. Ware, R. A.; Wei, J. Catalytic Hydrodemetallization of Nickel Porphyrins I. Porphyrin Structure and Reactivity. J. Catal. 1985, 93, 100−121.
24. Ali, M. F.; Abbas, S. A review of methods for the demetallization of residual fuel oils. Fuel Process. Technol. 2006, 87, 573−584.
25. Jarullah, A. T.; Mujtaba, I. M.; Wood, A. S. Kinetic model development and simulation of simultaneous hydrodenitrogenation and hydrodemetallization of crude oil in trickle bed reactor. Fuel 2011, 90, 2165−2181.
26. Rana, M. S.; Ancheyta, J.; Rayo, P.; Maity, S. K. Catal. Today 2004, 98, 151−160.
27. Ancheyta-Juárez, J.; Maity, S. K.; Betancourt-Rivera, G.; Centeno-Nolasco, G.; Rayo-Mayoral, P.; Gómez-Pérez, M. T. Comparison of different Ni-Mo/alumina catalysts on hydrodemetallization of Maya crude oil. Appl. Catal., A 2001, 216, 195−208.
28. Ware, R. Catalytic hydrodemetallization of Nickel Porphyrins. III. Acid-Base Modification of Selectivity. J. Catal. 1985, 93, 135−151.
29. Ancheyta, J. Reactors for hydroprocessing. In Hydroprocessing of heavy oils and residua; Ancheyta, J., Speight, J. G. Eds.; CRC Press: Boca Raton, 2007, p.71-120.
30. Reynolds, G. J.; Biggs, W. R. ; Bezman, S. A. Removal of heavy metals from residual oils. ACS Symposium Series 1987, 344, 205–219.
31. Atwood, L.; Atwood, W. Improvement in preparing oil from bitumens U.S. Patent 15,506, Aug. 12, 1856.
32. Burges, W. J. Removing grease from leather. U.S. Patent 176,423, April 25, 1876.

33. Maxwell, J. R.; Pillinger, C. T.; Eglinton, G. Organic geochemistry. Quarterly Reviews, Chemical Society 1971, 25, 571–628.
34. Arod, J.; Bartoli, B.; Bergez, P.; Biedermann, J.; Rossarie, J. Process for the treatment of hydrocarbon charge by high temperature ultrafiltration. US Patent No. 4,411,790, Assigned to Commissariat a l'Energie Atomique and Compagnie Francais de Raffinage, 1983.
35. Duong, A.; Chattopadhyaya, G.; Kwok, W.; Smith, K. An experimental study of heavy oil ultrafiltration using ceramic membranes. Fuel 1997, 76 (9), 821–828.
36. Awokoya, K.; Moronkola, B.; Chigome, S.; Ondigo, D.; Tshentu, Z.; Torto, N. Molecularly imprinted electrospun nanofibers for adsorption of nickel-5,10,15,20-tetraphenylporphine (NTPP) in organic media. J. Polym. Res. 2013, 20, 1−9.
37. R.E. Overfield, Integrated method for extracting nickel and vanadium compounds from oils. US Patent No. 4643821 Assigned to Exxon Research and Engineering Co., USA, 1987.\
38. Dietz, M. L.; Dzielawa, J. A. Ion-exchange as a mode of cation transfer into room-temperature ionic liquids containing crown ethers: implications for the 'greenness' of ionic liquids as diluents in liquid–liquid extraction. Chem. Commun. 2001, 20, 2124-2125.
39. Jensen, M. P.; Dzielawa, J. A.; Rickert, P.; Dietz, M. L. EXAFS investigations of the mechanism of facilitated ion transfer into a room-temperature ionic liquid. J. Am. Chem. Soc. 2002, 124, 10664-10665.
40. Dietz, M. L.; Dzielawa, J. A.; Laszak, I.; Young, B. A.; Jensen, M. P. Influence of solvent structural variations on the mechanism of facilitated ion transfer into room-temperature ionic liquids. Green Chem. 2003, 5, 682-685.
41. Gould, K. A. Oxidative demetallization of petroleum asphaltenes and residua. Fuel 1980, 59(10), 733–736.
42. Acevedo, D.; D'Elia Camacho, L. F.; Moncada, J.; Puentes, Z. Electrochemically assisted demetallisation of model metalloporphyrins and crude oil porphyrinic extracts in emulsified media, by using active permeated atomic hydrogen. Fuel 2012, 92 (1), 264−270.
43. Welter, K.; Salazar, E.; Balladores, Y.; Márquez, O. P.; Márquez, J.; Martínez, Y. Electrochemical removal of metals from crude oil samples. Fuel Process. Technol. 2009, 90, 212−221.
44. Ovalles, C.; Rojas, I.; Acevedo, S.; Escobar, G.; Jorge, G.; Gutierrez, L. B.; Rincon, A.; Scharifker, B. Upgrading of Orinoco Belt crude oil and its fractions by an electrochemical system in the presence of protonating agents. Fuel Process. Technol. 1996, 48, 159−172.

45. Greaney, M. A.; Kerby, M. C.; Olmstead, W. N.; Wiehe, I. A. Method for demetallating refinery feedstreams. U.S. Patent 8,440,438, June 25, 1996.
46. Mandal, P. C.; Wahyudiono; Sasaki, M.; Goto, M. Nickel removal from nickel etioporphyrin (Ni-EP) using supercritical water in the absence of catalyst. Fuel Process. Technol. 2012, 104, 67−72.
47. Mandal, P. C.; Wahyudiono; Sasaki, M.; Goto, M. Non-catalytic vanadium removal from vanadyl etioporphyrin (VO-EP) using a mixed solvent of supercritical water and toluene: A kinetic study. Fuel 2012, 92, 288−294.
48. Shiraishi, Y.; Hirai, T.; Komasawa, I. A Novel Demetalation Process for Vanadyl- and Nickelporphyrins from Petroleum Residue by Photochemical Reaction and Liquid−Liquid Extraction. Ind. Eng. Chem. Res. 2000, 39, 1345−1355.
49. Tu, S. P.; Yen, T. F. The Feasibility Studies for Radical-Induced Decomposition and Demetalation of Metalloporphyrins by Ultrasonication. Energy Fuels 2000, 14, 1168−1175.
50. Wang, S.; Yang, J.; Xu, X.; Gao, J. Influence of the Microwave Method on Vanadium Removal in Crude Oil. Pet. Sci. Technol. 2009, 27, 368−378.
51. Kim, D.; Tu, S. P.; Yen, T. F. Evaluation of Versatile Ultrasonic Effects on Degradation of Organometallics from Petroleum. Environ. Eng. Res. 2003, 8, 59−71.
52. Salehizadeh, H.; Mousavi, M.; Hatamipour, S.; Kermanshahi, K. Microbial Demetallization of Crude Oil Using Aspergillus sp.: Vanadium Oxide Octaethyl Porphyrin (VOOEP) as a Model of Metallic Petroporphyrins. Iran. J. Biotechnol. 2007, 5, 31−226.
53. de Souza, R. M.; Saraceno, A. L.; Duyck, C.; da Silveira, C. L. P.; Aucélio, R. Q. Determination of Fe, Ni and V in Asphaltene by ICP OES after Extraction into Aqueous Solutions Using Sonication or Vortex Agitation. Microchem. J. 2007, 87 (2), 99–103.
54. De Souza, R. M.; Meliande, A. L. S.; Da Silveira, C. L. P.; Aucélio, R. Q. Determination of Mo, Zn, Cd, Ti, Ni, V, Fe, Mn, Cr and Co in Crude Oil Using Inductively Coupled Plasma Optical Emission Spectrometry and Sample Introduction as Detergentless Microemulsions. Microchem. J. 2006, 82 (2), 137–141.
55. Serban, M.; Bhat-Tacharyya, A.; Mezza, B. J.; Vanden Bussche, K. M.; Nicholas, C.P.; Bennion, W. K. Patent WO 2011/090610 A2. 2011, Illinois, Patent Cooperation Treaty (PCT).
56. Tipman, R. Froth treatment. In Handbook on theory and practice of bitumen recovery from Athabasca oil sands. Vol. II. Industrial practice; Masliyah, J.; Xu, Z.; Dabros, M. Eds.; Kingsley Knowledge Publishing, 2013, p.211-253.

Appendix D –Benchtest Report by Shell at Imperial College of London (ICL)

Benchtest Report.docx

Metal Removal and Recovery from Crude Oils via Ionic Liquids (ILs)

Bench Test Report

Paul J. Corbett

March 2018

Revision	Author	Reviewers
1	Paul J. Corbett	Mrudula Paranjape (CNRL)
2	Paul J. Corbett	JT Steenkamp (Shell) Juan Dominguez (Shell)

Table of Contents

Extraction Study to Remove Porphyrinic Vanadium and Nickel Complexes Using ILs

In this section, we assess the capabilities of six ILs in the extraction of vanadium (V) and nickel (Ni) from dilbit samples via a biphasic extraction. We report the details of the ILs, why they are selected and the extraction percentages for a 1:1 (dilbit:IL) procedure.

A varying range of ILs were selected in the extraction of V and Ni from the dilbit samples:

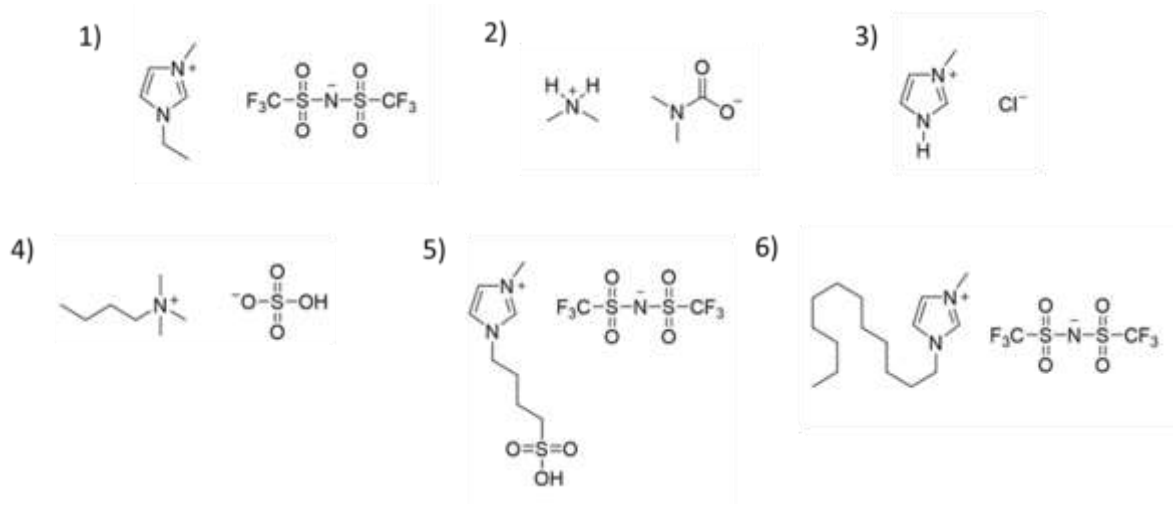

Figure 1 *– Chemical Structures for the ILs used in this study; 1) $[C_2C_1im][N(Tf)_2]$ (emim bisimide), 2) dimethylammonium dimethylcarbamate (dimcarb), 3) $[HC_1im]Cl$ (hmim chloride), 4) $[N_{4420}][HSO_4]$ (DMBA HSO_4) and 5) $[C_8H_{15}N_2O_3S][N(Tf)_2]$ (sulfonic bisimide), 6) $[C_{12}C_1im][N(Tf)_2]$ (dodecyl bisimide)*

The range of ILs were selected to determine which cationic and anionic components of ILs are effective in the extraction of V and Ni from dilbit samples. Dialkylimidazolium (with methyl, ethyl and dodecyl alkyl chains) and trialkylammonium (with methyl, ethyl and butyl alkyl chains) based ILs were selected due to their varying cationic properties, with individual ring structures, and their alkyl chain lengths yielding variety of structure without the incorporation of additional functional groups. Specific to the structures, the imidazolium-based cations contain a delocalized charged ring whereas the ammonium-based cations provide a charged atom. The anion will play the key part in chelation to the metal center we have selected here three ILs with the same $[N(Tf)_2]^-$ anion so that the effect of the cation can be monitored. The anions in this study were employed for a number of reasons in addition to being thought of as suitable candidates to coordinate to the metals. Specific details are below:

- The $[N(Tf)_2]^-$ anion were selected due to being widely used and thus there exists vast amounts of physical property data about them. Due to the electron withdrawing fluorine groups it would be expected that IL based in this anion will have a lower ability than the other ILs in the extraction of the target metals, however, it can be seen from a patent in this area[1], that $[C_2C_1im][N(Tf)_2]$ was able to remove both V and Ni in good yield from Medium Arabian Crude Oil.

- The $[HSO_4]^-$ anion was employed to allow the determination of whether anion-based H bond donation could have a major role in chelation. The $[HSO_4]^-$ based alkylammonium ILs are particularly inexpensive thus if they perform well in the metal extraction they would be very appealing to a scale up application.

- The chloride (Cl^-) anion was selected to examine possible formation of a metal precipitate within the extraction (after strong direct metal-anion coordination), and to determine how this could affect the purification approach. Cl^- based ILs have been known to also perform well in pervious extraction of metals from hydrocarbon streams due being small and highly charged thus having a large charge density.

Experimental

Figure 2 *– Hot Plate Stirrer with multi-welled heating blocks*

The ionic liquid of choice (Figure 1) (3.00g) was added to the dilbit sample (3.00 g) in a glass vial along with a cross magnetic stirrer. This was then heated to 50 °C and stirred in a carousel along with another two identical samples for repeatability. After one hour, the sample was left to settle overnight at 50 °C, where under LED and UV light a two-phase separation could be observed (Figure 3). 1 mL of each phase was then transferred to a centrifuge tube where centrifugation allowed any contaminants from the opposing phase to be removed. The samples would then be processed for ICP analysis via acid digestion. 200 mg of each phase of the extraction was transferred to high pressure microwave tube in addition to HCl (3 mL) and HNO_3 (9 mL). These were then sealed and digested in a high-pressure microwave oven for 10 minutes, the samples were then diluted and filtered accordingly ready for analysis via ICP-MS.

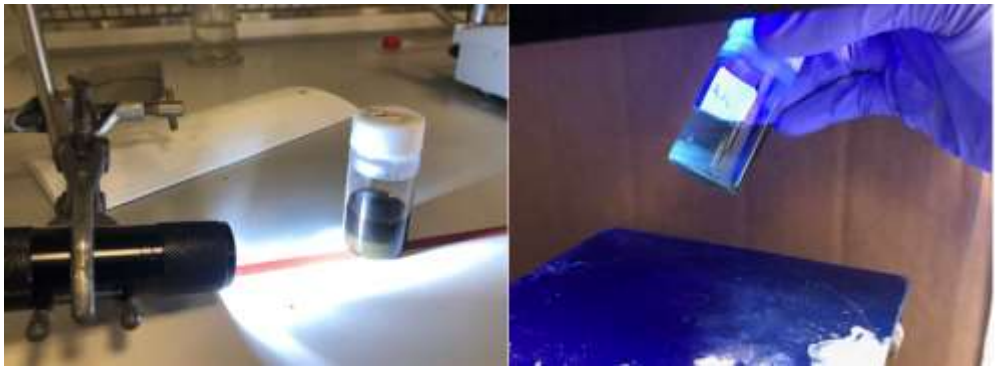

Figure 3 *– Biphasic separation of bitumen and dimcarb under an LED light (left) and under UV light (right)*

Results

The ILs provided a range of abilities to extract both V and Ni to varying degrees. However, it is assumed that there are mixing issues due to the sample on the inner of the carousel always providing a higher extraction. Thus, to provide more reliable results, complete mixing of the two phases needs to be ensured. This can be achieved by an overhead mixture or decreasing the sample frequency to provide a better interaction between the hotplate and magnetic stirrer.

Table 1 *- Extraction percentages for V and Ni from dilbit using a range of ionic liquids based on a dilbit pre-extraction concentration of 120 ppm and 46 ppm respectively.*

Ionic Liquid	V Extraction (%)	Ni Extraction (%)
$[C_2C_1im][N(Tf)_2]$	40.00	36.96
dimethylammnium dimethylcarbamate	13.33	4.35
$[HC_1im]Cl$	45.83	43.48
$[C_{12}C_1im][N(Tf)_2]$	13.33	2.17
$[C_8H_{15}N_2O_3S][N(Tf)_2]$	26.67	32.61
$[N_{4420}]HSO_4]$ (20% Water)	18.33	13.04

Electrochemical Study of Porphyrinic Vanadium Complexes in ILs

In the section, we assess 6 ILs for the electrochemical visibility of V complexes to determine the feasibility of isolating V complexes post-extraction. This is carried out via cyclic voltammetry which enables the potential to see redox reactions of the V in the IL. We report the cyclic voltammograms displaying the difference between the neat ILs and V-doped ILs.

Prior to the correct procedure being implemented enabling the recycling the IL and isolation of the metal compounds of desire, the electrochemistry of V in each IL needs to be assessed. The ILs will be doped with a V complex to resemble the structure and concentration seen in the field. The IL will then be filtered and the nature of the vanadium complex will be assessed via an electrochemical technique known as cyclic voltammetry.

This will provide us with data on the oxidation state of the V in the IL and allow the design of a suitable pathway to isolate the most suitable form of V.

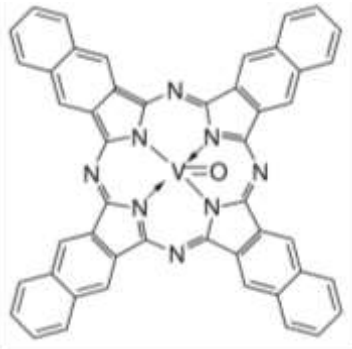

Figure 4 *- Chemical structure for vanadyl 2,3-naphthalocyanine*

The porphyrinic complex (Figure 4) was selected due to being inexpensive and displaying a similar structure to the complexes found naturally in crude oil. Figure 5 displays a Pourbaix diagram for vanadium complexes in water, due to the absence of data available for V in ILs this will be our reference to see what complexes are in solution as they will be roughly similar.

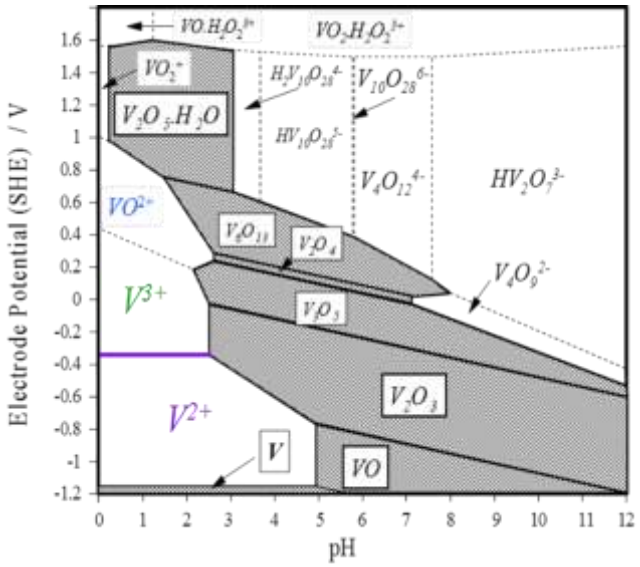

Figure 5 *- Pourbaix Diagram for Vanadium Complexes in Water*

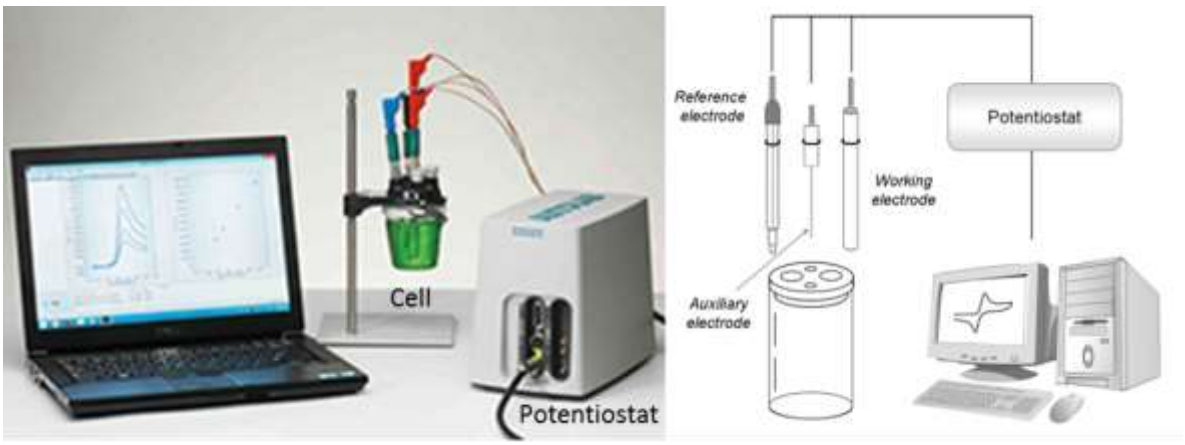

Figure 6 *– Setup for measurement of Cyclic Voltammetry; Photograph (Left) and Schematic (Right)*

Experimental

Two sets of the Ionic liquids were dried overnight with heating *in vacuo* to remove any water or gases. 5 mL was then measured out and under an inert atmosphere the vanadyl 2,3-naphthalocyanine (3.69 mg) was added to 1 set of the ILs. These were then stirred overnight at 30 ℃, sonicated and filtered using a PTFE microdisc. Cyclic voltammetry was run for both the neat ILs and V doped ILs using a Gamry Reference 3000 potentiostat (Figure 6). A 2-mm diameter glassy carbon (GC) working electrode was used in addition to a silver wire reference and a platinum wire counter electrode.

3.69 mg of vanadyl 2,3-naphthalocyanine was used as this provided similar concentrations shown in the IL phase of the extractions in part 1 (40 %).

Results

The results are displayed as cyclic voltammograms which show current density plotted against voltage. Current density, the amount of electric current flowing per unit cross-sectional area of an electrode material, enables us to see how much current would be required to initiate the redox reactions. Voltage relates to the sweeping scan that we performed and displays the voltage at which the redox reactions would happen at. To explain the cyclic voltammograms; the vanadium line indicates our vanadium doped sample, the background indicates the neat IL and the subtracted is vanadium – background so that we only see the effect of the vanadium species.

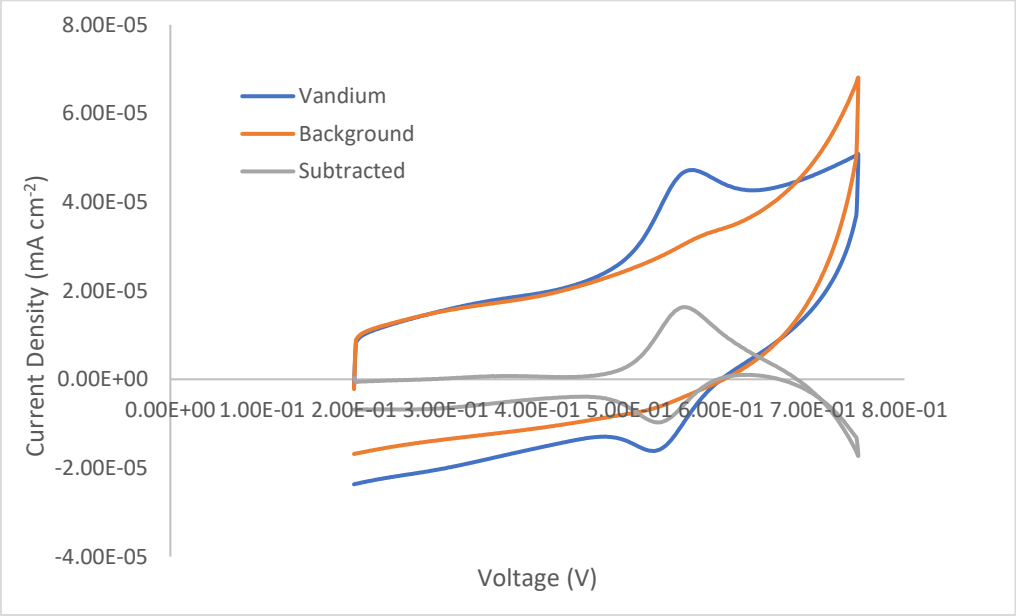

Figure 7 *– Voltammetry of Vanadyl 2,3-naphthalocyanine in [C_2C_1im][N(Tf)$_2$] at 0.20 – 0.75 V using a 2 mm-dia. GC disk*

The cyclic voltammograms for [C_2C_1im][N(Tf)$_2$] show promising results due to the peaks between 0.5 - 0.7 V displaying an oxidation and reduction. When referring to the Pourbaix diagram for V in water (Figure 4) we can see at the lower pH values around this potential range the VO^{2+} species exists. This

coordinated well with our sample due to the vanadyl 2,3-naphthalocyanine possessing V in the +4-oxidation state which is the same as for VO^{2+}. Showing the following reaction could take place

$$V^{IV} + e^- \longrightarrow V^{III} \qquad \text{Oxidation}$$

$$V^{IV} \longrightarrow V^{V} + e^- \qquad \text{Reduction}$$

Another interesting point to note from the CV is that the V in the IL appears to inhibit some oxidation reaction about 0.7 V thus potentially allowing the formation of +5 oxidation state (Figure 5) which is the state of V in V_2O_5 providing the promise of being able to separate the V in this form. This is a highly desirable due to being a solid and providing a feedstock for vanadium battery electrolytes.

For $[HC_1im]Cl$, once the CVs have been subtracted there appears to be a peak 0.11 V (Figure 6) which if due to the vanadium complex this would suggest a +3 oxidation state. This could suggest that this IL chelates differently to the $[C_2C_1im][N(Tf)_2]$ IL altering the oxidation state of the V in solution. This would need to be confirmed by running a lower scan to determine if there is a V^{2+} peak present on the reverse scan.

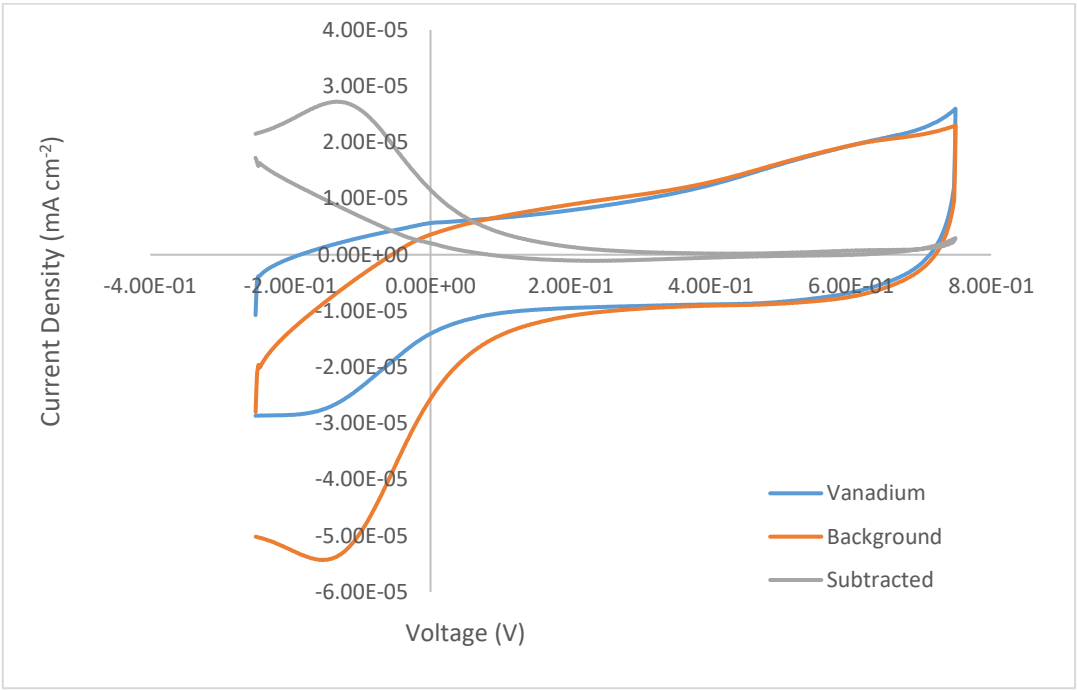

Figure 8 *- Voltammetry of Vanadyl 2,3-naphthalocyanine in $[HC_1im]Cl$ at -0.25 – 0.75 V using a 2 mm-dia. GC disk*

$[C_8H_{15}N_2O_3S][N(Tf)_2]$ again shows a different story with a peak in the reverse scan at 0.36 V (Figure 7) suggesting a potential +4 oxidation state. If this in fact due to V this could be paired with the highly increased current at the top end of the spectrum thus indicating a development to +5 oxidation state which is characteristic of the V_2O_5 species.

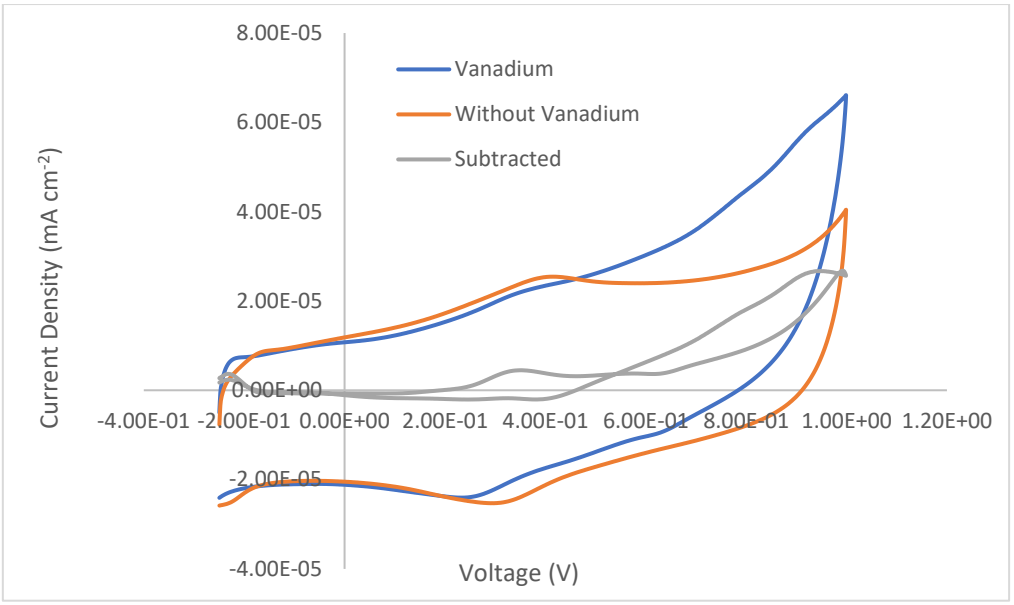

Figure 9 *- Voltammetry of Vanadyl 2,3-naphthalocyanine in* $[C_8H_{15}N_2O_3S][N(Tf)_2]$ *at -0.25 – 1.00 V using a 2 mm-dia. GC disk*

$[C_{12}C_1im][N(Tf)_2]$ does not show any clear peaks as the previous ILs have shown and appears relatively flat (Figure 8), this could suggest that the vanadium complex has a low solubility or that the sample preparation need to integrate increased heating or sonication.

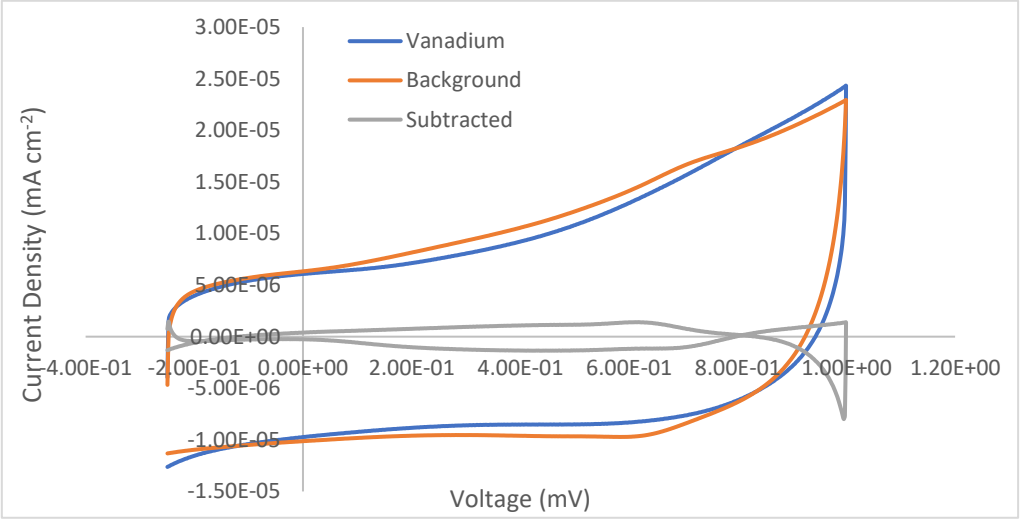

Figure 10 *- Voltammetry of Vanadyl 2,3-naphthalocyanine in* $[C_{12}C_1im][N(Tf)2]$ *at -0.25 – 1.00 V using a 2 mm-dia. GC disk*

Dimethylammnium dimethylcarbamate displays a clear negative peak in the reverse scan in comparison to the background scan at 0.5 V (Figure 9). This relates to a +4-oxidation state on the Parbaix diagram which could pair to the heightened peak at the high end of the CV scan.

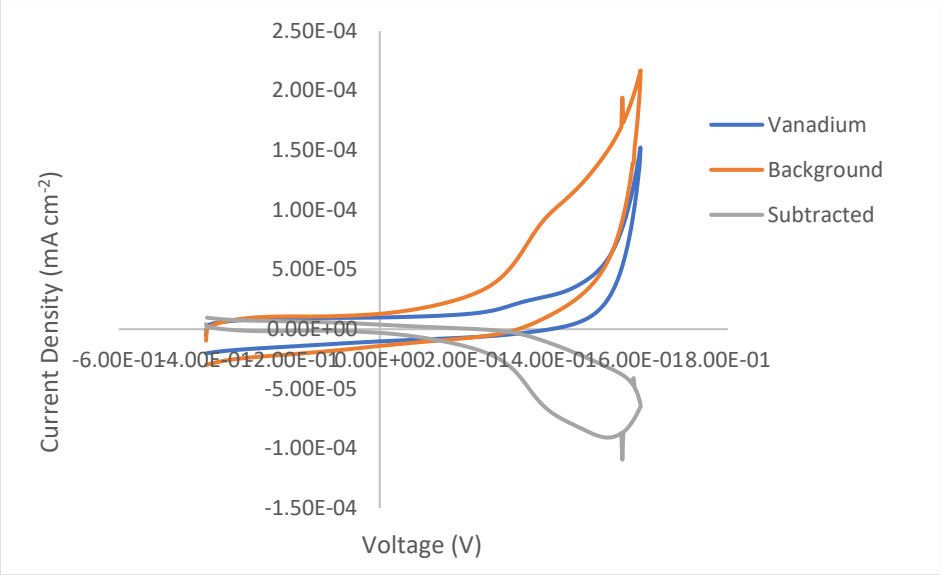

Figure 11 *- Voltammetry of Vanadyl 2,3-naphthalocyanine in dimethylammnium dimethylcarbamate at -0.25 – 1.00 V using a 2 mm-dia. GC disk*

$[N_{4420}]HSO_4]$ does not show any clear peaks appearing flat (Figure 10), this could suggest that the vanadium complex has a low solubility or that the sample preparation need to integrate increased heating or sonication.

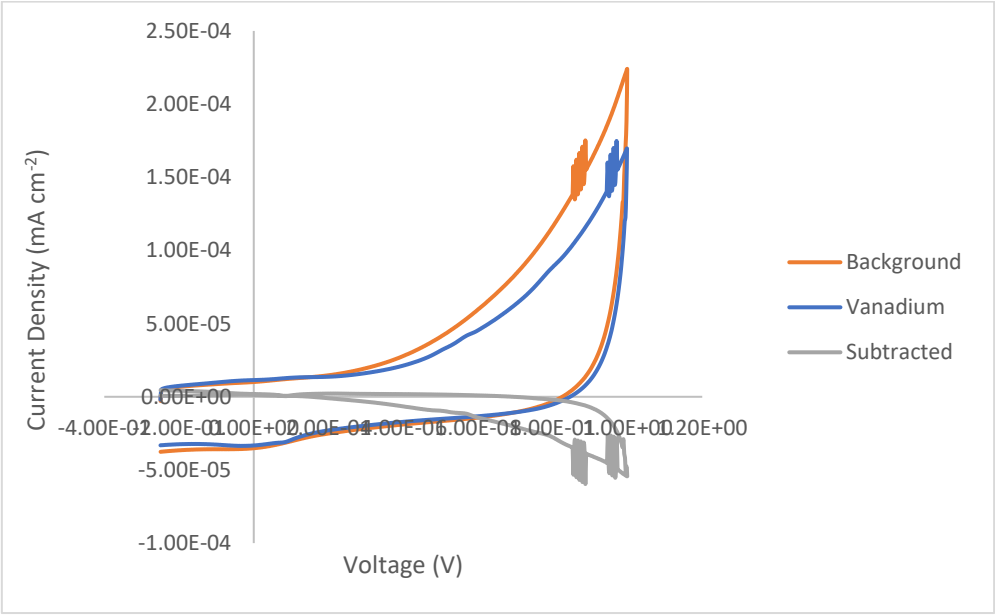

Figure 12 *- Voltammetry of Vanadyl 2,3-naphthalocyanine in $[N_{4420}]HSO_4]$ at -0.25 – 1.00 V using a 2 mm-dia. GC disk*

Conclusion

The ILs have shown a variety of abilities in the extraction of both V and Ni from the provided bitumen samples at ICL. $[C_2C_1im][N(Tf)_2]$ and $[HC_1im]Cl$ are by far the best performers giving a V extraction of 40.00% and 45.83% respectively based on a bitumen concentration of 120 ppm. For Ni, a 36.96% and 43.48 % extraction was achieved respectively based on a 46-ppm concentration. This shows that there is not a great amount of selectivity between the two elements by the IL however, other ILs in this study have given a greater selectivity towards V.

In the electrochemical studies, $[C_2C_1im][N(Tf)_2]$, $[HC_1im]Cl$ and $[C_8H_{15}N_2O_3S][N(Tf)_2]$ all displayed signs of vanadium speciation within the IL. These ILs also had the highest extraction efficiencies so could explain why there was little evidence in the remaining ILs. $[C_2C_1im][N(Tf)_2]$ showed the clearest vanadium peaks in the CV showing that the voltage can be altered to form the +3 and +4 and potentially +5 oxidation states within the IL. The +5-oxidation state is of high interest as this is characteristic of the V_2O_5 species which could precipitate out of the IL and be a valuable feedstock to produce vanadium battery electrolytes.

This preliminary work has provided an indicator that ILs are feasible in the extraction of V and Ni from dilbit samples with $[C_2C_1im][N(Tf)_2]$ scientifically being the strongest recommendation. However, further research need to continue in the following areas to assess the feasibility of the ILs:

- Economic assessment of the IL process including regeneration
- Assessing a range of temperatures and mixing instrumentation to determine if this increases extraction
- In-depth electrochemical analysis and analysis of samples post-extraction need to be compared with the model studies in the report to be fully certain on the removal of V in the most desired form.

Future Work

Based on this study I would highly recommend taking both the extractions and electrochemical work forward refining the following criteria:

- Seek alternative stirring methods during extractions to ensure full phase mixing.
- Trail more ILs to provide further information on the ideal chemical makeup for the application
- Explore electrochemistry further with exact known concentrations and implemented methods to increase solubility of vanadium complexes potentially offering further information regarding the nature of V in the ILs.

References

1. Serban, M, Bhat-Tacharyya, A, Mezza, B. J, Vanden Bussche, K. M, Nicholas, C.P, Bennion, W. K, (2011), *WO 2011/090610 A2*, Illinois, Patent Cooperation Treaty (PCT)